



National Library
of Canada

Bibliothèque nationale
du Canada

Acquisitions and
Bibliographic Services Branch

Direction des acquisitions et
des services bibliographiques

395 Wellington Street
Ottawa, Ontario
K1A 0N4

395, rue Wellington
Ottawa (Ontario)
K1A 0N4

Your file *Votre référence*

Our file *Notre référence*

NOTICE

The quality of this microform is heavily dependent upon the quality of the original thesis submitted for microfilming. Every effort has been made to ensure the highest quality of reproduction possible.

If pages are missing, contact the university which granted the degree.

Some pages may have indistinct print especially if the original pages were typed with a poor typewriter ribbon or if the university sent us an inferior photocopy.

Reproduction in full or in part of this microform is governed by the Canadian Copyright Act, R.S.C. 1970, c. C-30, and subsequent amendments.

AVIS

La qualité de cette microforme dépend grandement de la qualité de la thèse soumise au microfilmage. Nous avons tout fait pour assurer une qualité supérieure de reproduction.

S'il manque des pages, veuillez communiquer avec l'université qui a conféré le grade.

La qualité d'impression de certaines pages peut laisser à désirer, surtout si les pages originales ont été dactylographiées à l'aide d'un ruban usé ou si l'université nous a fait parvenir une photocopie de qualité inférieure.

La reproduction, même partielle, de cette microforme est soumise à la Loi canadienne sur le droit d'auteur, SRC 1970, c. C-30, et ses amendements subséquents.

Canada

**VERTICAL DISTRIBUTION AND TRANSPORT PROCESSES OF
MARINE PARTICLES**

by

Kumiko Azetsu-Scott

Submitted in partial fulfilment of the requirements
for the degree of Doctor of Philosophy

at

Dalhousie University
Halifax, Nova Scotia
April, 1992

© Copyright by Kumiko Azetsu-Scott, 1992



National Library
of Canada

Bibliothèque nationale
du Canada

Acquisitions and
Bibliographic Services Branch

Direction des acquisitions et
des services bibliographiques

395 Wellington Street
Ottawa, Ontario
K1A 0N4

395, rue Wellington
Ottawa (Ontario)
K1A 0N4

Your file *Voire référence*

Our file *Notre référence*

The author has granted an irrevocable non-exclusive licence allowing the National Library of Canada to reproduce, loan, distribute or sell copies of his/her thesis by any means and in any form or format, making this thesis available to interested persons.

L'auteur a accordé une licence irrévocable et non exclusive permettant à la Bibliothèque nationale du Canada de reproduire, prêter, distribuer ou vendre des copies de sa thèse de quelque manière et sous quelque forme que ce soit pour mettre des exemplaires de cette thèse à la disposition des personnes intéressées.

The author retains ownership of the copyright in his/her thesis. Neither the thesis nor substantial extracts from it may be printed or otherwise reproduced without his/her permission.

L'auteur conserve la propriété du droit d'auteur qui protège sa thèse. Ni la thèse ni des extraits substantiels de celle-ci ne doivent être imprimés ou autrement reproduits sans son autorisation.

ISBN 0-315-80080-1

Canada

TABLE OF CONTENTS

	Page
List of Figures	vi
List of Tables	x
Abstract	xi
Abbreviations and Symbols	xii
Acknowledgement	xiv
Chapter 1: General Introduction	
Marine Particles: Key to Understanding Biogeochemical Cycles in the Ocean.....	2
Purpose of The Study.....	11
Organization of the Thesis.....	12
Chapter 2: Time Series of the Vertical Distribution of Particles During and After a Spring Phytoplankton Bloom in Bedford Basin, Nova Scotia	
Introduction.....	16
Methods.....	19
Results.....	23
Discussion.....	50
Conclusions.....	61
Chapter 3: An Intermittent Intermediate Nepheloid Layer in Emerald Basin, Scotian Shelf	
Introduction.....	64
Materials and Methods.....	66
Observations.....	69
Discussion.....	77
Conclusions.....	93

Chapter 4: Measuring Physical Characteristics of Particles: A New Method of Simultaneous Measurement for Size, Settling Velocity and Density of Constituent Matter

Introduction.....	96
Methods.....	98
Results and Discussion.....	111
Conclusions.....	127

Chapter 5: Density Structure of the Water Column and Marine Particle Distribution

Introduction.....	129
Results and Discussion for the Field Data.....	130
A Model.....	147
Discussion.....	159
Conclusions.....	168

Chapter 6: Summary and Conclusions..... 170

Appendix I: Estimate of the Noise Level for Light-Scatter Measurements..... 176

References..... 181

Copyright Acknowledgement..... 198

LIST OF FIGURES

		Page
Fig. 2-1	Map of Bedford Basin, Nova Scotia, Canada and the sampling station	20
Fig. 2-2	Correlation of light-scatter and SPM concentration and linear regressions for total (0-60m), surface (≤ 5 m), 20m and bottom(50-60m)	25
Fig. 2-3	Time series of sigma t and light-scatter profiles	28
Fig. 2-4	Sackville River discharge during the study, in March (Water Survey of Canada, Halifax, Nova Scotia)	30
Fig. 2-5	Repeated measurements of sigma t and light-scatter within 105 minutes on May 16	33
Fig. 2-6	Time series of SPM and POC concentration profiles	35
Fig. 2-7	Surface (5m) Chl.a concentration change with time	38
Fig. 2-8	Time series of Chl.a profiles. Mar.10 was the bloom peak	40
Fig. 2-9	Inverted microscope photographs of suspended particles collected from (1) 1.5m, (2) 15m, (3) 25m, (4) 40m, and (5),(6) 60m on April 7	43
Fig. 2-10	Inverted microscope photographs of suspended particles collected from (1) 8m, (2) 20m and (3) 60m on April 13. (4) 1.5 m, (5) 40 m and (6) 60 m on April 26	45
Fig. 2-11	Inverted microscope photographs of suspended particles collected from (1) 1.5m, (2) 30m and (3) 60m on May 16. (4) 5 m, (5) 10 m and (6) 60 m on April 26	47
Fig. 2-12	Sigma t change with time in the deep water, as an indicator of intrusion events	54
Fig. 2-13	Integration of light-scatter in total (0-60 m) and three layers (0-20 m, 20-40 m and 40-60 m) of the water column	56

Fig. 3-1	Study area. Station 1 is at the deepest point of Emerald Basin (270 m). Station 1-3, 5 and 6 are in Emerald Basin and Station 4 is in the adjacent basin.	67
Fig. 3-2	Vertical profiles of salinity, temperature, sigma t and light-scatter at Station 1	70
Fig. 3-3	Vertical profiles of salinity, temperature, sigma t and light-scatter at Station 2 to 6	73
Fig. 3-4	Chlorophyll a concentration at Station 1	75
Fig. 3-5	Salinity and Temperature diagram for the water from 150 m, 200m and the intermediate nepheloid layer	80
Fig. 3-6	The V component (towards the north) and U component (towards the east) of the wind at the Sable Island weather station	82
Fig. 3-7	The topographic slope, α , calculated from the bathymetric chart over 10 m contour intervals and the characteristic slope, c	87
Fig. 3-8	V component (towards the north) of the semidiurnal (M_2 , N_2 and S_2) tide velocity calculated at Station 1	90
Fig. 4-1	System configuration	100
Fig. 4-2	Density profile of the column	103
Fig. 4-3	(a) Settling of a particle (sample no.21 in Table 2-1) through the density gradient column as a function of time. (b) Plot of $Y = t/y$ against t and linear regression for $t > 40$ minutes	109
Fig. 4-4	The relationships between diameter and length, diameter and settling velocity, diameter and density of constituent matter and density of constituent matter and settling velocity of aggregates from both Bedford Basin and diatom culture	117
Fig. 4-5	The relationships between diameter and length, diameter and settling velocity, diameter and density of constituent	119

	matter and density of constituent matter and settling velocity of aggregates from Bedford Basin	
Fig. 4-6	Changes of diameter, length, settling velocity, diameter/length, density of constituent matter of aggregates from diatom (<i>Chaetoceros</i>) culture with time.	122
Fig. 4-7	Change of the porosity of aggregates from diatom (<i>Chaetoceros</i>) culture with time	125
Fig. 5-1	"Halifax Transect" stations in the western North Atlantic	131
Fig. 5-2	Vertical distribution of light-scatter and sigma t at three stations from "Halifax Transect"	133
Fig. 5-3	Profiles of light-scatter and the density gradient of the water column from the "Halifax Transect"	137
Fig. 5-4	The relationship between light-scatter and the density gradient of the water column	139
Fig. 5-5	Profiles of light-scatter and the density gradient of the water column at Station 1 and Station 4 in Emerald Basin	143
Fig. 5-6	Profiles of light-scatter and the density gradient of the water column on Mar. 10, Apr. 13 and Aug. 16 Bedford Basin	145
Fig. 5-7	Two compartment model for the particle distribution at the pycnocline	149
Fig. 5-8	A sketch of the density profile for the constituent matter, ambient water, bulk density of particle and density difference between the particle bulk density and ambient water at the density discontinuity layer.	151
Fig. 5-9	Light-scatter measurement and SPM concentration relationship for the "Halifax Transect"	156
Fig. 5-10	Particle accumulation change with the proportion of the interstitial water exchange with various porosity and density gradients	160

Fig. 5-11 Saturation of ambient water in aggregates by diffusion process as a function of time. Solid line is for the saturation using the diffusion coefficient of salt for porous medium ($D_s=0.88 \times 10^{-5} \text{ cm}^2 \text{ s}^{-1}$) and dashed line is for the saturation using the diffusion coefficient of heat for porous medium ($D_T=0.88 \times 10^{-3} \text{ cm}^2 \text{ s}^{-1}$). 164

Fig. I-1 Autocorrelation coefficient of light-scatter with lag Δz . 179

LIST OF TABLES

	Page
Table 4-1 Diameter, maximum length, settling velocity, density of constituent matter, excess density, bulk density and porosity of aggregates from Bedford Basin sea water samples.	112
Table 4-2 Diameter, maximum length, settling velocity, density of constituent matter, excess density, bulk density and porosity of aggregates produced in laboratory diatom (<i>Chaetoceros</i>) culture	114
Table 5-1 Linear regression between depth and light-scatter and standard error of estimate	142

ABSTRACT

Marine particles play a key role in biogeochemical cycles in the ocean as primary sites of chemical transport, as microcosms for biological communities and as a food source for larger animals. Fundamental questions that need to be answered include; what does the particle distribution in the ocean look like and what causes that distribution? In this work the hypothesis that the density structure of the water column affects the vertical distribution of marine particles was tested in various marine environments, in the laboratory and by modelling.

The particle distribution profile was measured using a recording backward light-scattering meter that enables the collection of a continuous, real time data set, that also included measurements of salinity and temperature. A time series study of the particle distribution was conducted during a six month period, including the spring phytoplankton bloom, in a coastal basin, Bedford Basin, Nova Scotia, Canada. A high particle load at the pycnocline, particle patchiness in mid-depth and the formation of bottom nepheloid layers (BNL) were observed. The BNL is not a steady state but rather is a dynamic phenomenon. In Emerald Basin on the Scotian Shelf, there was also a high particle load on the pycnocline. In contrast, strong intermittent intermediate nepheloid layers (INL) were recorded in mid-depth. Depths of INLs coincided with the critical depth for possible generation, amplification and breaking of internal waves with semi-diurnal (M_2) internal tide frequency. Intermittent particle resuspension at the "critical" depth on the Basin slope, together with temporal variability of the currents, appear to be the likely cause of the observed intermittency of the INLs.

Particle distributions were significantly different for the two environments investigated in the field (a coastal and a shelf basin) as were the respective controlling factors. However, the two areas had a common feature - a high particle load always on the surface pycnocline. The distribution of particles below the pycnocline, in mid- and deep water, was not related to water density structure. Instead the particle distribution below the mixed layer was characterized by biological (in the coastal basin) or local physical factors (in the shelf basin).

The hypothesis of control of the distribution of particles by density structure was also approached from the perspective of particle characteristics. A new method was developed to measure physical properties of aggregates. The method measures aggregate size, settling velocity and density of constituent matter simultaneously and independently for each aggregate. This last property, density of constituent matter, is presented for the first time for marine aggregates. A high density of constituent matter of aggregates ($>1.095 \text{ g/cm}^3$) relative to sea water, considered with measured settling velocities, suggests that aggregates have high porosity ($>94\%$).

A simple model, using measurements obtained both in the field and in the laboratory, demonstrates that constituent matter density, porosity and exchange rate of interstitial water of aggregates are important parameters for particle settling behaviour and consequently for explaining the distribution of particles at the density discontinuity layer in the ocean. Of the three parameters, two of them (constituent density and porosity) were obtained in this study.

ABBREVIATIONS AND SYMBOLS

BNL	bottom nepheloid layer
c	wave characteristic slope
Chl.a	Chlorophyll a
$C_i(t)$	concentration of suspended particulate matter in component i at time t
E	mathematical expectation
f	local inertial frequency
g	gravitational acceleration 980 cm s^{-2}
GMT	Greenwich mean time
INL	intermediate nepheloid layer
$LS(z)$	light-scatter measurement at depth z
M_2	semidiurnal components of the tide
N	Brunt-Väisälä frequency
$N(z)$	noise for the light-scatter measurement at depth z
P	significance level
PCC	particulate organic carbon
r	particle size
Re	Reynolds number
SPM	suspended particulate matter
t	time
U	eastward component of the wind
V	northward component of the wind
V	volume of particle (Chapter 4)
v_i	settling velocity of particles in compartment i
w	settling velocity of particle
W_∞	terminal settling velocity of particles
$W_{0.99}$	99% of terminal settling velocity of particle

α	topographic slope (Chapter 3)
α	porosity (Chapter 4)
β	proportion of interstitial water exchange with ambient water
τ	necessary time for complete water exchange
σ	wave frequency
μ	dynamic viscosity
ρ_c	density of constituent matter of aggregates
ρ_f	density of ambient fluid
ρ_s	particle bulk density
$\Delta\rho$	density difference between particle and ambient fluid

ACKNOWLEDGEMENTS

I would like to thank my supervisor, Bruce Johnson, for his continuous encouragement, constructive criticism and perseverance. I am grateful to my committee members, Kate Kranck, Barry Ruddick and Pete Wangersky, who were always helpful to solve any problems I encountered during the program.

Discussions with Kee Muschenheim, Brian Petrie and Motoyoshi Ikeda (*Bedford Institute of Oceanography*), David Slauenwhite and David Scott facilitated my research.

Many people helped over the years. In particular, I wish to thank Regina Maas, Xianliang Zhou, Bob Pett, Frederika Schneider, Francine McCarthy, Wolfgang Kuhnt, Eric Collins and Roly King, the captain of the M.V. Sigma t, for help in the field and in the laboratory.

I thank my parents for their support all through the school life.

David Scott gave encouragement, professional advice and two babies. Erica Scott and Tarou Scott, you are the joys.

Financial support was provided by a Killam Scholarship, a Dalhousie Graduate Fellowship and NSERC operating grants awarded to B. Johnson and P. Wangersky.

Chapter One

General Introduction

Marine Particles :

Key to Understanding Biogeochemical Cycles in the Ocean

The existence of marine particles is easily confirmed by examining a sample of sea water under intense light. In 1953, macroaggregates were observed *in situ* by Japanese researchers looking through the viewing ports of a submersible. These large aggregates were named "marine snow" (Suzuki and Kato, 1953). Since then, marine particles have attracted substantial attention from oceanographers. Organic aggregates in tropical and subtropical surface waters of the north Atlantic Ocean were studied by Riley *et al.* (1964). They showed that the abundance of particulate organic carbon (POC) was not uniform and that higher concentrations of aggregates were found in upwelling regions. Riley (1963) observed the seasonal cycle of organic aggregates in Long Island Sound. Wangersky (1974) demonstrated the sampling variability of POC measurement due to the patchy distribution of POC. In the 1970's, the distribution of particulate matter in the Atlantic Ocean was mapped using Niskin bottle sampling in the GEOSECS program (Brewer *et al.*, 1976). These extensive measurements of suspended particulate matter (SPM), employing a gravimetric method, revealed regional variation of SPM concentration as well as depth variation. Wangersky (1976) showed that POC concentrations in the Pacific and Atlantic oceans were roughly comparable and that both oceans showed a logarithmic decrease with depth, along with occasional anomalously high values. Extensive utilization of sediment traps, for example in association with GOFS (Global

Ocean Flux Study) of the 1980's, has resulted in much new data on particle fluxes in various marine environments.

The importance of marine particles in biogeochemical cycles in the ocean has been recognized for about 10 years. Marine particles are carriers of heavy metals (for example, Bruland, 1983; Noriki *et al.*, 1985), radionuclides (Bacon and Anderson, 1982; Livingston and Anderson, 1983;), organic materials (for example, Wangersky, 1978, 1984; Karl *et al.*, 1988) and nutrients (Eppley and Peterson, 1979). These chemical substances are incorporated in and/or are attached to the surface of marine particles and are transferred from the surface waters of the ocean to the deeper waters. Some particles reach the seabed and are incorporated into the sediments. During transport, chemical substances may associate and dissociate with marine particles because of reversible chemical reactions at the particle surface (Martin and Knauer, 1985). Decomposition, formation and aggregation processes of marine particles are of primary importance in the cycling of chemical substances in the ocean.

Marine snow, macroscopic aggregates of detritus, living organisms and inorganic matter, are significant as microcosms. Marine snow contains an enriched community of living phytoplankton, cyanobacteria, protozoa, and bacteria at densities two to five orders of magnitude higher than populations found freely dispersed in the surrounding seawater. Therefore, marine snow represents an isolated microenvironment where carbon fixation by autotrophs, decomposition of organic

matter and nutrient regeneration by a dense heterotrophic bacterial community are enhanced (e.g., Silver *et al.*, 1978; Silver and Alldredge, 1981; Shanks and Trent, 1979; Prezelin and Alldredge, 1983; Knauer *et al.*, 1982; Alldredge *et al.*, 1986; Caron *et al.*, 1986; Alldredge and Cohen, 1987; Alldredge and Silver, 1988 as review). In addition, marine particles are important food sources for various zooplankton and fish (Alldredge, 1972, 1979; Wotton, 1990; Vanderploeg, 1990). Further, response of the benthic community to surface biological activity through the settling of particles has been observed with relation to population dynamics, reproductive cycles (Goody and Lamshead, 1989; Goody and Turley, 1990, a review) and seasonality of oxygen consumption (Smith and Baldwin, 1984; Smith, 1987; Cole *et al.*, 1987).

Composition and Sources of Marine Particles

"Marine particles" can be anything from sub-micron size particles to whales. However, the definition of "marine particles" as used in Oceanography is operational and depends on the sampling method. If bottle sampling or an *in situ* filtration system is used, the pore size of the filter determines the lower end of the size spectrum and sampling bottle and screen size determine the upper end of the size spectrum (Wangersky, 1990). If a camera system is used, the resolution of the photographs and the depth of field typically control the range of the size spectrum.

Sources of marine particles include authigenic production by biological activity, physical processes that cause aggregation of molecular or colloidal matter (e.g., Johnson and Cooke, 1980; Johnson *et al.*, 1990), precipitation of inorganic minerals,

fluvial input (Nittrouer *et al.*, 1986), aeolian input (Buat-Ménard *et al.*, 1989), input from ice melt in polar region, shore erosion, resuspension of sediment, and input from submarine volcanism and hydrothermal activity (Comita *et al.*, 1984).

Marine particles, including biogenic and non-biogenic materials, often form aggregates containing both kinds of materials. Sources of non-biogenic particles include terrigenous material transported through the atmosphere or by rivers, erosion of sediment and shoreline and authigenic precipitation. Intact organisms and plankton hard parts, faecal pellets and amorphous macroaggregates - marine snow - are the major components of the biogenic particles. Most biogenic materials are produced in the upper layer of the ocean, where primary productivity can be high. The abundance of biogenic particles has strong regional and seasonal variation - factors that influence the vertical flux of particulate material to the deep water. Faecal pellets produced by protozoans (Gowing and Silver, 1985), zooplankton (Bruland and Silver, 1981), and fish (Robison and Basiley, 1981), appear to be important in vertical flux of particles in the ocean. Small particles with low settling speeds as individual particles are packaged and transformed into rapidly settling faecal pellets (Emery and Honjo, 1979) or are aggregated and contribute to the mass flux to the deep sea (Honjo, 1980), and to the sediment in coastal waters (Knauer *et al.*, 1979) and in fjords (Syvitski and Murray, 1981). Intact organisms and the hard parts of plankton are the major components of biogenic particles. Although most biogenic particles are produced in the surface water, they are also found in deep water sediment trap samples (Takahashi and Honjo, 1981, 1983; Takahashi, 1986;

Honjo, 1978; Honjo *et al.*, 1982) and comprise a portion of the large particle flux (Fowler and Knauer, 1986). Marine snow is ubiquitous and contains living organisms, detritus, faecal pellets and inorganic minerals. Data from Asper (1987) suggested that most of the flux of particles entering a trap is carried in aggregates. Because marine aggregates are fragile and tend to break up during sampling, detailed study has not been conducted until recently. *In situ* studies using SCUBA and optical methods are now widely used. Physical characteristics, dynamics, and significance of marine snow have been recently summarized by Alldredge and Silver (1988).

Sampling Methods

Studies of marine particles have evolved with invention of new sampling techniques and with changing scientific focus. Conventional bottle sampling is a widely used technique to collect marine particles for measurement of weight/volume concentration, determination of chemical composition and for microscope investigation. There are some disadvantages associated with the method, in that bottle samples can not provide continuous data and consequently patchiness of the particle distribution is difficult to detect. In addition, large, rapidly sinking particles are under-represented in sampling bottles that have a side mounted spigot, because some of the particles settle below the spigot height during recovery. This may cause an underestimate of SPM concentration (Gardner, 1977; Calvert and McCartney, 1979). Finally, large aggregates are fragile and are broken up easily by bottle sampling procedures (Nishizawa *et al.*, 1954; Riley, 1963; Gibbs and Konwar, 1983).

Large-volume *in situ* pumps such as the "LVFS"-large volume *in situ* filtration system (Bishop and Edmond, 1976) and "WHISP"-Woods Hole *in situ* pump (Wakeham *et al.*, 1984a,b) sample large volumes of water in a short period of time and consequently minimize errors caused by bacterial decomposition of particles and by chemical contamination during sampling. Because of the large volume of water filtered, samples include large, rare particles. Disadvantages, however, are the discrete nature of sampling and, as well, some particle disruption may occur even though filtration speed is slow ($<2\text{cm/sec}$) (Simpson, 1982; Fowler and Knauer, 1986; Alldredge and Silver, 1988). Large volume filtration systems average over the period of pumping and particles are collected on a filter surface and hence often it is not possible to identify whether particles were discrete or part of an aggregate.

In situ collection by SCUBA diving and submersible allows recovery of intact, large, fragile marine aggregates, and permits determination of abundance and size distribution (Trent *et al.*, 1978; Alldredge and Gotschalk, 1988), microbial population (Caron *et al.*, 1982; Alldredge *et al.*, 1986), chemical composition (Alldredge, 1979) and *in situ* settling velocity (Shanks and Trent, 1980; Alldredge and Gotschalk, 1988). The SCUBA method has proven especially effective; however, the method is limited to surface waters and is subject to some variability with ability of divers, water conditions (ambient light level, visibility and size and colour of aggregates) and particle size (correctly assesses particle size $>0.5\text{ mm}$) (Alldredge and Silver, 1988). Only a few studies are available describing collection of particles by submersibles (Kajihara, 1971; Silver and Alldredge, 1981), although there are many accounts of

observation of particles through submersible windows (Kato and Suzuki, 1953, Aybulatov and Novikova, 1984; Ebara and Asaoka, 1985). Collection of particles using submersibles solves the problem of depth limitation of SCUBA diving.

Moored or floating sediment traps were developed for measurements of particulate matter flux. Studies have focused on mass and composition of settling particles and associated chemical substances such as trace elements, radionuclides and various pollutants. Since the flux of particles in the ocean is a necessary parameter to assess the global cycle of chemical substances and energy input to the benthic community, numerous studies that use sediment traps have been conducted over the world oceans (e.g., Honjo, 1978, 1982; Deuser *et al.*, 1981, 1988; Sasaki and Nishizawa, 1981; Livingston and Anderson, 1983; Ittekkot *et al.*, 1984, 1991; Wakeham *et al.*, 1984; Bacon *et al.*, 1985; Deuser, 1985; Noriki and Tsunogai, 1986; Takahashi, 1986; Karl *et al.*, 1988; Moore and Dymond, 1988; Grimalt *et al.*, 1990; Albert *et al.*, 1991). Problems inherent in use of sediment traps result in variable and unpredictable trapping efficiency caused by: hydrodynamic effects (Gardner *et al.*, 1980a,b; Gardner, 1985; Butman 1986; Butman *et al.*, 1986; Baker *et al.*, 1988; Siegel *et al.*, 1990; Buesseler, 1991), organisms swimming into traps (Knauer *et al.*, 1979; Gardner *et al.*, 1983; Knauer *et al.*, 1984), degradation of organic materials (Gardner *et al.*, 1983; Banse, 1990; Michaels *et al.*, 1990) and dissolution of some metals from the particulate phase within the traps (Knauer *et al.*, 1984). Sediment traps are the only direct method available for measuring the *in situ* particulate matter flux, although careful considerations in developing a sampling strategy and design of the

trap are necessary to minimize the associated errors (Asper, 1987).

In situ optical methods of measuring particle abundance are classified into two types of measurements. Transmissometry (light attenuation) or light-scattering can be used to measure the distribution of particles. The other, photography, can also be used for studying the distribution of large particles (Honjo *et al.*, 1984; Johnson and Wangersky, 1985; Gardner and Walsh, 1990), but is most often used to measure particle size distribution or to investigate morphology of particles. There have been a growing number of studies using transmissometer measurements and optical scattering during the last decade. These studies have demonstrated the existence of discrete layers of high particle loading (e.g., Pak *et al.*, 1980a,b; Dickson and McCave, 1986; Thorpe and White, 1988), which might be overlooked by conventional bottle sampling (Sternberg *et al.*, 1974; Wangersky, 1990). Transmissometer and light-scatter methods usually provide a direct readout aboard ship, and can aid in the selection of depths for further sampling of particles. Moreover, a transmissometer or a light-scatter meter can be deployed easily with other instruments that measure the physical, chemical and biological characteristics of the water column - instruments that include CTD's, current meters, oxygen probes and fluorometers. Since these systems can be lowered repeatedly at short intervals or can be moored over a long period, they can be used to study episodic events such as benthic storms (Gardner and Sullivan, 1981; McCave, 1983; Hoilister and McCave, 1984), sediment resuspension by internal tides in submarine canyons (Gardner, 1989a,b) or diel variation due to biological activity (Siegel *et al.*, 1989). The major problem with *in*

situ optical methods lies in calibration with SPM concentration. Correlation between light attenuation or light-scatter and SPM concentration is affected by the concentration, size distribution, refractive index and shape of particles (Richardson, 1987; Gardner *et al.*, 1990). Therefore, the correlation can vary regionally or with depth (Biscaye and Eittreim, 1974; Sternberg *et al.*, 1974; Spinrad *et al.*, 1983; Gardner *et al.*, 1985). *In situ* photography has been used for measurements of the particle size distribution and particle settling velocity (Honjo *et al.*, 1984; Asper, 1985). Photography has also been used for observations of the flocculation process during a diatom bloom (Kranck and Milligan, 1988) and in studies of morphological change of the seabed due to particle flux (Billet *et al.*, 1983; Lampitt, 1985; Hecker, 1990). Because, in general, large aggregates are very fragile, this non-invasive method is suitable for measuring the particle size distribution and settling velocity - measurements that can not be obtained by bottle sampling, *in situ* filtration or sediment trap collection.

A combination of sediment trap and camera system has been developed to measure the flux and concentration of marine snow (Asper, 1987). The vertical particle distribution and morphological change of particles with depth were studied using light-scatter and an *in situ* camera system (Johnson and Wangersky, 1985). Since no available method is perfect for deriving all the information on marine particles, combinations of existing tools need to be used together with the development of new techniques.

The Purpose of the Study

Fundamental problems to be solved in studying particulate matter in the ocean include determination of the spatial and temporal distribution of particulate matter and identification of mechanisms that control marine particle dynamics. The purpose of this study is to contribute to an understanding of the vertical distribution of particulate matter under various marine conditions. Chemical characteristics of the water column such as oxygen concentration and biological effects such as patchiness of heterotrophic organisms affect the distribution of particles; however, this study focuses on the physical characteristics of water, specifically density structure. The questions that are asked include;

(1) What is the relationship between the distribution of particles and density structure of the water column ? The hypothesis that density discontinuities act as sediment traps in the ocean is tested. Knowing the regions of high particle concentration is important because these represent sites of active chemical dynamics including desorption and adsorption of trace elements, and sites of food concentration for heterotrophs and attendant nutrient regeneration.

(2) What are the mechanisms that cause the observed particle distributions in the ocean ? When density structure of the water column does not affect the distribution of particle, what causes the observed distribution ? Identification of the controlling factors for the distribution of particles in various marine environments helps in understanding general mechanisms and the significance of local processes of particle

dynamics.

(3) How can physical characteristics of marine particles be measured ? The distribution of particles in the ocean is the consequence of ambient water characteristics and particle properties. Among the basic physical parameters that affect particle dynamics, including size, density and settling velocity, density is least known. Since the density difference between particles and ambient water controls the settling behaviour as well as particle size and shape, it is essential to obtain the density of marine particles for the study of particle dynamics, especially where the ambient water density changes sharply. A system that measures the size, density and settling velocity is developed.

(4) What are the areas requiring further study ? Through this study, new questions arise that pertain to what parameters are important for understanding marine particle dynamics and how well these are now known.

Organization of the thesis

The thesis consists of field observations (Chapters 2 and 3), laboratory measurements (Chapter 4) and a model study using the results from both the field and the laboratory (Chapter 5).

First, a field study was conducted in coastal and offshore basins to describe the relationship between the distribution of particles and the density structure of the water column, and to identify the controlling factors for the observed particle distribution. In Chapter 2, the distribution of particles was studied in a coastal basin

during and after a spring phytoplankton bloom. These results are related to the density structure of the water column and auxiliary biological and chemical measurements. Because the phytoplankton bloom is a major source of marine particles and biological productivity is especially high in coastal waters, the distribution of particles in coastal waters has a strong impact on biogeochemical cycles in the ocean. After demonstrating domination of biological effects on the distribution of particles in a coastal basin, Chapter 3 treats the particle distribution in an offshore basin. In the offshore basin, intermediate nepheloid layers were featured in the distribution of the particles. Using existing hydrographic and atmospheric data, it is concluded that the observed intermediate nepheloid layers were caused by local physical processes - instability of internal waves. From these results the hypothesis that density discontinuities act as a sediment trap appears to be true only in the surface pycnocline, not in mid- and deep water.

To understand the settling behaviour of particles in response to strength of the density stratification observed in the field, it is necessary to know the physical characteristics, especially density, of particles - a parameter that has not previously been measured directly for marine aggregates. In Chapter 4, a method that measures size, settling velocity and the density of constituent matter of aggregates is illustrated with results from coastal water and from a diatom culture.

Finally, in Chapter 5, general features of the relationship between density structure and particle distribution are reviewed by comparing the observations in coastal water, on the shelf, on the slope and in the open ocean. Using these results

and the measurements conducted in the laboratory (Chapter 4), a simple model is constructed to help in understanding the effect of the density discontinuity on the distribution of particles as a function of the strength of stratification, particle density, porosity and water exchange rates. This model clarifies which parameters need to be further studied in the future.

Summary and conclusions are presented in Chapter 6. In Appendix I, the noise level for light-scatter measurements is estimated. A combined reference list is placed at the end of the thesis.

Chapter Two

Time Series of the Vertical Distribution of Particles During and After a Spring Phytoplankton Bloom in Bedford Basin, Nova Scotia

INTRODUCTION

Relative to the open ocean, particle dynamics in coastal waters are more strongly affected by biological, chemical and physical processes on shorter time scales. High surface biological activity and fluvial input represent the main sources of particles to coastal regions. In addition, lateral transport of particles from other water masses by tide and/or current can be locally very important in some areas. Input of particles is followed by cycling and sorting. Some particles, consumed by zooplankton and fish, are packaged as faecal pellets that contribute to the vertical flux through increases in particle size and density. Some particles undergo flocculation and deflocculation - processes that also affect vertical transport. Ultimately particles are transported offshore by tide and current, or settle through the water column to the sea floor. There, they may be resuspended before being incorporated into the sediments.

Seasonality of the vertical flux of organic matter due to surface primary production has been recognized from sediment trap results (for example, Hargrave and Taguchi, 1978; Deuser, 1981; Honjo, 1982; Takahashi, 1986; Riebesell 1989), from *in situ* photography (Billet *et al.*, 1983; Lampitt, 1985; Rice *et al.*, 1986) and from sediment core samples (Goody and Lambshead, 1989). Mass flocculation of spring phytoplankton blooms (marine snow formation) has been observed in Nova Scotia (Kranck and Milligan, 1988) and California (Alldredge and Gotschalk, 1989) coastal waters, and in the southern North Sea (Riebesell, 1991a,b). In spite of the

evidence of a strong influence of the spring phytoplankton bloom on particle flux, less is known about the vertical distribution of particles in the water column - information that may be important as an indicator of oceanic biogeochemical processes (Gardner *et al.*, 1990).

In situ optical methods that include transmissometry, light-scattering, photography and/or a combination of these offer advantages for determining marine particle distributions. Large aggregates, proven to be of major importance in vertical transport (Bishop and Edmond, 1976; Honjo *et al.*, 1984; Asper, 1987; Gardner and Walsh, 1990), are both rare and fragile - two properties that make them especially suited to measurement using non-invasive *in situ* optical methods. Since beam attenuation or light-scattering provides a continuous measurement of the particle distribution, *in situ* optical methods are very powerful for studying particle patchiness - features of the distribution that might be missed by conventional bottle sampling. Examples of these features include intermediate nepheloid layers (e.g., Pak *et al.*, 1980a,b; Dickson and McCave, 1986; Thorpe and White, 1988) and the accumulation of particles observed associated with strong density gradients or discontinuities such as pycnoclines or fronts (Pak *et al.*, 1980a; Gardner *et al.*, 1990); however, the mechanism by which these higher concentrations are sustained is not clear. In addition, optical methods can be used to measure vertical profiles of the particle distribution repeatedly within a short period of time or can be moored over a long period. Consequently such methods can be used to detect episodic events such as benthic storms (Gardner and Sullivan, 1981; McCave, 1983; Hollister and McCave,

1984) and diel variations of particle distribution resulting from biological activity (Siegel *et al.*, 1988). However, there are also disadvantages of *in situ* optical methods. Such methods do not give the chemical composition of particles. Vertical flux is not accurately estimated with optical methods because of errors associated with size measurement and assumptions of particle density and settling velocity. Further, the conversion of the signal from a transmissometer or light-scatter nephelometer to mass/volume concentration is not always linear, in part because of variation in the size distribution, composition and surface characteristics of particles (Richardson, 1987). Finally, for camera systems there is a size limitation for small particles.

Cognizant of the advantages and disadvantages of optical methods, a time series study of the particle distribution over the spring phytoplankton bloom period was conducted using a backward light-scattering meter, a CTD and bottle sampling. The purposes of this study include the following:

- (1) to describe the change of the particle distribution in the water column during and after the spring phytoplankton bloom. Phytoplankton blooms in surface waters are a major source of marine particles and resulting vertical mass flux. However, little is known about the distribution of marine particles during and after the bloom - information that is important in understanding biogeochemical cycles including trace element dynamics in relation to adsorption and desorption sites, food abundance for heterotrophic organisms and nutrient regeneration.
- (2) to clarify the relationship between water structure and the patchiness of the particle distribution.

(3) to identify particle characteristics and changes in these characteristics with progression of the surface phytoplankton bloom. Characteristics that were measured include POC, mass/volume concentration and Chl.a, and size, shape and particle type determined from microscope observation.

METHOD

From February to August, 1988, profiles of light-scatter, salinity and temperature (CTD, Guildline 8709) and water samples were taken in Bedford Basin, Nova Scotia, Canada (Fig. 2-1). The Basin is 2.7 km wide and 4.3 km long, and is characterized by a 20 m sill at the mouth where the basin is connected to Halifax harbour and the open ocean. The sampling station was at the deepest point, 70 m, and almost in the centre of the Basin. Using the M. V. Sigma-T of the Bedford Institute of Oceanography, sampling was conducted 15 times during this study; two times each week in March when the spring bloom was observed, and less frequently through the remainder of the study period.

A recording backward scattering meter, developed by Johnson and Wangersky (1985), was used to measure relative backscatter at a fixed angle of 30° (the instrument condition has been changed slightly since 1985). The observed volume *in situ* by the instrument is about 10 cm³. The measurement was recorded as backscatter/intensity of light emitted. Offset of the light-scatter measurement is 2.88

**Fig. 2-1 Map of Bedford Basin, Nova Scotia, Canada. The
sampling Station is marked as S.**

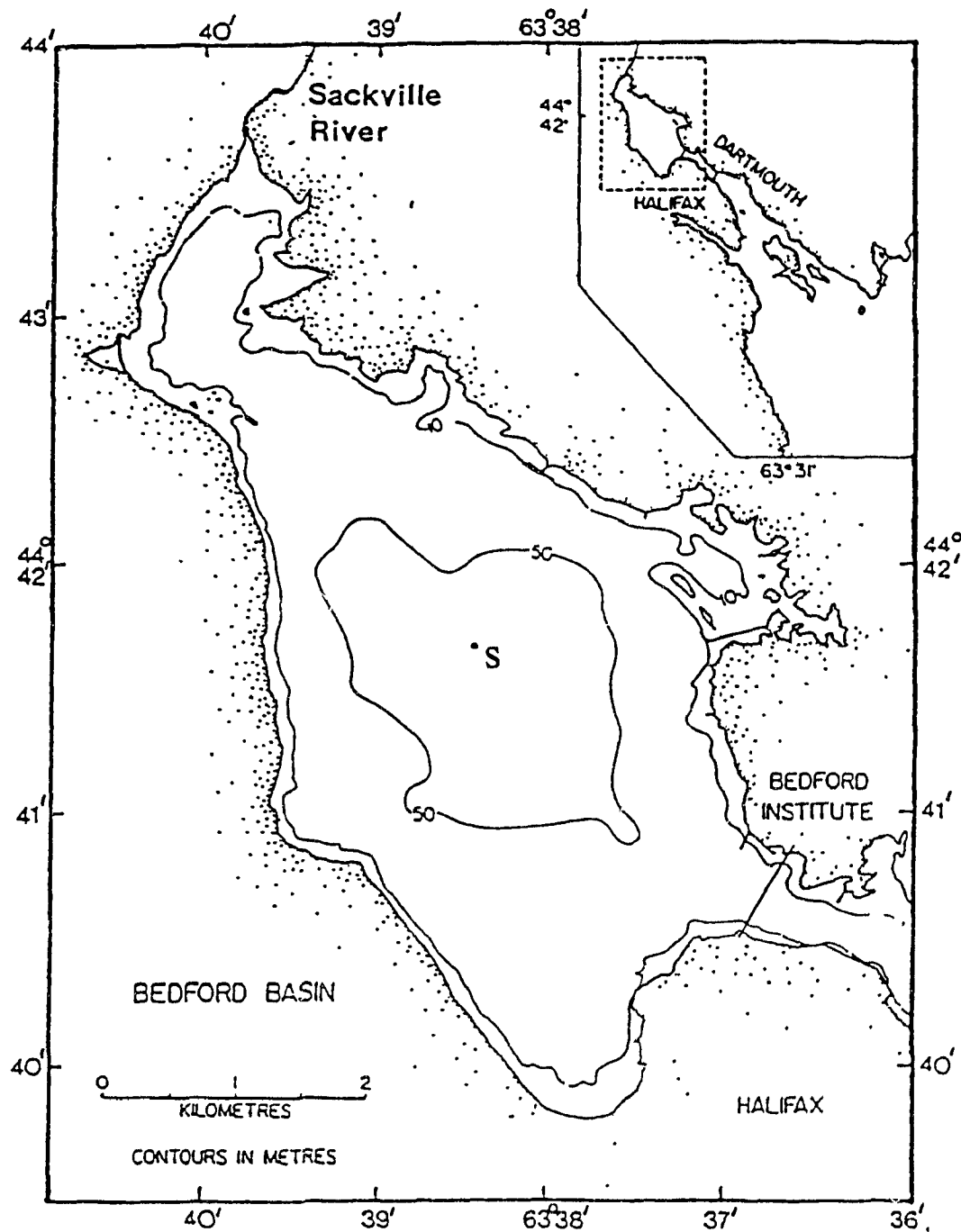


Fig. 2-1

units and variance of the light-scatter signal due to noise is 0.009 units. Estimate of the noise level for light-scatter measurements is described in Appendix I. Because the CTD resolution is about 0.1 m, data were recorded at 0.1 m intervals and both CTD and back scatter data were recorded in real time as a function of depth on a Hewlett-Packard 110 computer on the deck of the sampling vessel. At least 2 casts were made with the CTD - light-scatter system to test repeatability. On one occasion, May 16, 5 profiles were taken to observe the stability of the observed patchiness.

From the CTD and backscatter profiles plotted on deck, typically 6 different water sampling depths were chosen. These water samples were used for measurements of mass concentration of suspended particulate matter (SPM), particulate organic carbon (POC) and for microscope examination. Water samples were taken by Go-Flo bottles within 10 minutes of the CTD and light-scatter measurements. These water samples were transferred to polyethylene containers from the bottom of the Go-Flo bottles to avoid leaving fast settling particles in the bottles below the spigots (Gardner, 1977). Water samples were brought back to the laboratory where they were processed for analysis within one hour.

For mass concentration of particles, preweighed 47mm Millipore filters (0.45 μm pore size), were prepared according to the method of Winneberger et al. (1963). For each SPM measurement five litres of water sample were filtered. Following filtration, filters were rinsed with distilled water and kept in individual desiccators to dry for two days. The filters were then weighed to 0.01 mg (error was $\pm 2\%$).

For POC analyses, 500 ml of sample were filtered onto 25 mm Whatman GF/C glass fibre filters and then frozen at -20°C until analysis. POC was determined using

the dry combustion method of Wangersky (1976) with the blank error 0.1 ± 0.07 mgC/L. For microscope study of particle characteristics, one hundred millilitres of sample were placed in settling cylinders overnight. The settled particles were examined with an inverted microscope (Wild M40) and photographed. Chlorophyll a was measured at the same sampling station almost daily in February and March and on selected days in April (unpublished data, Biological Oceanography Division, Bedford Institute of Oceanography).

RESULTS

Correlation of light-scatter measurements with SPM concentration

Light-scatter observation is a measurement of scattering cross section of particles (Plnak, et al., 1972) rather than mass and is affected by the particle size distribution, particle surface characteristics and refractive index (Richardson, 1987). On the other hand, SPM concentration is influenced by the type of filter used and is a measure of the weight of marine particles. In other words, light-scatter and SPM concentration measure different aspects of the particle distribution. SPM concentration is the important parameter for mass flux estimates, however, there is no method for measuring SPM continuously. Therefore the light-scatter measurements have been calibrated with SPM concentration determined using bottle samples or *in situ* filtration systems in various marine environments. The correlations between light-scatter and SPM concentration typically differ regionally or with depth (for example,

Biscaye and Eittrheim, 1974; Sternberg, *et al.*, 1974; Carder *et al.*, 1974; Spinrad *et al.*, 1983; Biscaye *et al.*, 1985; Gardner *et al.*, 1985; Richardson, 1987). Because biological diversity is greater and particle composition is more complex in coastal areas, more scatter in the correlation between SPM concentration and light-scatter is observed in this study (Fig. 2-2) than in similar studies in the open ocean (Richardson, 1987). The correlation between light-scatter and SPM concentration in the surface water, excluding the data when the Sackville River discharge was more than 10 m³/sec (Fig. 2-5) and August data when the dominant species in the surface water became dinoflagellates, was significant at the level $P < 0.002$ (Fig. 2-2). At mid-depth (20 m), however, less scatter in the relation was observed ($P < 0.001$). These results suggest that the particle composition is more homogeneous in the clear-water minimum than in the surface mixed layer or in deep water. In the deep water, particle composition and size distribution are complicated, reflecting surface biogenic and fluvial input, as well as particle degradation. It is worth noting that the slopes of the regression lines relating light-scatter to SPM concentration changed with depth, being highest in the surface water and decreasing to the bottom. Although relationships between light-scatter and SPM concentration changed with depth, the overall correlation is still significant at the level $P < 0.005$ and therefore the light-scatter can be a good indicator of the particle mass distribution.

Light-scatter and water structure

The time series observations of light-scatter showed transition of the particle

Fig. 2-2 Correlation of light-scatter and SPM concentration.

Linear regressions for total (0-60 m), surface (≤ 5 m),
20 m and bottom (50-60 m) were as follows;

depth	equation	correlation coeff. (r)	significance level (P)
0-60m	$Y=0.248X-0.207$	0.49	<0.005
≤ 5 m	$Y=0.683X-1.961$	0.85	<0.002
20m	$Y=0.277X-0.234$	0.96	<0.001
50-60m	$Y=0.125X+0.079$	0.57	<0.01

Y = SPM concentration (mg/l), X = light-scatter

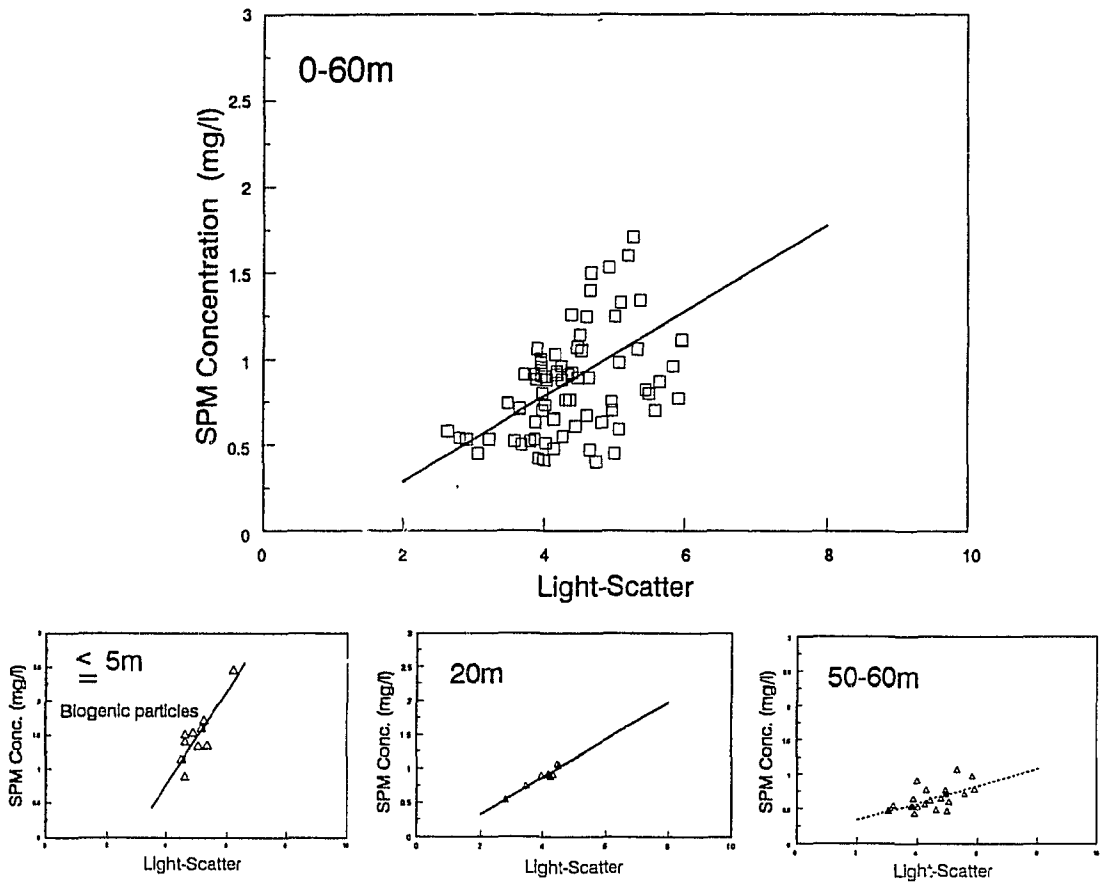


Fig. 2-2

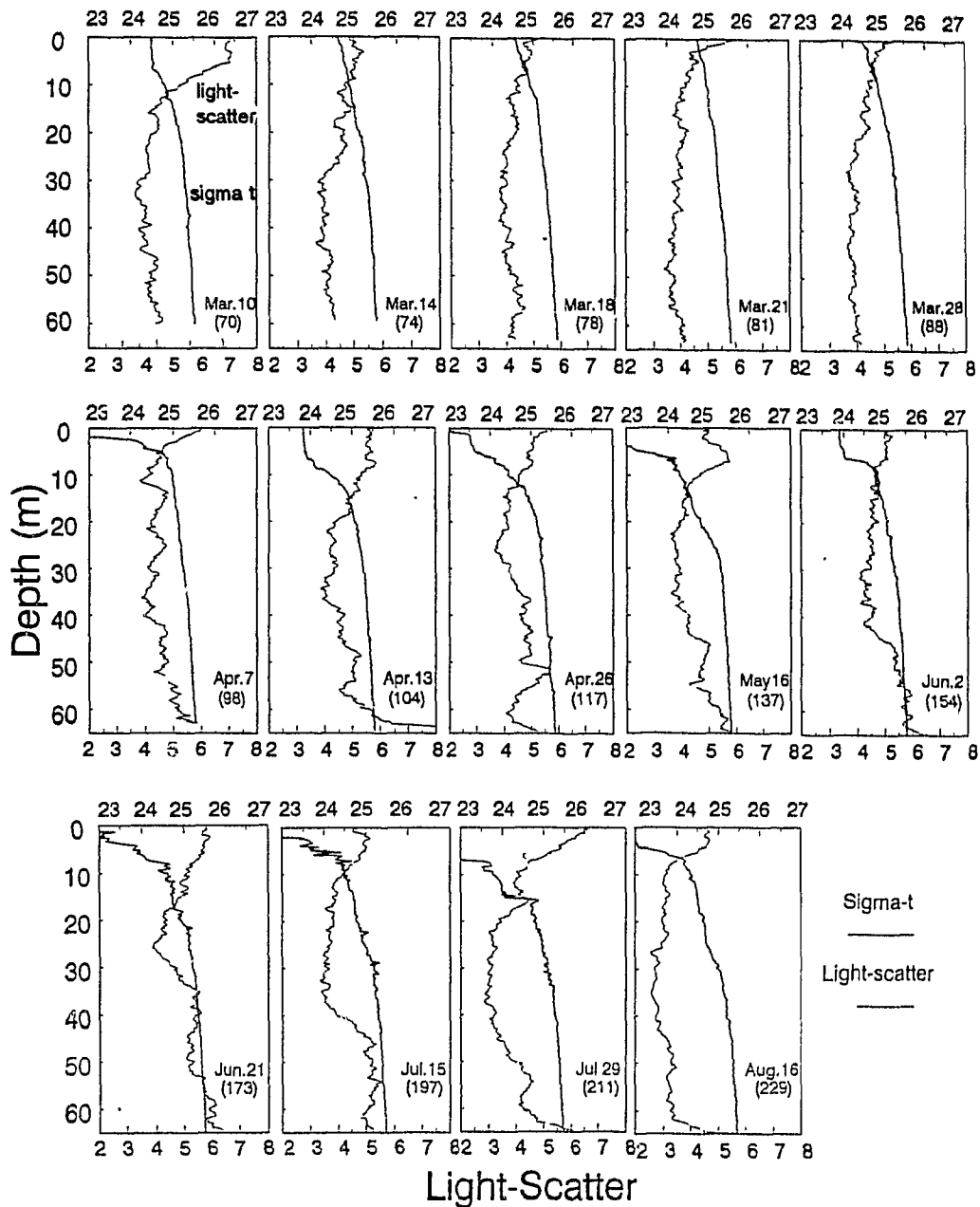
distribution from high light-scatter above the pycnocline and low light-scatter below during March, to bottom nepheloid layer formation in April, May, June and July. This pattern gave way to very low light-scatter in the middle water and thinning of the bottom nepheloid layer in late July and August (Fig. 2-3). This general trend, however, was also affected by local episodic events such as fresh water input from the Sackville River (Fig. 2-1 and 2-4), storm mixing (March 14, 18 and 21 when wind speed was 20-40 km/h at the sampling station) and patchiness of biological activity in the water column.

On March 10, light-scatter peaked on top of the pycnocline and was high throughout the surface mixed layer (Fig. 2-3). A subsequent wind mixing event weakened the pycnocline (March 14, 18 and 21), reduced light-scatter in the surface layer and increased near-bottom light-scatter on March 18. On March 28, surface water (0-20 m) warmed to 2.5 °C and light-scatter increased in the resulting broad thermocline. For the April 7 profile, input of warm fresh water, high in inorganic particle concentration from the Sackville River (Fig. 2-4) established a sharp pycnocline and high light-scatter in the surface layer. In addition, in this profile there were two distinct peaks of light-scatter, one at 15 m and the other at 25 m, for which there were no corresponding density discontinuities at either depth. Light-scatter in the bottom water increased with depth to the bottom.

Development of the bottom nepheloid layer intensified about one month after the bloom peak in the surface water. A typical particle distribution reported for the open ocean, i.e., high in the surface mixed layer, minimum in mid-water and high

Fig. 2-3 Time series of sigma-t and light-scatter profiles. The numbers in parentheses are days of the year.

Sigma-t



Time Series of Sigma-T and Light-Scatter Profile

Fig. 2-3

Fig. 2-4 **Sackville River discharge (m^3/sec) during the study. In March, except March 1-4, 10 and 24-31, ice conditions at the edge of the Basin were reported. (Water Survey of Canada, Halifax, Nova Scotia)**

Sackville River Discharge

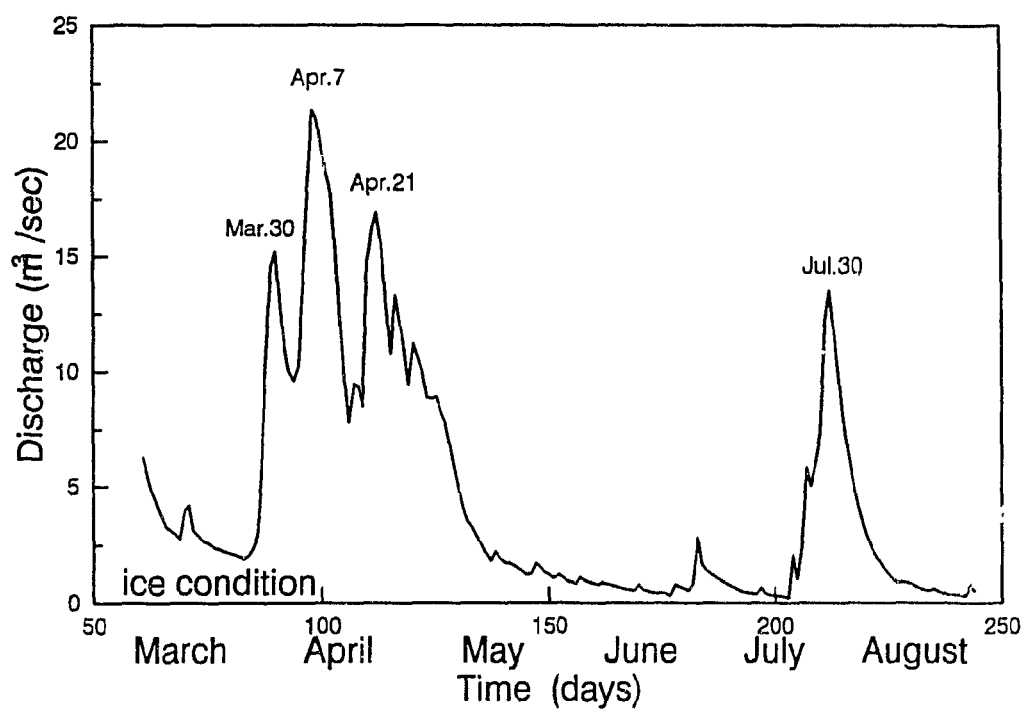


Fig. 2-4

near the bottom (bottom nepheloid layer), developed as the surface water warmed and the thermocline intensified. The position of the clear water minimum changed slightly during the study, but remained in the range of 20 m to 40 m depth. Light-scatter in the bottom nepheloid layer became more intense and increased in depth range until the end of June. Profiles of July 29 and August 16 show a reduced light-scatter at the mid-depth minimum and reduction in thickness of the bottom nepheloid layer.

To examine the temporal stability of the observed patchiness, the system was deployed 5 times within 105 minutes on May 16 (Fig. 2-5). The resulting profiles were very similar, although surface light-scatter above 15 m did show some change. Light-scatter in very surface water (<3m) might be affected by the research vessel.

POC and SPM concentration

Profiles of SPM and POC concentration, usually from 6 depths, are shown in Fig. 2-6. These profiles typically feature high SPM concentration in the surface and a decreasing concentration with depth. An exceptionally high SPM concentration measured at 35 m on June 21 included many zooplankton. The nepheloid layer, clearly detected in the light-scatter profile, was less apparent in the SPM concentration profile. Since light-scatter at 30° is more sensitive to small particles ($\leq 5\mu\text{m}$), this might suggest that particles in the bottom nepheloid layer are predominantly small size grains.

Surface SPM concentration (5 m) ranged from 0.8 mg/l measured on April 13, to 2.63 mg/l measured on August 16 and varied considerably with time (S.D.=0.54 mg/l). In contrast, in the mid-depth region (20 m), the SPM concentration was low

Fig. 2-5 Repeated measurements of sigma t and light-scatter within 105 minutes on May 16.

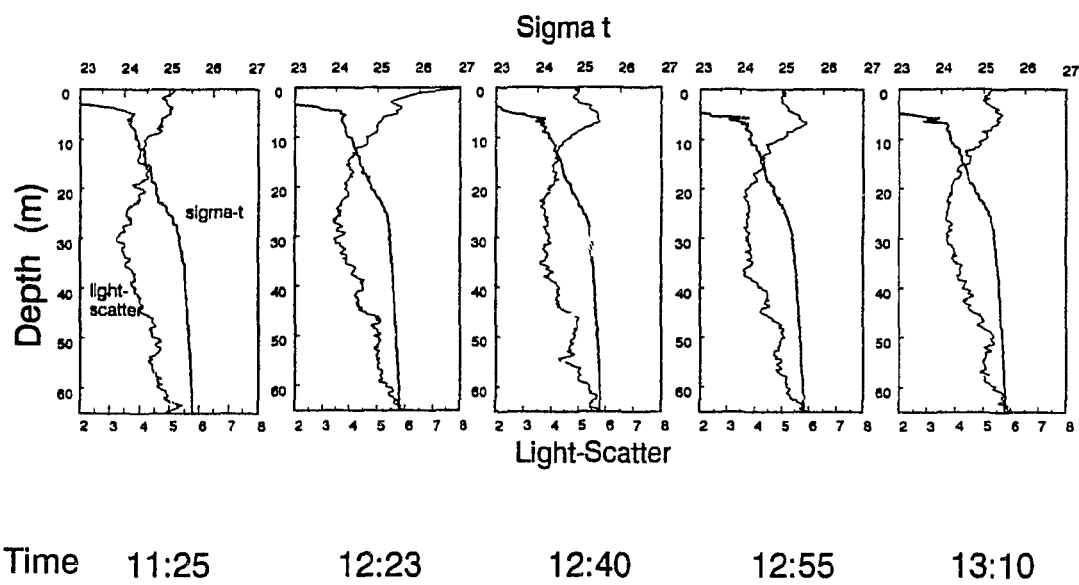


Fig. 2-5

Fig. 2-6 Time series of SPM and POC concentration profiles.
The numbers in parenthesis are days of the year. SPM
concentration at 5m on Aug. 16 was 2.63 mg/l.

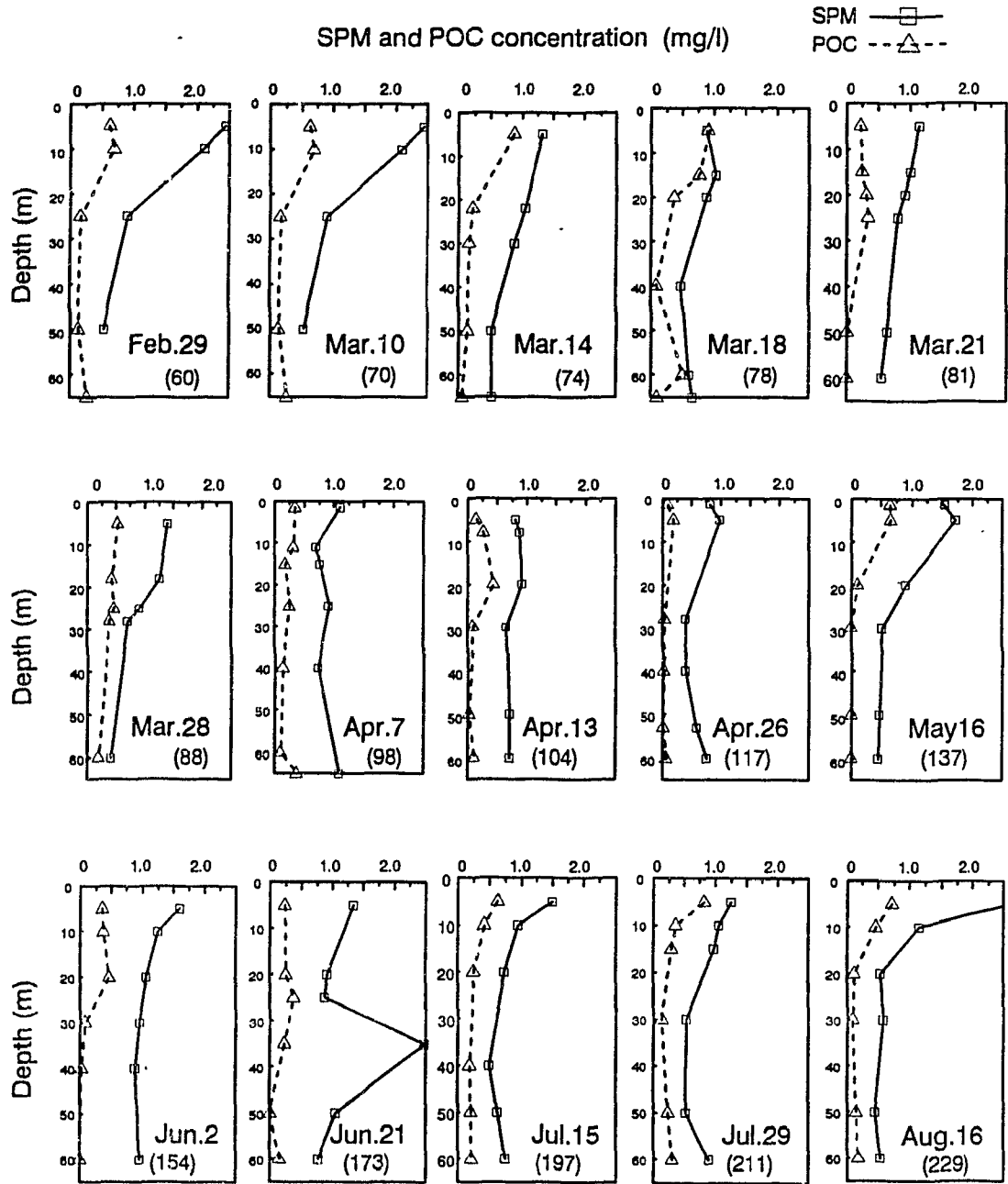


Fig. 2-6

and less variable, ranging from 0.5 mg/l to 1.07 mg/l (S.D.=0.16 mg/l). The bottom water SPM concentration was between 0.42 mg/l and 1.09 mg/l with a S.D. of 0.18 mg/l.

In general, the POC concentration was high in the surface water and low in the middle and deep water. In the middle and/or bottom water samples of March 21, April 26, May 16, June 2 and June 21, the POC concentration was below the detection limit of the method. Surface POC concentration varied from 0.144 mg/l to 0.914 mg/l (S.D.=0.274 mg/l). At 20 m depth, POC concentrations were within the range of 0.108 mg/l to 0.472 mg/l (S.D.=0.133 mg/l). Although the bottom water (60 m) sample of March 18, corresponding to the settling and the mixing down of surface diatoms by a storm, had a high POC concentration (0.503 mg/l), other bottom sample concentrations were less than 0.295 mg/l.

Chl.a concentration

The highest Chl.a concentration, 40.88 $\mu\text{g/l}$ was observed at 4 m depth on March 11, coinciding with the peak of the spring bloom (*Chaetoceros* spp.) which occurred on March 10 and 11 (Fig. 2-7). A typical Chl.a concentration profile for the spring bloom period was observed on both days (Fig. 2-8). In the surface mixed layer, upper 10 m of the water column, the Chl.a concentration was high and uniform, while below the pycnocline the Chl.a concentration decreased rapidly with depth. This profile changed as the bloom proceeded. The surface concentration of Chl.a declined and the surface peak became less well defined. During the same period,

Fig. 2-7 Surface (5m) Chl.a concentration change with time.

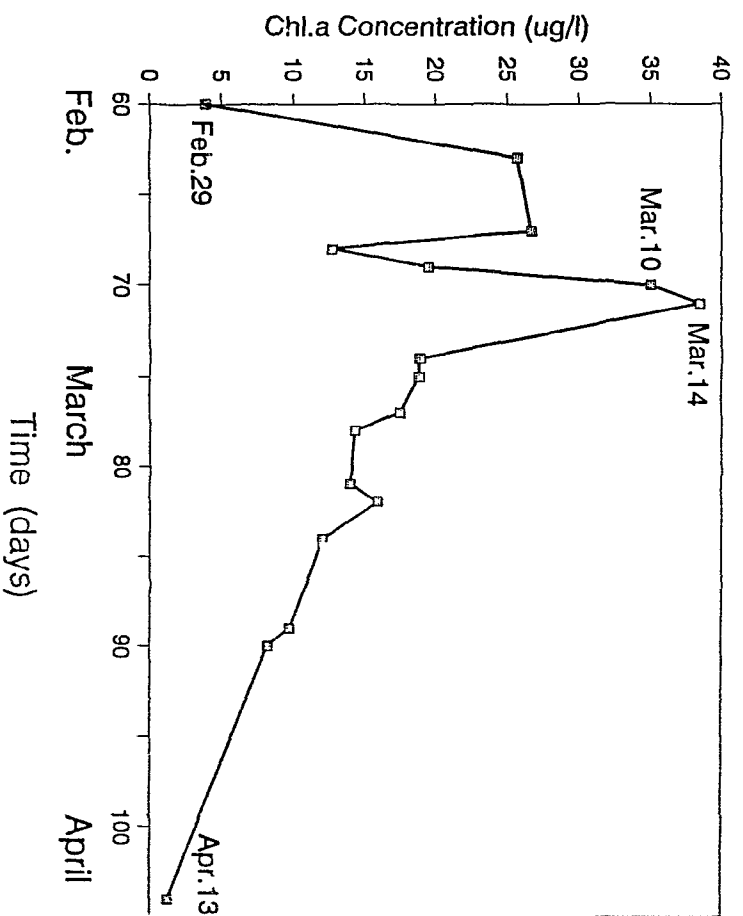


Fig. 2-7

Fig. 2-8 Time series of Chl.a profiles. Mar. 10 was the bloom peak.

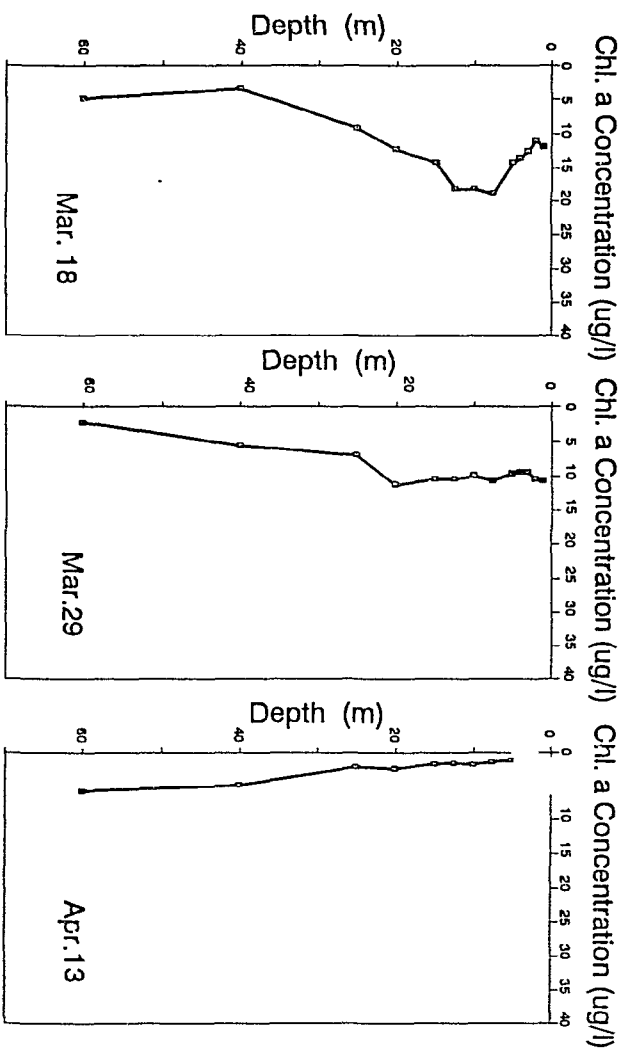
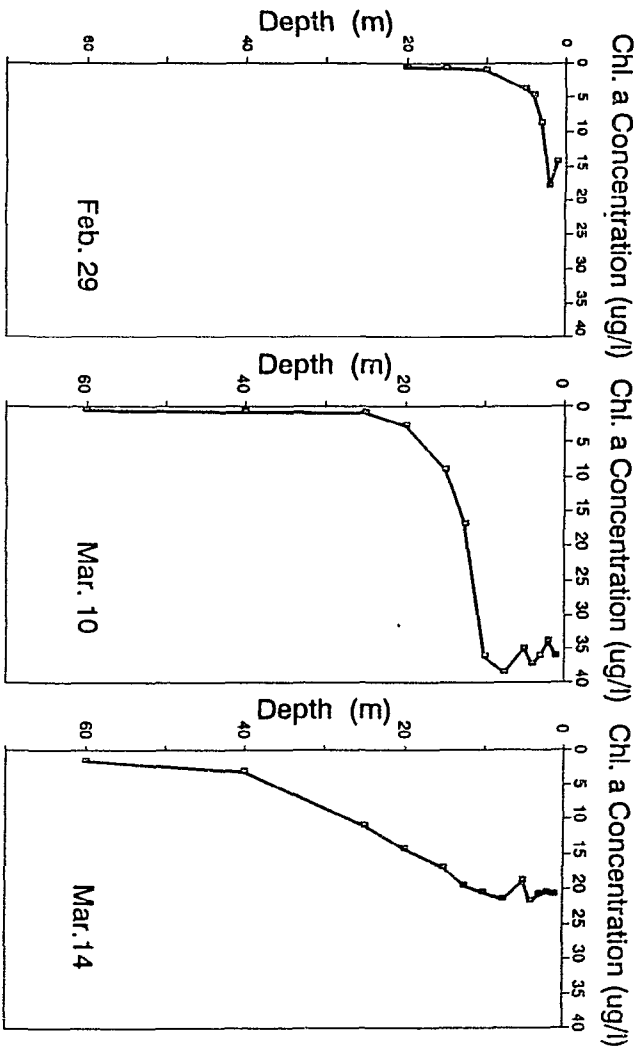


Fig. 2-8

the middle and deep water Chl.a concentration increased. On March 10 the concentrations of Chl.a at 40 m and 60 m were 0.881 $\mu\text{g/l}$ and 0.586 $\mu\text{g/l}$ respectively. By April 13 the concentrations at these depths had increased to 4.915 $\mu\text{g/l}$ at 40 m and 5.793 $\mu\text{g/l}$ at 60 m.

Microscope observation

Particles collected from specific depths, chosen from the light-scatter profiles, were examined under a microscope. Morphological change of particles with depth as well as with time was observed. Photographs were taken from April 7 to June 2. Malfunction of the microscope-camera system precluded further use, however, microscope observation was continued through the sampling period.

At the beginning of the bloom, particles in the surface water were composed of small diatom chains ($\approx 40 \mu\text{m}$), while neither diatoms nor their aggregates were observed below the thermocline. On March 18, long and tangled diatom chains were found at mid-depth (20 m, $>100 \mu\text{m}$) and in deep water (50 m, $>200 \mu\text{m}$), although small diatom chains were still dominant in the surface water. Faecal pellets appeared in the surface sample from April 7 (Fig. 2-9-1). After a week of rain, the surface sample of April 26 included small biogenic particles (Fig. 2-10-4). Long diatom chains, their aggregates and zooplankton, were found again in the surface water from May 16 (Fig. 2-11-1) and for the remainder of the sampling period. On June 2, a large aggregate ($\approx 1 \text{ mm}$), including phyto-detritus and faecal pellets, was observed in the sample from the top of the pycnocline (Fig. 2-11-4). In contrast, particles in the bottom water sample (50-60 m) changed from large biogenic particles, including

Fig. 2-9 **Inverted microscope photographs of suspended particles collected from (1) 1.5 m, (2) 15 m, (3) 25 m, (4) 40 m, and (5),(6) 60 m on April 7 (See Fig. 2-3). Scales in the photographs are 300 μ m. Dark shaded region in the centre of photograph (1) is a scratch on the microscope slide.**

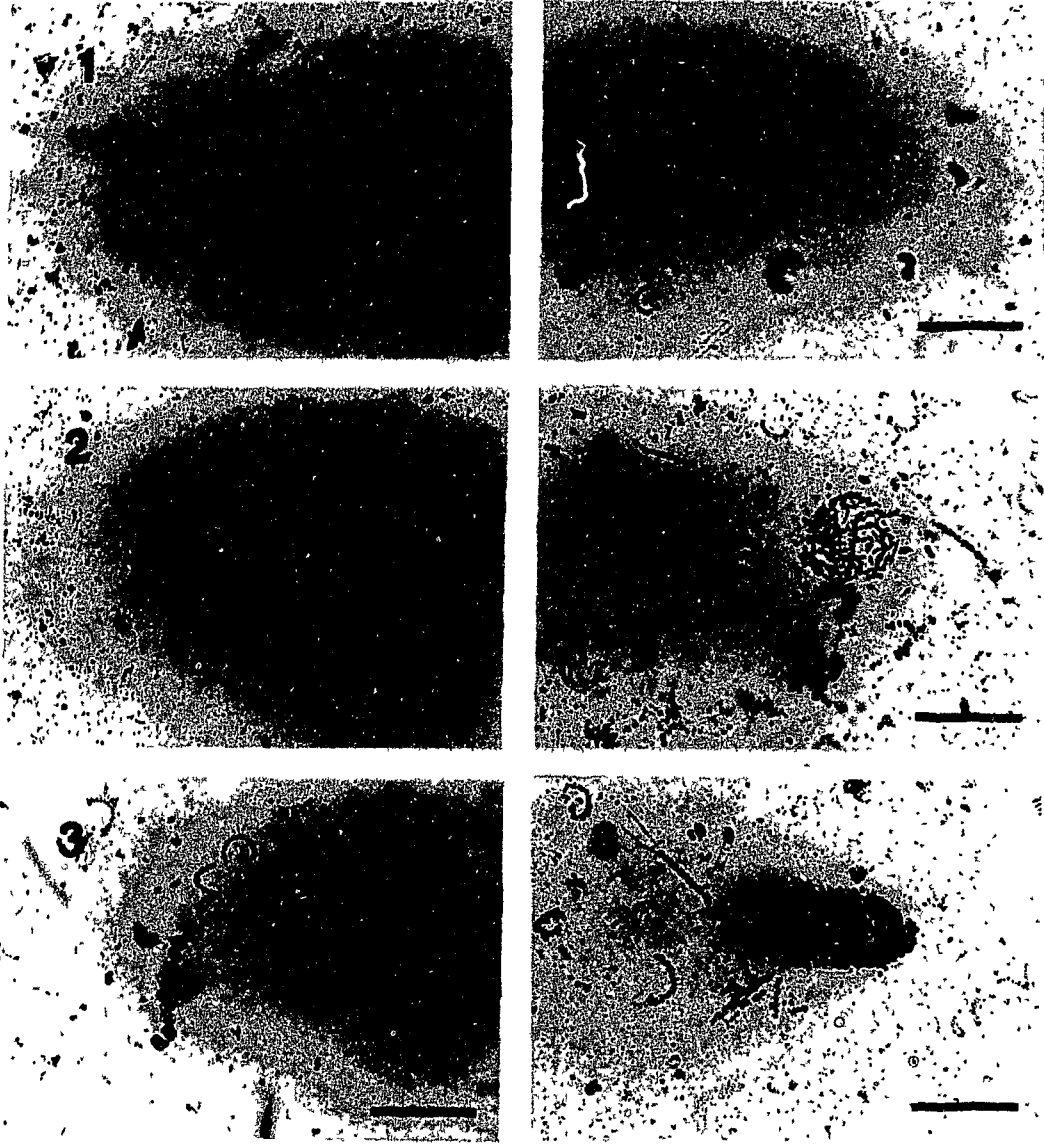


Fig. 2 - 9

Fig. 2-10 **Inverted microscope photographs of suspended particles collected from (1) 8 m, (2) 20 m and (3) 60 m on April 13. (4) 1.5 m, (5) 40 m and (6) 60 m on April 26. Scales in the photographs are 300 μm .**

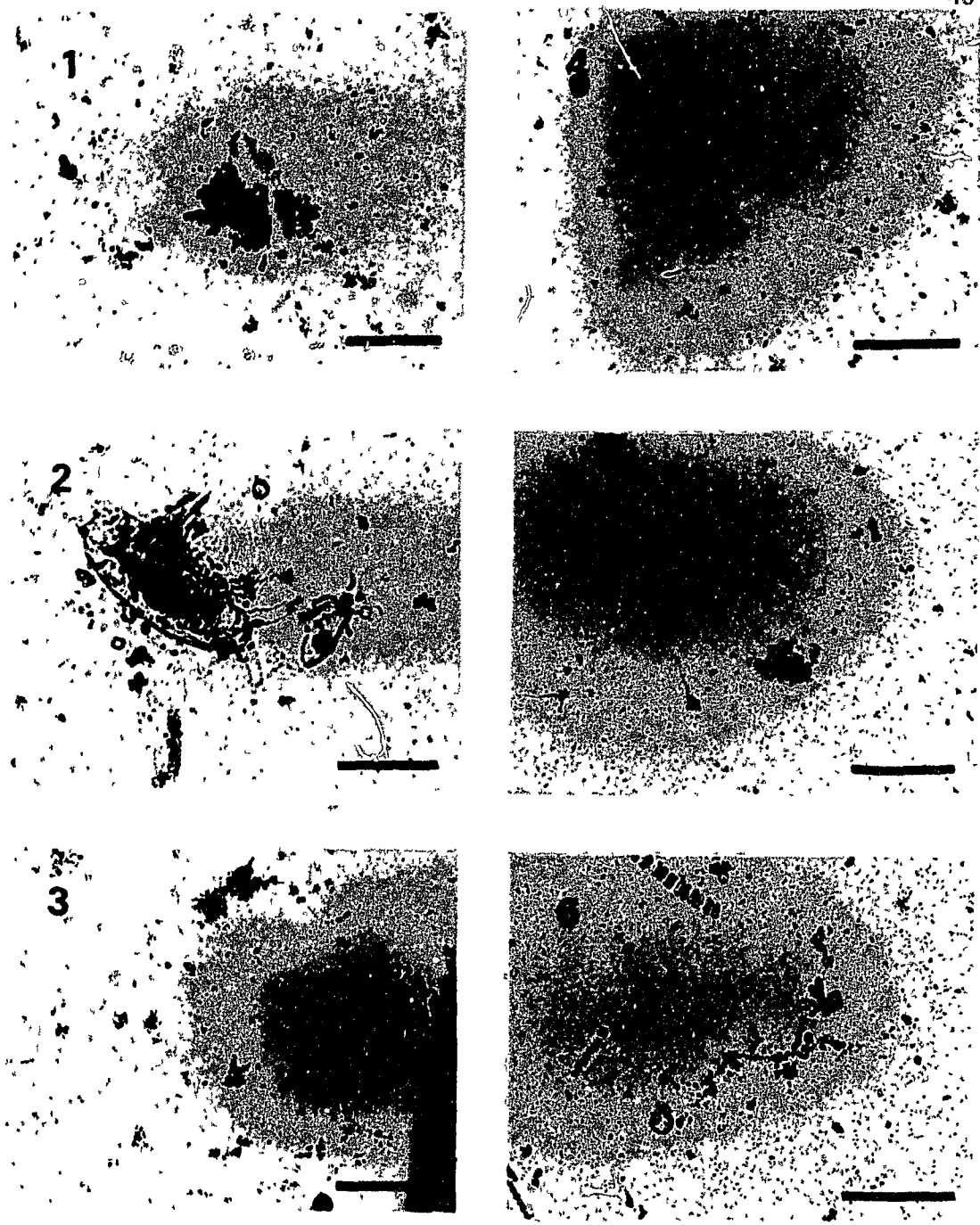


Fig. 2 - 10

Fig. 2-11 **Inverted microscope photographs of suspended particles collected from (1) 1.5 m, (2) 30 m and (3) 60 m on May 16. (4) 5 m, (5) 10 m and (6) 60 m on April 26. Scales in the photographs are 300 μm .**

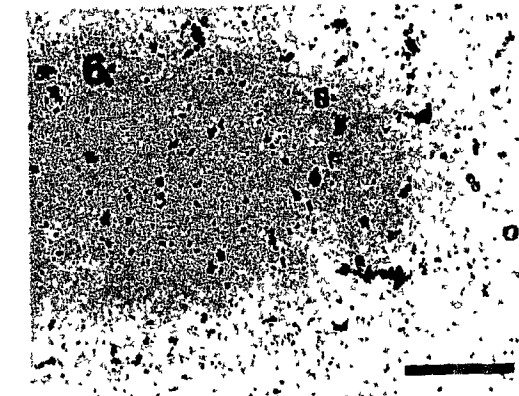
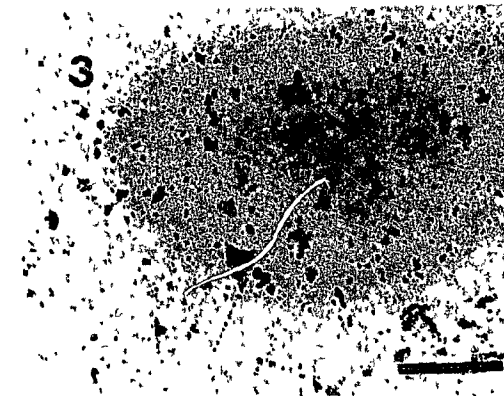
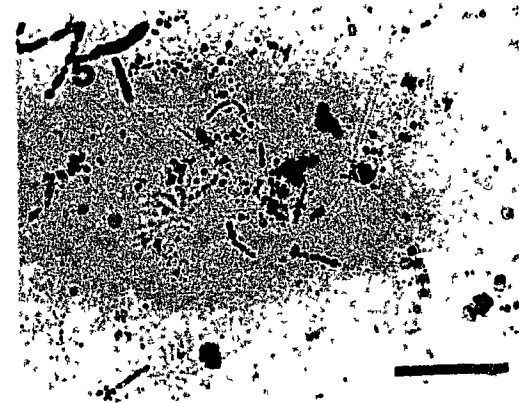
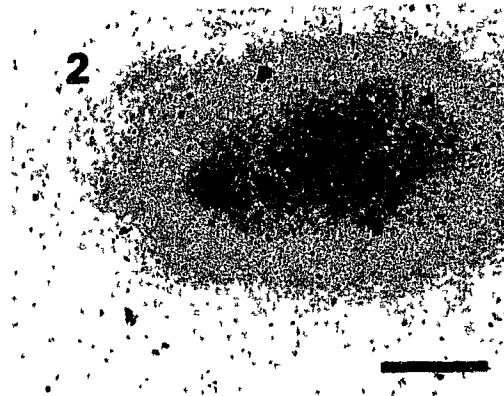
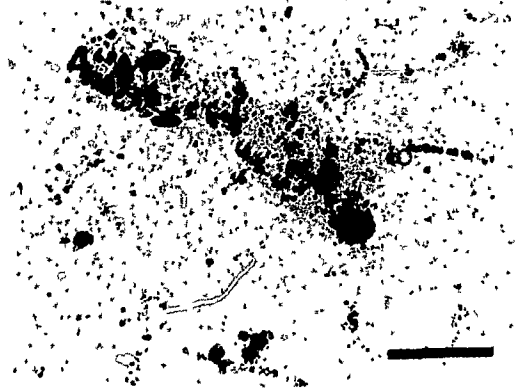
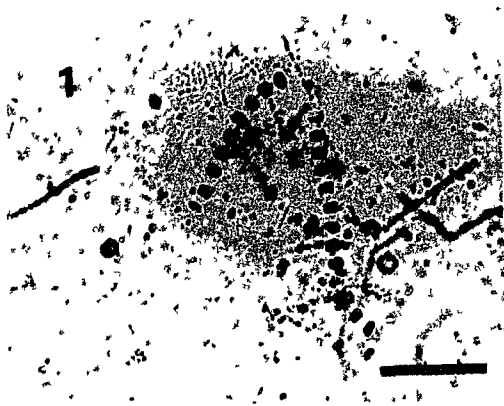


Fig. 2 - 11

tangled diatom chains ($>200 \mu\text{m}$) and faecal pellets ($> 500 \mu\text{m}$) on April 7 (Fig. 2-9-5,6), April 13 and 26 (Fig. 2-10-3,6), to smaller and more degraded particles as the bottom nepheloid layer became thicker and stronger (Fig. 2-11-3,6). Large aggregates in the water column are very fragile and tend to disaggregate during sampling (Kranck and Milligan, 1988), therefore these observations are not representative of size or shape of particles *in situ*. However, aggregates in the bottom nepheloid layer that settle during or immediately after the surface bloom are more robust and harder to disaggregate than those found later in the season. Particles at mid-depth (20-40 m) did not always reflect the surface water sample in size and morphology (Fig. 2-9-3,4, Fig. 2-11-2) or in size (Fig. 2-10-5).

Heterogeneity of the vertical particle distribution was observed on April 7. Samples corresponding to distinct peaks of light-scatter in the April 7 profile corresponded to particles of differing characteristics (Fig. 2-9). In the surface (1.5 m) peak, aggregates of small mineral grains and small faecal pellets ($<150 \mu\text{m}$) were dominant. Particles from the second peak of light scatter, 15m deep, included many ciliates and some short diatom chains. In the third light scatter peak at 25m, particles were mainly diatom chains longer than those in the 15m sample along with bigger faecal pellets ($\approx 300 \mu\text{m}$). Particles forming the bottom nepheloid layer mainly consisted of entangled aggregates of diatom chains and single diatom chains. Big faecal pellets of more than $500 \mu\text{m}$ in size were also found in the bottom samples.

DISCUSSION

Settling velocity of biogenic particles is reported to be in the range of 10 - 200 m/day as determined from laboratory settling experiments of aggregates of *Chaetoceros* spp., the dominant spring bloom species in Bedford Basin (Azetsu-Scott and Johnson, 1992) and from *in situ* observations in coastal water (Aldredge and Gotschalk, 1989). Kranck and Milligan (1988) reported that flocculated diatoms appeared in the near bottom water within 3 days of the bloom in Bedford Basin, and Aldredge and Gotschalk (1988) observed flocculation in as little as 24 hours in coastal California waters. Since depth of the water in this study site is 70 m, one week is sufficient for a bloom to settle to the bottom. Although the profile of March 18 (about one week after the bloom peak) featured a small bottom nepheloid layer and diatom chains were observed in the bottom water under the microscope, the steady and strong peak of light scatter in the bottom water appeared at the beginning of April (Fig. 2-3). Photographic evidence for the deposition of a spring bloom and subsequent resuspension - about 2 weeks after the phytodetritus arrived at the sea bed has been described for the bottom of the continental slope in the North Atlantic (Lampitt, 1985). In this study, the bottom nepheloid layer did not develop until the beginning of April, while aggregates of tangled diatom chains were observed in the bottom water one week after the peak of the surface bloom. Thus, in this study the time lag between sinking of the bloom and bottom nepheloid layer formation was 2-3

weeks. No clear reasons for this time lag between the arrival of phyto-detritus on the seabed and resuspension has yet been demonstrated, however, Lampitt (1985) suggested that the degradation of settled detrital aggregates is necessary for erosion to occur. There are numerous studies on the effect of benthos on sediment transport (for example, Nowell *et al*, 1981; Eckman *et al*, 1981; Jumars and Nowell, 1984). Studies on seafloor stability in Long Island Sound (Rhoads *et al*, 1978; Yingst and Rhoads, 1978) showed that the seasonal change of critical rolling and saltation velocities, which is lowest in early summer, is a result of destabilization of the sediment surface by the reworking activities of meio- and macrofauna that break up the boundary layer of aggregates. Hargrave (1978) showed that biological respiration by sediment cores from Bedford Basin increased towards the summer and reached the highest value in early July. He suggested that this reflected delayed incorporation of freshly deposited phytoplankton in the benthic food web. There is no quantitative evidence for degradation of phytodetritus on the sea bed, but microscope observation of bottom water samples shows some morphological changes of particles in the nepheloid layer (Fig. 2-9-10). Further, POC concentration decreased and fell below the detection limit on May 16 and June 2. These results may support the mechanism suggested by Lampitt (1985), i.e., resuspension occurs only if the sediment-water interface is composed of a detrital layer and only if the detrital aggregates have degraded somewhat. At this study site, however, the nepheloid layer existed longer (over 3 months) than was reported for the open ocean (about 20 days at the deep sea-floor)(Lampitt, 1985). This is primarily because in coastal waters surface

biological activity is much higher than in the open ocean and consequently more material settles to the bottom. Also, nutrients are less limiting than in the open ocean and thus, surface biological activity is still high even after the spring phytoplankton bloom. At this study site Chl.a concentration stayed within a range of 2.5 to 8.5 $\mu\text{g/l}$ through the summer (Irwin, 1991).

Changes in thickness and composition of the bottom nepheloid layer with time were also found in this study. The bottom nepheloid layer became thicker and reached 30 m above the bottom on June 21, followed by clearing at mid-water and thinning of the bottom nepheloid layer. Three factors affecting formation of the nepheloid layer can be identified. The first is the quantity of "rebound" materials, i.e., particles that have settled through the water column but have not become incorporated into the sediment (Walsh *et al.*, 1988). The second is the energy to resuspend particles. The third possible factor is the decrease of particle settling velocity in the deep water due to the increase of water density with depth. The quantity of rebound materials increases with surface biological activity and with high fluvial input from the end of March to the end of April (Fig. 2-4). Increase of rebound material, along with some degradation of particles, contributes to the quantity of resuspendable materials forming the bottom nepheloid layer. Lampitt (1985) suggested tidal currents as the source of energy to resuspend particles. In this study the relationship between tidal mode and strength of the bottom nepheloid layer was not clear. Low frequency intrusion events are the primary mechanism for the replacement/renewal of bottom water in Bedford Basin (Ruddick, 1986). Two

intrusion events were observed from sigma t change on March 18 and April 26 (Fig. 2-12) and were manifest in high light-scatter between 50 m and 60 m on both days. There were no other intrusion events during the study. The probable energy sources in this study site include vertical mixing by tidal friction acting on the bottom water at the sill depth (20 m), wind mixing that is larger than that due to tidal friction at this sampling station, and seiching. None of these three energy sources appeared to increase during the period of bottom nepheloid layer formation (April to July). Accumulation of particles in the deep water caused by decreased particle settling velocity in higher density deep water is one possible mechanism of bottom nepheloid layer formation. However, sigma t in the deep water decreased slightly towards the summer and consequently this effect does not explain the development of the bottom nepheloid layer in this study. Therefore, the increase in resuspendable material on the sea bed, originating from surface biological activity, must be the most important among the three possible factors for development of the bottom nepheloid layer in this study.

Integration of light-scatter in total (0-60 m) and in three layers (0-20 m, 20-40 m and 40-60 m) was calculated for the results (Fig. 2-13). Although there is scatter in the linear relationship between light-scatter and SPM concentration, integrated light-scatter with depth gives an approximation of the change of particle mass distribution in the water column with time. Highest total light-scatter was observed on June 21 (173rd day of the year) corresponding to the existence of the thickest bottom nepheloid layer. This was followed by a decreasing total light-scatter. At the

Fig. 2-12 Σt change with time in the deep water, as an indicator of intrusion events. Note that there are two peaks in 50 m and 60 m sample on March 18 and April 26.

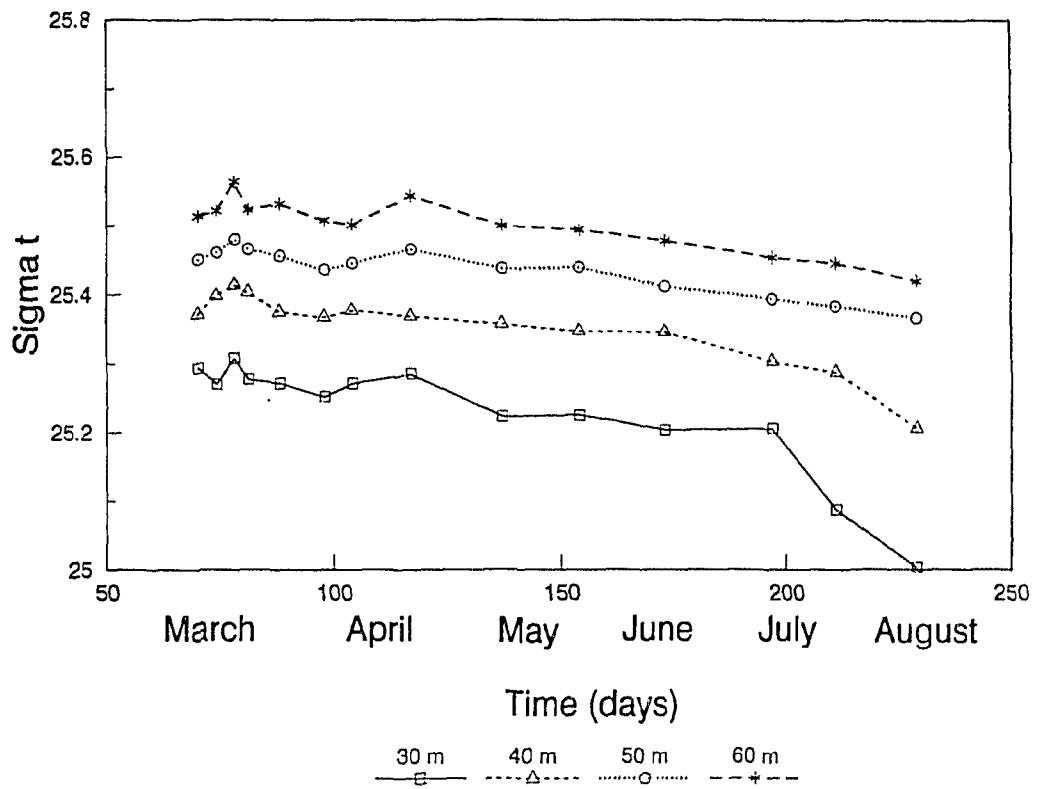


Fig. 2-12

Fig. 2-13 **Integration of light-scatter in total (0-60 m) and three layers (0-20 m, 20-40 m and 40-60 m) of the water column.**

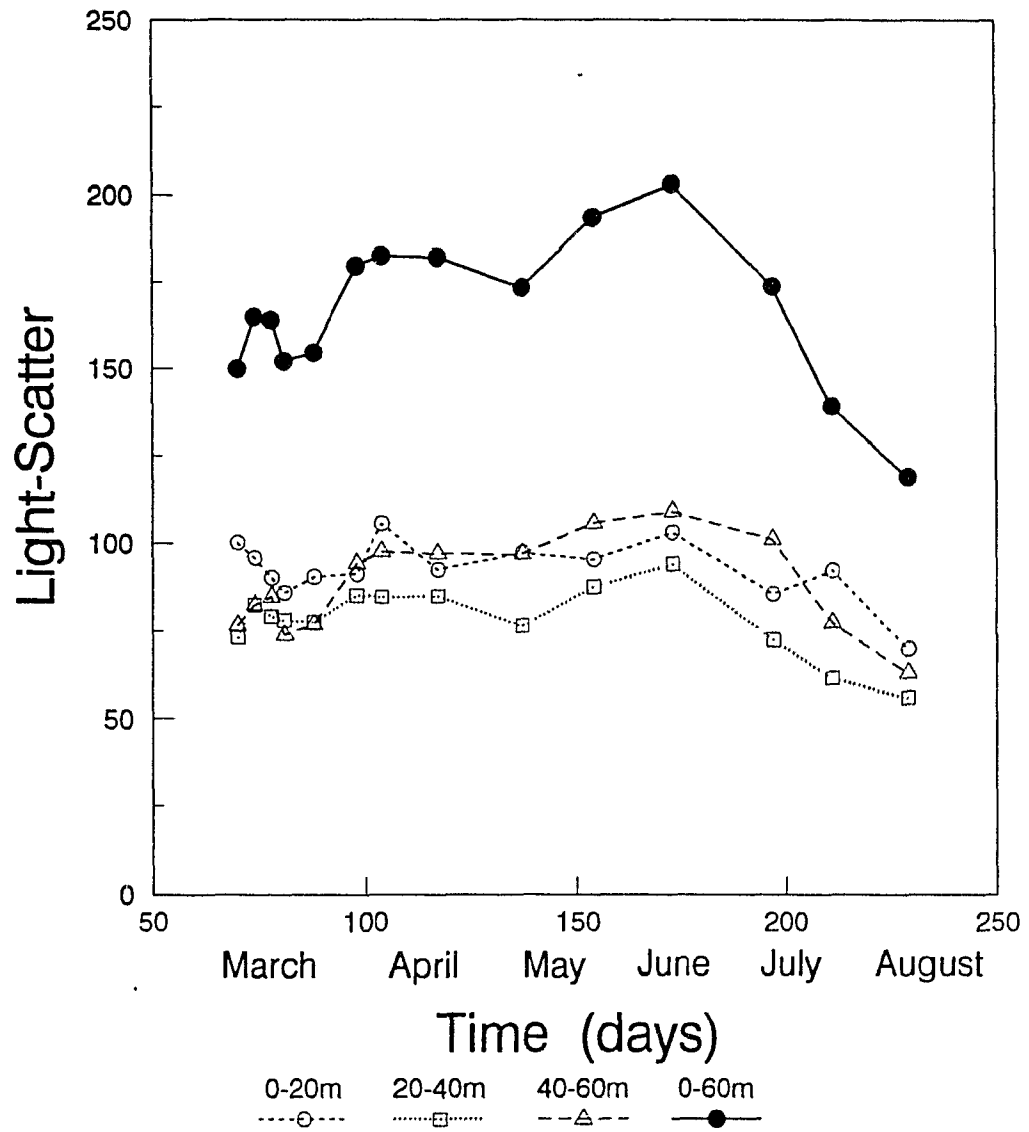


Fig. 2-13

beginning of the bloom, the bottom light-scatter was lower than the surface light-scatter. As the bloom proceeded, the bottom light-scatter increased and during May to mid-July was higher than the surface light-scatter. Where the linear relation between light-scatter and SPM concentration is strong and changes little with depth, such as in the open ocean, particle flux in each layer can be calculated using the time series of integrated light-scatter. However, this approach does not seem reasonable in this study.

The composition of particles in the bottom nepheloid layer varied from biogenic aggregates to small grain size particles. Many entangled diatom chains ($\approx 300 \mu\text{m}$) and faecal pellets ($>500 \mu\text{m}$) were observed in the 50-60 m samples on April 7 and 13 (Fig. 2-9, 3-9). In the 60 m samples on April 26 and May 16, the particle size is smaller and fewer diatom aggregates were identified. POC concentration decreased and fell below the detection limit on May 16 and June 2, when microscope observation revealed that samples were composed entirely of small grains. This change in composition might be caused by one or both of the following:

- (1) decomposition of organic material of settled biogenic particles and
- (2) stratification of suspended particles. Since a specific depth (60 m) was sampled, the vertical distribution of particle composition within the nepheloid layer is not clear. Active decomposition of organic matter by a large microbial community has been reported for Halifax Harbour (Novitsky, 1990), and thus decomposition of settled organic matter is strongly suggested. However, particle stratification may also be an important factor. The height from the bottom that particles reach by resuspension is a function of turbulence intensity or upwelling speed and particle gravitational

settling. This latter parameter is affected by particle size, density and surface drag, and therefore less dense, fluffy, biogenic particles and dense, small-grain, inorganic particles with relatively smooth surfaces can be stratified within a nepheloid layer. In this study, however, I do not have clear evidence for this stratification.

Patchiness in the particle distribution is caused by both biological and physical characteristics of the water mass. The former includes growth, mortality, sinking, and migration rate of plankton and their predators (Parsons *et al.* 1984). The latter includes the density and turbulence structures of the water mass - the effects of which on the particle distribution are not yet well known. When the pycnoclines existed in surface water, high light-scatter was always observed on top of the pycnocline. However, below the pycnocline, high light-scatter did not appear to have any relationship with the density structure of the water column. For example, on April 7, there were light-scatter peaks at 15 m and 25 m, while the density profile showed no discontinuity at either depth. Moreover, bottom nepheloid layers were observed associated with water of homogeneous density.

Change of particle characteristics with depth was also observed. Microscope photographs and POC concentration measurements on April 7 showed that each peak in light-scatter represented a different type of particle (Fig. 2-3, Fig. 2-6 and Fig. 2-10). In the surface water (1.5 m) aggregates of small mineral grains and small faecal pellets (<150 μm) were dominant. Particles from the second peak of light scatter, 15 m deep, included many ciliates and some short diatom chains. In the third light scatter peak at 25 m, POC concentration is high and particles were larger faecal

pellets ($\approx 300 \mu\text{m}$) and diatom chains that were longer than those in the 15 m sample. In the bottom nepheloid layer particles consisted primarily of large faecal pellets of more than $500 \mu\text{m}$ in size and loosely entangled aggregates of diatom chains and single diatom chains - particles resulting in a high POC concentration. The time or spatial scale of this distinct patchiness are unknown, however, the observations of April 7 present an example of the heterogeneity of the vertical particle distribution.

CONCLUSIONS

Bottom nepheloid layer formation was observed through a time series study of the vertical distribution of suspended particles conducted during and after a phytoplankton bloom in a small coastal basin (Bedford Basin, Nova Scotia, Canada).

Measurements of continuous light-scatter profiles over a six month period using a recording backward light-scatter meter reveal that the bottom nepheloid layer in Bedford Basin is not a steady state but rather a dynamic phenomenon. At this coastal study site, the formation of the bottom nepheloid layer started 2-3 weeks after the settling of the surface spring phytoplankton bloom and persisted for a much longer period of time (3 months) than has been reported for the open ocean (20 days) (Lampitt, 1985). Microscope observations and POC measurements showed that the particles in the bottom nepheloid layer changed from intact diatom chains and large faecal pellets to more degraded small particles with lower POC concentrations as the bottom nepheloid layer became thicker and stronger.

Although the profiles of the particle distribution reflected episodic events such as fresh water river input and storm mixing, three general stages were observed through the period of the study. During the peak of the spring bloom in March, the water column was characterized by a high particle load in the surface mixed layer (0-8 m) with a smaller but uniform particle load in the middle and bottom water. The second stage (mid-April to July) featured bottom nepheloid layer formation (45-65

m) and a high particle load in the surface water with minimum light-scatter at mid-depth. In late July to August the bottom nepheloid layer thinned and the mid-water became progressively clearer.

High light-scatter was always observed on and in the pycnocline in the surface water; however, below the pycnocline, occurrence of light-scatter peaks was not related to the density structure of the water column. Rather, particle patchiness observed in mid-water often reflected the biological patchiness of different species of organisms or different stages of the same organisms. In deep water, accumulation and degradation of surface derived phytodetritus were the likely cause of bottom nepheloid layer formation. In this study, strong biological influence on the distribution of particles not only in surface but also in mid- and deep water was demonstrated.

Continuous light-scatter profiles also delineated the vertical extent and strength of particle patchiness in the water column. Characteristics of some of this patchiness were identified using conventional bottle sampling. These results illustrated that in this coastal basin the composition of particles varies with depth as well as with time.

Chapter Three

*An Intermittent Intermediate Nepheloid Layer
in Emerald Basin, Scotian Shelf*

INTRODUCTION

Continental shelves are regions where a high rate of terrigenous input (Ittekkot, 1988) and high primary productivity (Berger, 1989) introduce new materials to the margins of the ocean. The significance of the continental shelves in biogeochemical cycles, especially with regard to the global carbon cycle, has been recognized for the last ten years (Deuser, 1979; Berner, 1982; Walsh, 1991; Rowe *et al.*, 1986). The Scotian Shelf, which is located on the east coast of Canada, off Nova Scotia, is one of the broadest (200 km) continental shelves in the world. The topography of the shelf is complicated by the presence of numerous shallow banks and deep basins. While high biological productivity in the surface waters on the shelf has been reported (Fournier *et al.*, 1977), large areas of the shelf show little net deposition (Piper, 1991). However, fine-grained, pelagic sediment that is characterized by high organic carbon, nitrogen and carbon/nitrogen ratio (Pocklington *et al.*, 1991; Buckley, 1991) and enhanced benthic biological activity (Grant *et al.*, 1991) have been reported in the basin areas. While storm induced sediment transport of 0.35 mm sand on the Shelf was observed and predicted through a model of resuspension (Amos and Judge, 1991), there is little information about the transport processes affecting particles in the water column.

Optical methods for continuously measuring the vertical particle distribution reveal the non-uniform distribution of particles in the water column. High particle

concentration is usually observed in the surface mixed layer and originates from biological activity and from the terrigenous input through rivers, wind-blown dust and in some polar coastal areas, from glaciers. A decrease in particle concentration usually occurs below the surface mixed layer and forms the "clear-water minimum" that is due to particle dissolution, decomposition and consumption at mid-water depths (Biscaye and Eitrem, 1977). Bottom nepheloid layers have been reported both in coastal regions and in the deep ocean (e.g., Hollister and McCave, 1984; McCave, 1986; Gross *et al.*, 1988), and are formed by resuspension of particles from the seabed. These general features are often modified by biological and physical events - such as biological patchiness, water stratification and turbid water intrusion as a nephel signal in the mid-water column. Intermediate nepheloid layers have been detected on the continental slope off Oregon and Washington (Pak *et al.*, 1980a), off the west coast of Africa (Pak *et al.*, 1980b), off England (Dickson and McCave, 1986; Thorpe and White, 1988) and off submarine canyons (e.g., Gardner, 1989). These intermediate nepheloid layers are considered very important for transporting particulate matter from the ocean margin to the ocean interior (Murray, 1987). The distribution of particles in continental shelves is influenced by the high particle supply from coastal area and biological productivity in the surface water and resuspension of bottom sediment, which are transported by the mean circulation of the shelf and water exchange with the open ocean.

As a part of the "Halifax Transect" cruise, September 1986, salinity, temperature and light-scatter were measured in Emerald Basin. Measurements showed an

intermediate nepheloid layer at 180 m depth, 90 m above the bottom, while there was no change in density structure at this depth. At the same station seven months later, measurements for this station were taken to confirm the existence of this intermediate nepheloid layer, to determine its constancy and to identify the mechanism of formation.

MATERIALS AND METHODS

Emerald Basin is situated at the centre of the southeastern Scotian Shelf and is open to the slope through the Emerald Bank - LaHave Bank gap often called the "Saddle" (Fig. 3-1). Emerald Basin is 50 km wide, 100 km long and 270 m deep at the deepest point. Surficial geology and sediment stratigraphy of the Basin are well described by King (1970) and King and Fader (1986), and have recently been summarized by Piper (1991). Sampling stations are shown in Fig. 3-1. Station 1, in the deepest part of the Basin, is located at the site of one of the "Halifax Transect" hydrographic stations of Bedford Institute of Oceanography, and consequently there is a long term record of the water properties (Drinkwater and Taylor, 1982). Station 2 is located on the western flank of the Basin, 30 km north-northwest of station 1. Station 3 is in the northern end of the Basin, 63 km northeast of station 1. Station 4 is in the adjacent basin, which is located north of and is connected to Emerald Basin through a narrow channel 180 m deep. Stations 5 and 6 are at the east and

Fig. 3-1 Study area. Station 1 is at the deepest point of Emerald Basin (270 m). Station 1-3, 5 and 6 are in Emerald Basin and Station 4 is in the adjacent basin.

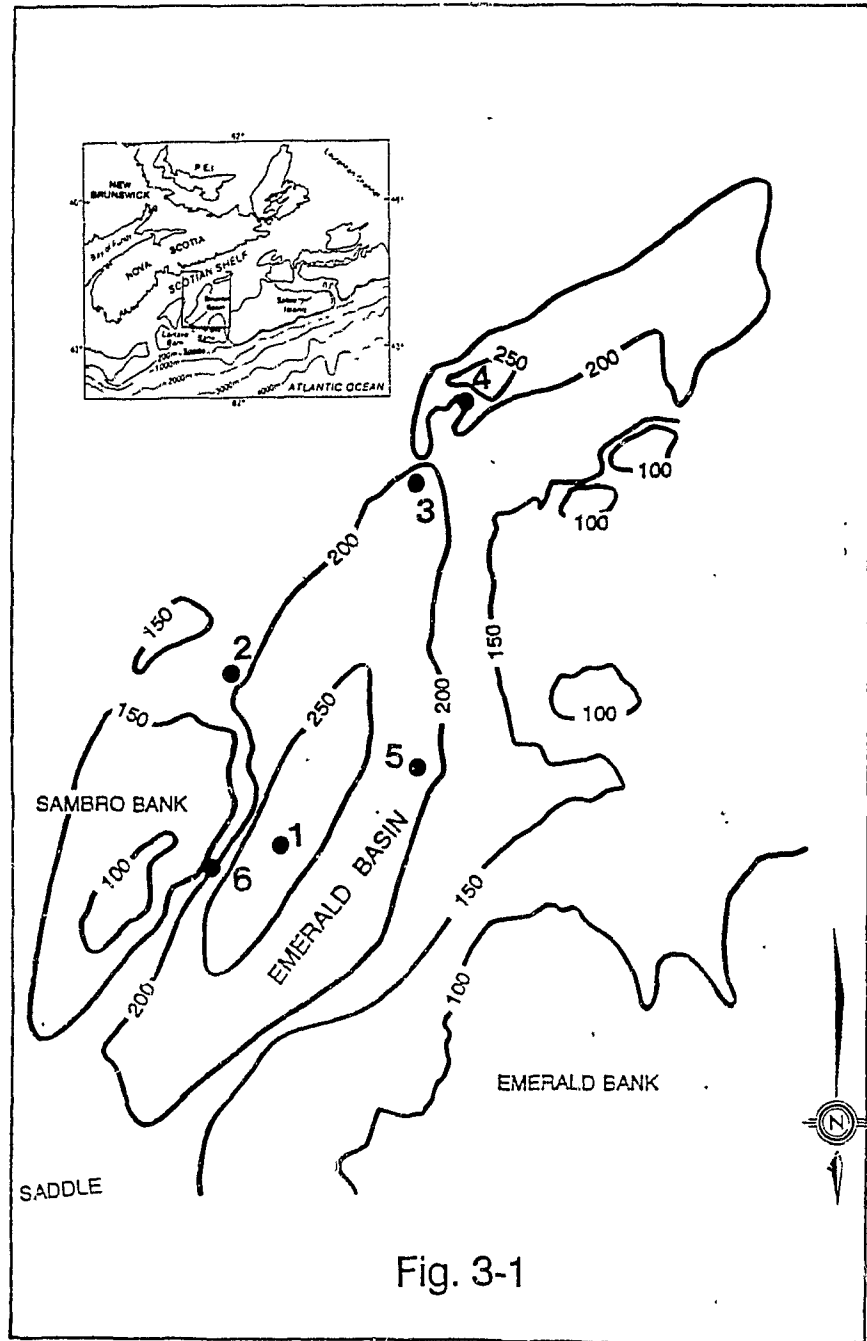


Fig. 3-1

west slopes of Emerald Basin, respectively.

Measurements were made, aboard *C.S.S. Dawson* April 22 to 26, 1987, using a recording backward light-scattering meter for particle distribution measurement (Johnson and Wangersky, 1985) attached to a CTD (Guildline 8709) for salinity and temperature measurement. The condition of the instrument is changed from the study in Chapter Two (baseline of the instrument is lower than 2.88). Variance of the light-scatter by noise is 0.004 (estimated as shown in appendix I). Water samples for Chl.a measurement were taken by rosette sampler at depths selected on the basis of the light-scatter profile. There is no measurement of SPM concentration available in this study. Calibration of the light-scatter measurements and SPM concentration in Chapter Two (Fig. 2-2) might be referred, although the relationship obtained in Fig. 2-2 will not be applied directly to this area.

OBSERVATIONS

A time series of depth profiles of light-scatter, salinity and temperature were taken from April 22 to 24 and April 26 at station 1 (Fig. 3-2). Some profiles show a weak maximum in light-scatter just above the pycnocline (80-100 m) (Fig. 3-2a,b and e), but these are not as strong as reported elsewhere for slope regions (Therpe and White, 1988; Dickson and McCave, 1986; Pak *et al.*, 1980a,b). A bottom nepheloid layer was observed in all profiles (except Fig. 3-2b, for which data were

Fig. 3-2 Vertical profiles of salinity, temperature, sigma t and light-scatter at Station 1 (270 m deep). Sampling time (local time) and day is **a**, 1:30, April 22; **b**, 10:00, April 22; **c**, 19:36, April 22; **d**, 15:45, April 23; **e**, 19:50, April 23; **f**, 9:30, April 24; **g**, 1:35, April 26, respectively. The bottom nepheloid layers appear in all the profiles except **b** (malfunction of the instrument below 200 m). Arrows show the appearance of the intermediate nepheloid layers in **a**, **d** and **f**.

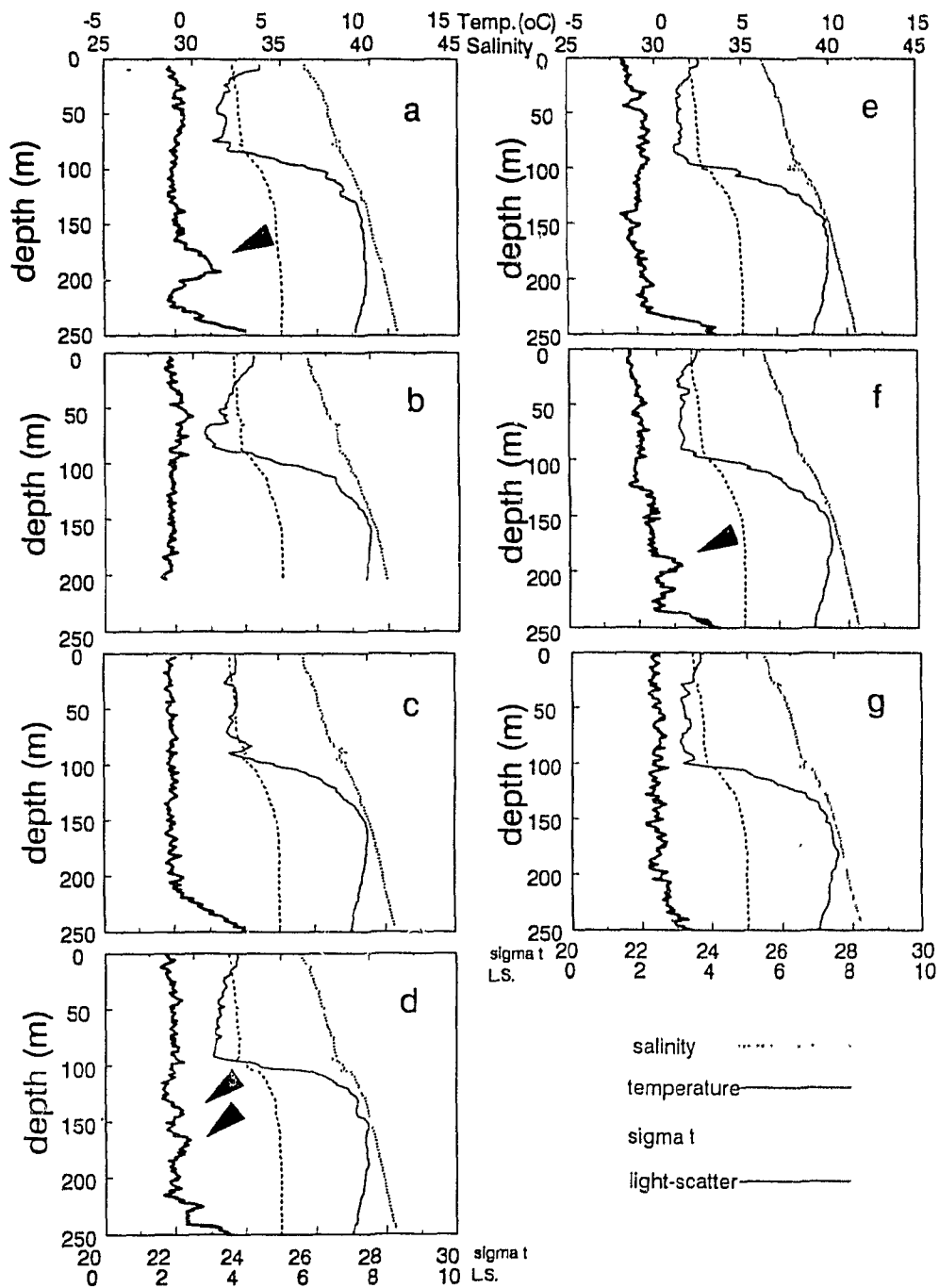


Fig 3-2

taken only to 200 m because of a malfunction of the instrument). A distinct feature of the light-scatter profiles is the intermittent occurrence of an intermediate nepheloid layer. A strong (30 m thick) nephel signal was observed on the first day of sampling at a depth of about 180-190 m (Fig. 3-2a). Thirty eight hours later, two small peaks at 140 m and 170 m (Fig. 3-2d) were recorded. At 56 hours, a small narrow peak appeared at 190 m depth (Fig. 3-2f). Other possible nepheloid layers include a weak, broad light-scatter peak at 130-150 m in Fig. 3-2f, and 130-150 m and 160-170 m in Fig. 3-2g, but these are not as distinct as other nephel signals. Light-scatter profiles from the five other stations are shown in Fig. 3-3. Intermediate nepheloid layers were observed at 130 m depth (40 m thick) at station 4, which is located in the adjacent basin north of Emerald Basin; at 170 m (40 m thick) at station 5 and as a small peak at 170 m at station 6, in Emerald Basin. All of the intermediate nepheloid layer signals in Emerald Basin occurred at a depth between 150 m and 200 m, except one (upper light-scattering signal, 140 m deep, in Fig. 3-2d).

Chl.a concentration, from samples taken at the time of the light-scatter measurements shown in Fig. 3-2a, shows a strong peak at around 30 m with relatively high concentration ($>1 \mu\text{g/l}$) at the top of the pycnocline ($\approx 80 \text{ m}$) (Fig. 3-4). There is also a small peak of Chl.a around 190 m depth that corresponds to the light-scatter peak.

Three water masses were observed from salinity and temperature profiles, and are in agreement with previous descriptions of this region: (1) Surface water flowing

Fig. 3-3 Vertical profiles of salinity, temperature, sigma t and light-scatter at Station 2-6. Bottom depth, sampling time and day in each stations are Station 2, 180m, 23:50, April 24; Station 3, 215 m, 10:35, April 25; Station 4, 195 m, 13:30, April 25; Station 5, 220 m, 21:50, April 25; Station 6, 188 m, 11:15, April 26, respectively. Station 4 is at the adjacent basin and others are at Emerald Basin stations. Arrows show the appearance of the intermediate nepheloid layers in Station 4, 5 and 6. The intermediate nepheloid layer in Station 4 is at the depth of 120-150 m, which is shallower than those observed in Emerald Basin stations.

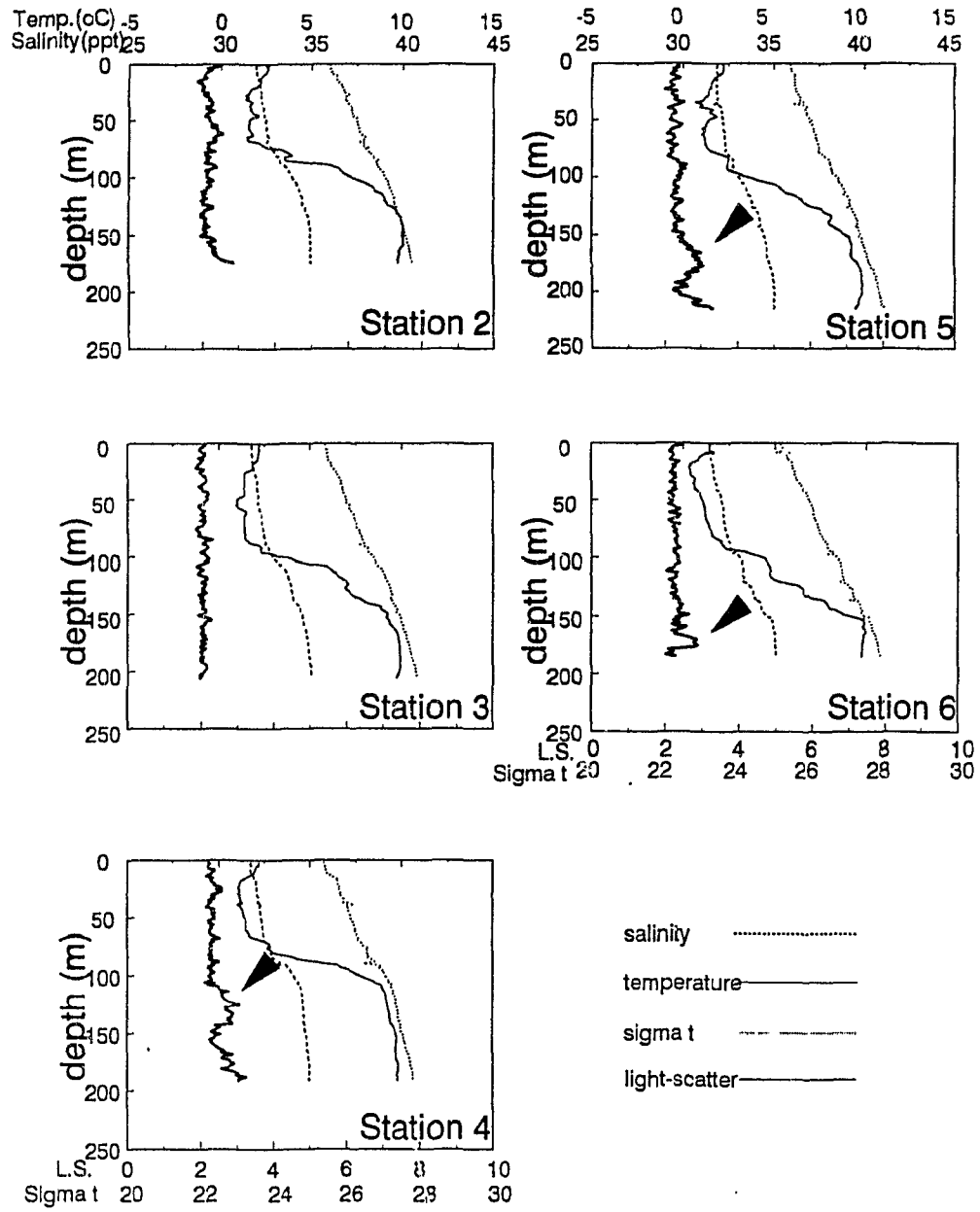


Fig. 3-3

Fig. 3-4 Chlorophyll a concentration at Station 1. Note a small peak at the depth 180 m that corresponds to the depth of the intermediate nepheloid layer in Fig. 2.

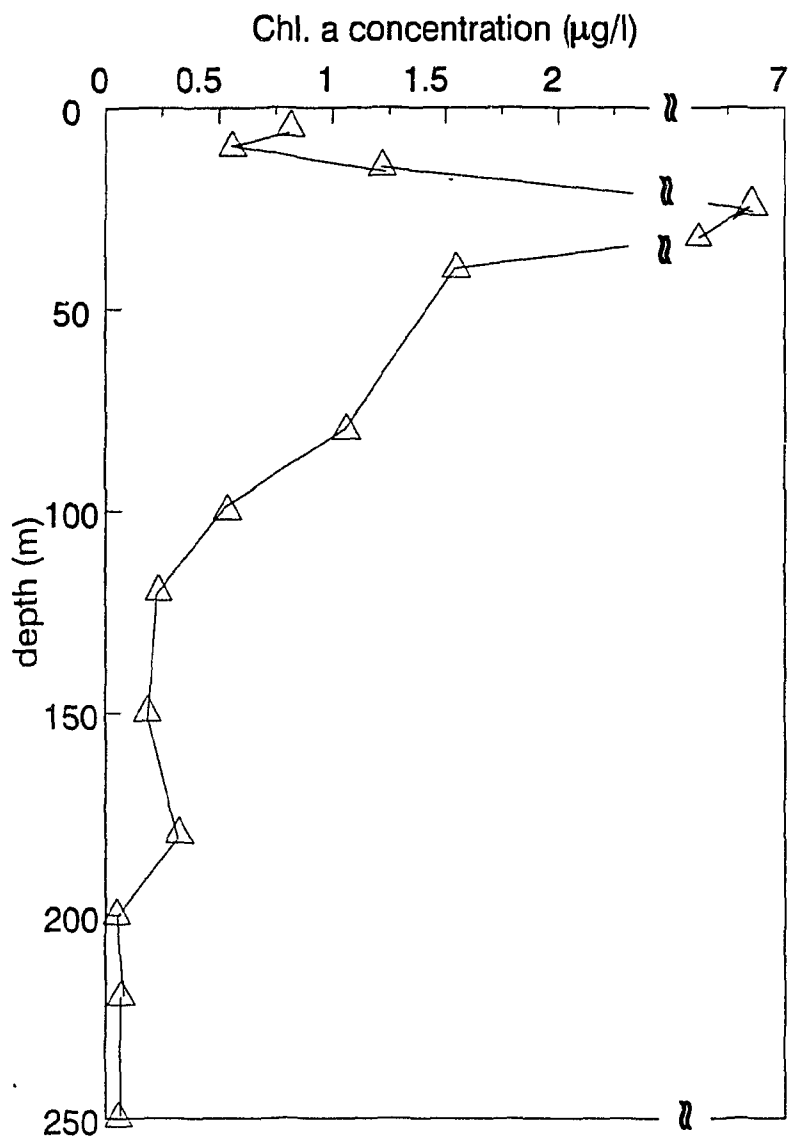


Fig. 3-4

from the Gulf of St. Lawrence on the western side of Cabot Strait; (2) Subsurface water from the Cabot Strait; (3) A warm saline bottom layer that is characteristic of slope water (Warner, 1970; Houghton *et al.*, 1978; Smith *et al.*, 1978). The water mass in which the intermediate nepheloid layers occurred has characteristics of water mass (3). There were no density discontinuities at the depths corresponding to the occurrence of observed intermediate nepheloid layers.

DISCUSSION

Causes of non-uniform distribution of particles in the ocean are roughly categorized into those due to biological control and those due to physical control, although these two factors are sometimes closely related. The former includes biological patchiness in the water column (Fowler and Knauer, 1986; Alldredge and Silver, 1988) and the latter includes particle patchiness associated with a strong halocline or thermocline and attendant pycnocline (Drake, 1974), and patchiness due to turbid water intrusion (Gibbs, 1974), turbulence caused by bottom current stress (Smith and Hopkins, 1972; Sternberg and McManus, 1972; Gross *et al.*, 1988; Gardner and Sullivan, 1981; Hollister and McCave, 1984; Newberger and Caldwell, 1981) and internal waves (Caccione and Drake, 1986; Dickson and McCave, 1986; Thorpe and White, 1988; Gardner, 1989b). Possible mechanisms for the observed intermittent intermediate nepheloid layers on the Scotian Shelf will be assessed from

both biological and physical considerations.

A regional spring phytoplankton bloom occurs during April following winter mixing of high nutrients to the surface from the deep central basins (Herman *et al.*, 1991). Chl. a concentration in the surface water (2.52 $\mu\text{g/l}$, surface layer, 0-80 m, average, Fig. 3-4) is comparable to the reported value (2-3 $\mu\text{g/l}$) measured during a spring phytoplankton bloom at the same station (Herman *et al.*, 1991), although a peak value at 30m depth (6.81 $\mu\text{g/l}$) is much higher than the previously reported data (3.5 $\mu\text{g/l}$). It is concluded that a spring phytoplankton bloom occurred in the surface layer during the sampling. In addition, this profile has a small peak of Chl. a concentration, corresponding to the light-scatter peak at 180 m. Therefore, particles in the intermediate nepheloid layer must include biogenic particles produced in the surface water. However, this small peak is too deep for biological patchiness of phytoplankton; furthermore, it is not likely to be due only to the settling of a phytoplankton population from the surface because a corresponding nephel signal occurs repeatedly at almost the same depth. Seasonal vertical migration of zooplankton in Emerald Basin has been well described by Sameoto and Herman (1990) and Herman *et al.*(1991). The period of maximum aggregation of copepods within the Basin occurs during September-October. During March, they begin migrating into the surface waters and by April the deep basin is virtually devoid of copepods while early stages of *Calanus* appear in the surface water in large concentrations. Therefore, the intermediate peak of light-scatter does not seem to have a biological cause.

The physical oceanography of the Scotian Shelf has been well characterized in

terms of water mass structure (Warner, 1970), circulation and variability (Smith *et al.*, 1978; Smith and Schwing, 1991), mixing (Houghton *et al.*, 1978) and low-frequency motions that result from wind forcing (Petrie and Smith, 1977; Petrie, 1983; Petrie *et al.*, 1987). Because Station 1 is at the same location as one of the hydrographic stations of the "Halifax Transect" of Bedford Institute of Oceanography, salinity and temperature have been measured there on an ongoing basis since 1950 (Drinkwater and Taylor, 1982). Moreover, since the Basin has been the site of several current meter moorings, current statistics, including tidal analyses, are available (Lively, 1988; Gregory and Smith, 1988). The intermediate nepheloid layer is found in water whose temperature (9-10 °C) and salinity (34.7-35) properties characterize it as slope water (Fig. 3-5).

Low-frequency slope water intrusions onto the shelf and into Emerald Basin, in response to transient wind forcing, were observed and analyzed by Petrie and Smith (1977) and Petrie (1983). Since the depth of the intermediate nepheloid layer is close to the depth of the Saddle (150m) connecting the slope and the Basin, one hypothesis is that upwelled slope water resuspends particles on the Saddle and flows into the Basin causing intermediate nepheloid layer formation. Wind direction and speed, from the Sable Island weather station (Fig. 3-1, courtesy of Environment Canada, Bedford, Nova Scotia), were decomposed into U (positive eastward parallel to the shelf break) and V components (positive northward) (Fig. 3-6). Petrie (1983) has found that significant upwelling and deep, onshelf flow with velocities of about 40 cm/s occur at the shelf break under the condition of moderate (10 to 20 m/s)

Fig. 3-5 Salinity and Temperature diagram for the water from 150 m, 200m and the intermediate nepheloid layer.

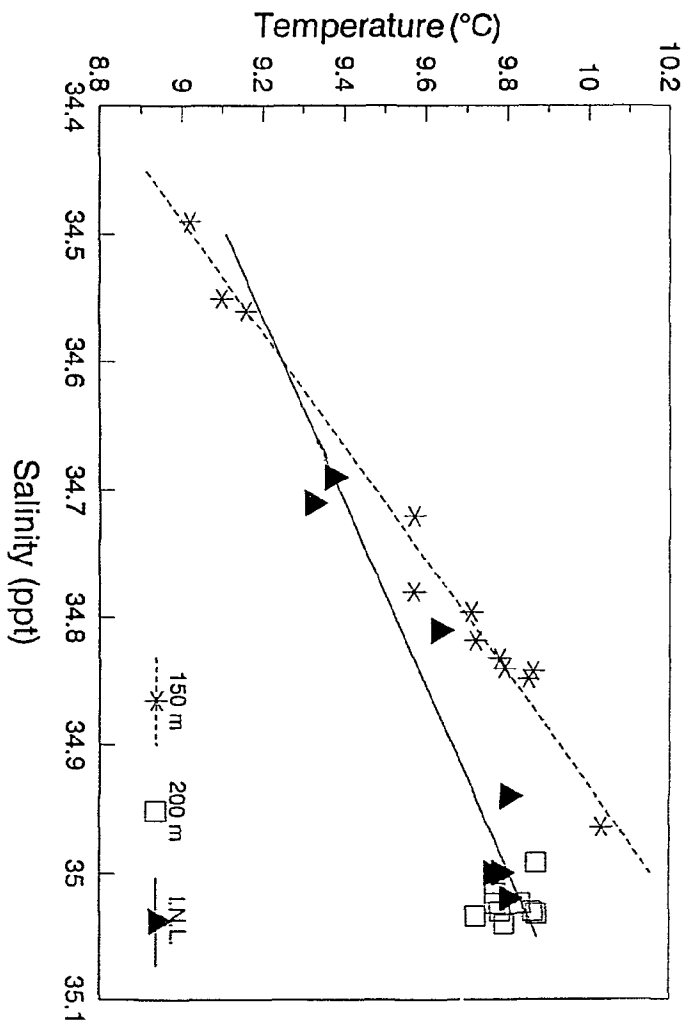


Fig. 3-5

Fig. 3-6 The V component (towards the north) and U component (towards the east) of the wind at the Sable Island weather station. More variance was in the U component than the V component and 15 m/sec was recorded on April 10 in the U component.

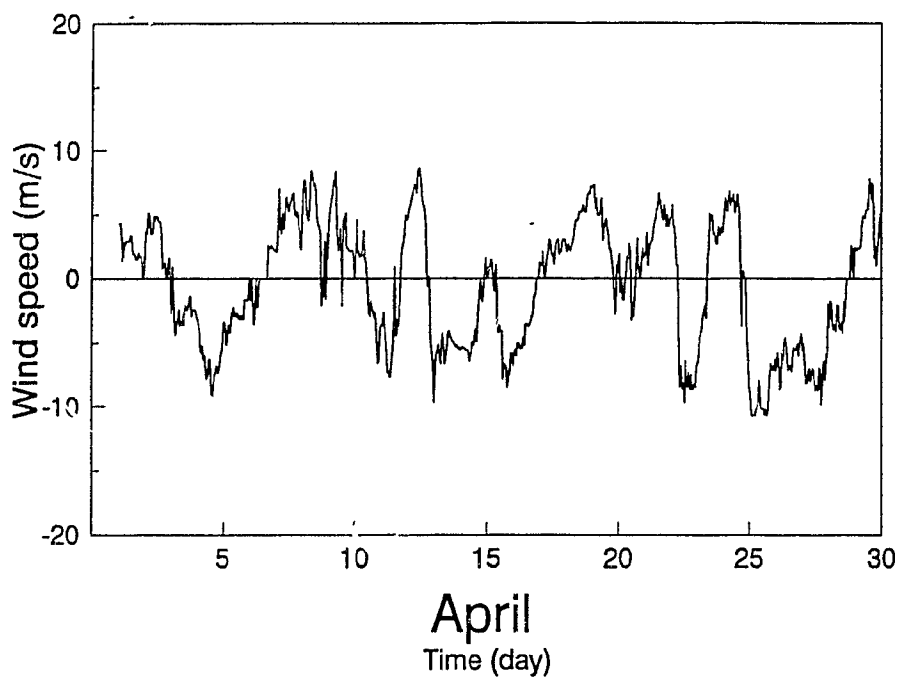
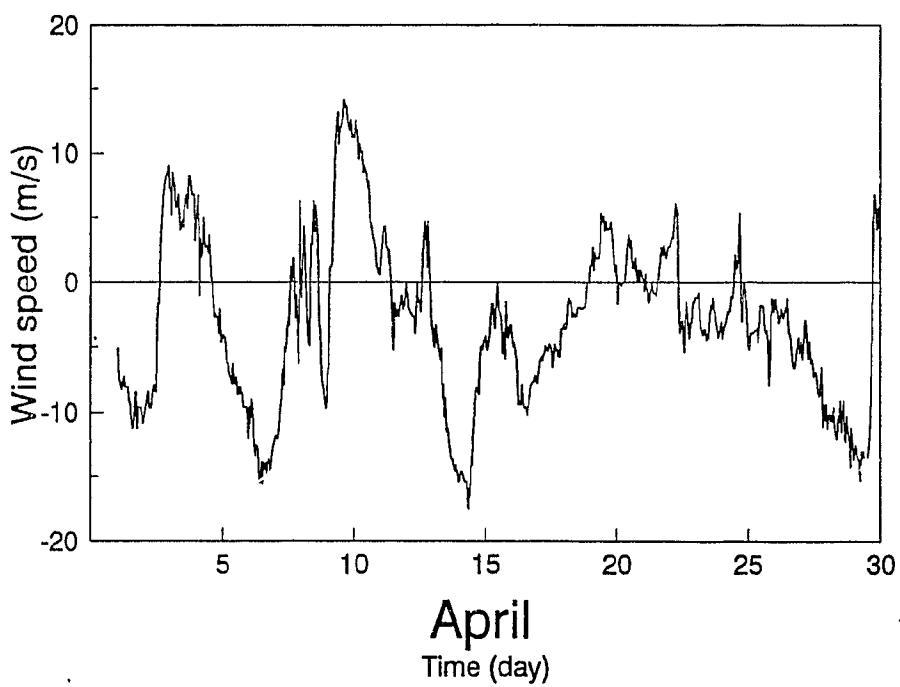
V COMPONENT**U COMPONENT**

Fig. 3-6

transient eastward wind of 2 or more days duration. An event of about 1 day duration when the U component equalled or exceeded 10 m/s occurred on April 9, two weeks before the sampling in the Basin. Using 40 cm/s and the 80 km between the middle of the Saddle to Station 1 in the Basin as a representative velocity and distance, then the time scale of slope water intrusion to reach the deepest area of Emerald Basin is about 2 days. That is, there appears to be sufficient time (about 2 weeks) for an intrusion to reach the sampling sites. There is little information available for the settling velocity of particles associated with the layer of water intrusion; however, the reported value for settling velocity of particles in nepheloid layers at the Nova Scotia Continental Rise, 12 m/day (McCave, 1983), gives the time scale of 3-4 days for particles settling from 150 m deep to the observed intermediate nepheloid layer depth, 180-190 m. That is, it would appear that any particles resuspended during the wind event would have sunk below the observed nepheloid layer depth. In addition, a nepheloid layer was observed at shallower depth at Station 4, farthest from the channel. From the above results, the wind event recorded on April 9 (13 days before the first observation) is unlikely to have caused any of the intermediate nepheloid layers observed in this study; moreover, no favourable wind event for upwelling, stronger than 10 m/s, was recorded after April 10. This mechanism, however, can be very important during winter when strong eastward winds are dominant and many upwelling events with strong, onshore flow (Petrie, 1983) and significant flushing of the Basin (Herman *et al.*, 1991) occur. This might explain the thick pelagic deposition in the Basin (Buckley, 1991; Pocklington

et al., 1991) with little deposition on the Saddle (Piper, 1991). There are possible local upwelling events that are attributed to coastal-trapped waves caused by remote forcing (Smith and Schwing, 1991). Such events can cause density-driven intrusion into the Basin. However, no evidence for this kind of event is available for this study.

Evidence for the role of internal waves in nepheloid layer formation has emerged from results on the continental slope, e.g., off southern California (Cacchione and Drake, 1986), off Porcupine Bank (Dickson and McCave, 1986; Thorpe and White, 1988) and in Baltimore Canyon (Gardner, 1989). Internal waves of varying frequencies can generate intensified bottom velocities and breaking by upslope shoaling. The "critical" depth of this boundary-layer instability is estimated from the wave characteristic slope, c and the topographic slope, α .

$$c = \left(\frac{\sigma^2 - f^2}{N^2 - \sigma^2} \right)^{1/2} \quad (1)$$

in which σ is the wave frequency, f is the local inertial frequency and N is the Brunt-Väisälä frequency. Energy concentrated in a narrow, near-bottom band grazes the slope where $\alpha/c \rightarrow 1$. Therefore, the formation of turbid lenses or plumes of off-slope flow and transport of fine sediment particles seaward may occur. This is as a result of intense zones of turbulent mixing and sediment resuspension on the slope in cases where the direction of internal wave energy propagation coincides with the bottom slope (Cacchione and Drake, 1986). In addition to focusing the energy of internal waves, the slope can serve as a generation site for internal waves. Baines

(1974), who concentrated primarily on internal tides, has shown that the most effective generation areas are those where the topography is convex upward and where $c \approx \alpha$.

The characteristic slope with M_2 internal tide frequency was significant on the slope off Porcupine bank (Dickson and McCave, 1986; Thorpe and White, 1988), while the characteristic slope of higher frequency internal waves was critical off southern California (Cacchione and Drake, 1986). There are no internal wave measurements available at the sampling station in Emerald Basin. However, the M_2 constituent is the dominant barotropic tide on the shelf, with the north-south component (about 7.4 cm/s, amplitude at 250 m in the Basin) exceeding the east-west component (about 5.8 cm/s); furthermore, semi-diurnal internal tides have been found in the Basin (Petrie, 1974, 1975).

The topographic slope, α , was calculated from the local bathymetric chart (Natural Resources Series, Department of the Environment, Canada, 15132-A, 15142-A) and the characteristic slope, c , was calculated from the salinity and temperature data at station 1 (Fig. 3-7-(1)). It is important to note that the sigma t profile at Station 1 did not change significantly over the sampling period. Examination of the topography of the Basin in the vicinity of Station 1 showed that along 320-330 T, coinciding with the direction of the major axis of the M_2 tidal ellipse, the slope was the most favourable for the intensification and generation of semi-diurnal internal waves. There, the parameter $\alpha/c \rightarrow 1$ at the depth of 160-170 m. However, since this area on the slope and Station 1 are separated by 5 km, a mechanism is needed

Fig. 3-7 The topographic slope, α (circle), calculated from the bathymetric chart along 320-330 T from Station 1 in Emerald Basin (1) and along 180 T from Station 4 in adjacent basin (2) over 10 m contour intervals and the characteristic slope, c (asterisk), calculated from equation (1). Error bars show 95 % confidence interval. Points without error bars indicate that the 95 % confidence interval is smaller than the size of the marks. Note that the "critical" depth is at 160-170 m in (1) corresponding to the main basin, and at 130 m in (2) corresponding to the smaller basin to the northeast.

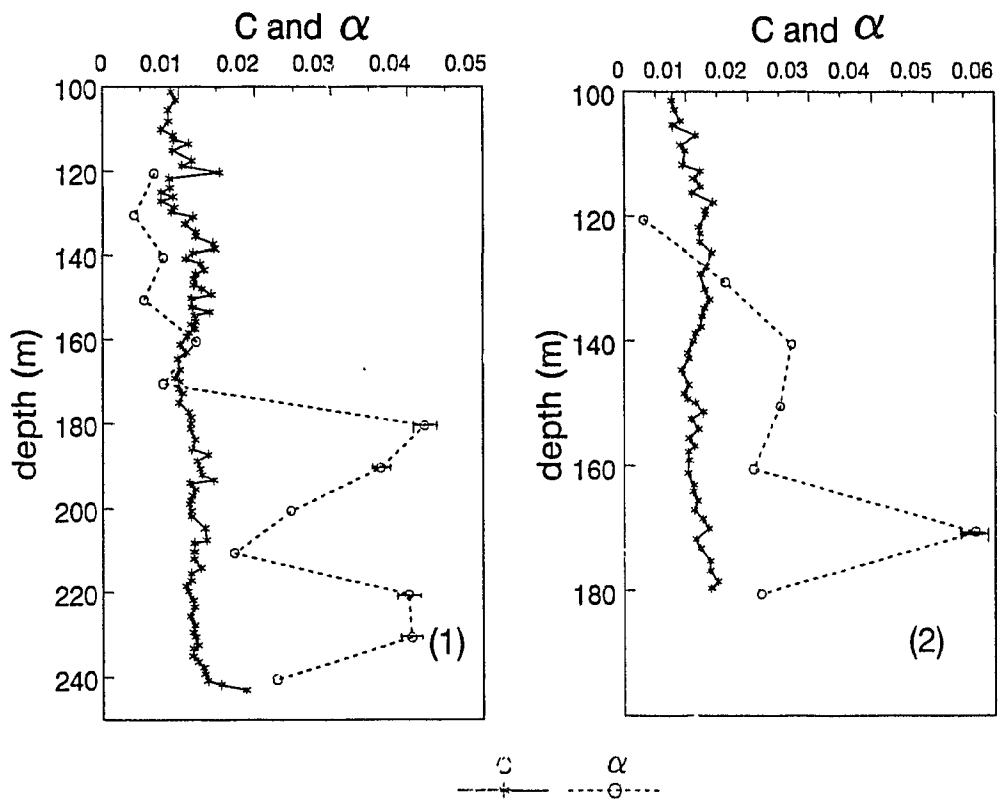


Fig.3-7

to transport the suspended particles. Current meter data, collected within a few kilometres of Station 1 during the spring of 1967 and 1968, have mean (root mean square amplitude of low frequency currents, maximum) flows of 0.03 m/s along 130 °T (0.11 m/s, 0.23 m/s) at 95 m and 0.01 m/s along 297 °T (0.11 m/s, 0.29 m/s) at 250 m. A flow represented by the mean current at 95 m would carry the particles from the critical area of the slope to Station 1 in about 2 days. During this time they would sink approximately 25 m (assuming a 12 m/d sinking rate) to 185-205 m, in reasonable agreement with profiles "a" and "f" in Fig. 3-2. If the flow had the magnitude of the root mean square current, only 0.5 d would be required, giving particles time to settle between 165-185 m at Station 1 as observed with the deeper nephel signal in Fig. 3-2d. However, this explanation cannot account for the shallower of the two nephel signals in "d" (Fig. 3-2) nor for the intermediate nepheloid layer at Station 5 (Fig. 3-3), which is far from any potential critical area. On the other hand, coincidence of the critical depth and observed intermediate nepheloid layer occurred at a depth of 130 m for the adjacent basin (station 4), north of Emerald Basin (Fig. 3-7-(2)). It is worth noting that the Brunt-Väisälä frequency had a minimum at the nephel signal depth. This implies that well mixed water with a higher particle load generated elsewhere was advected to this area.

Since the depth of the intermediate nepheloid layer appears to match the "critical" depth of the M_2 internal tide, the intermittency of co-occurrence in terms of phase was investigated. The U component (toward the east) and V component (toward the north) of the semi-diurnal tidal velocity were calculated at station 1 from the available hydrographic data (Drinkwater and Taylor, 1982)(Fig. 3-8). Among

Fig. 3-8 **V** component (towards the north) of the semidiurnal (M_2 , N_2 and S_2) tide velocity calculated at Station 1. Intermediate nepheloid layers were observed at **a**, **d** and **f**. (Time is GMT)

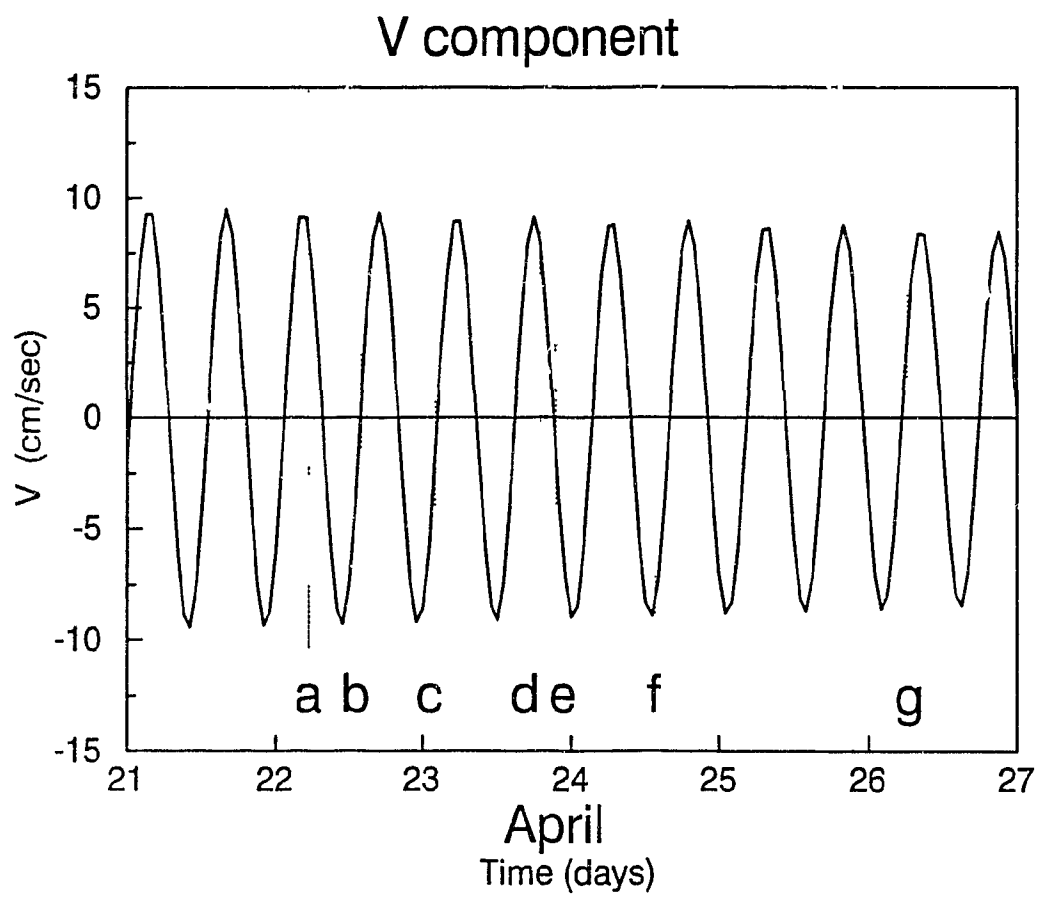


Fig. 3-8

intermediate nepheloid layers observed at the critical depth, "a" and "d" have the same phase relation to the surface tide, i.e. they occurred when the V component was strongest to the north. In contrast profile "f" shows the intermediate nepheloid layer 180 degrees out of phase. In both cases, the intermediate nepheloid layers appear when the V component is strongest. The close relationship between the M_2 tidal cycle and the sediment resuspension (particles on the sea-bed are resuspended when the tidal velocity is strong) has been reported for the continental rise off Nova Scotia (Pak, 1983), for the Porcupine Seabight (Lampitt, 1985) and for Baltimore Canyon (Gardner, 1989). Intermittent resuspension of particles on the slope at the "critical" depth, along with temporal variability of the currents, appears to be the likely cause of the observed intermittency of the intermediate nepheloid layers in Emerald Basin.

The intermittency of nephel signals at Station 1 also implies that other areas of the Basin may be deposition zones of the resuspended particles, because in the 9 hours between profile "a" and "b", and 4 hours between profile "d" and "e", nephel signals disappeared. This time scale is not long enough for particles to settle to the bottom, i.e. they must have been advected elsewhere. The surficial geology of the Basin (King, 1970) indicates that clay is dominant in the eastern part of the Basin, while the site of possible resuspension is exposed bedrock. This suggests that the likely fate of these particles is deposition in the eastern part of the Basin.

CONCLUSIONS

Intermittent intermediate nepheloid layers in Emerald Basin on the Scotian Shelf were found at a depth for which generation and/or energy concentration are most likely to occur for the internal tide with M_2 frequency. A reasonable explanation of this observation would be that the particles are resuspended by the internal tide on the Basin slope at the "critical" depth and then are transported by the variable flows and mean circulation in the Basin. Intermittence of the light-scatter signal at the critical depth appears to be ascribable to the intermittency of particle resuspension on the Basin slope and temporal variability of the currents. These mechanisms appear to be significant over the entire basin. Accumulation of particles in Emerald Basin is probably episodic and is related to major storms during winter that resuspend surface sediment in shallower areas with little net deposition (Piper, 1991; Amos and Judge, 1991). However, sediments carried onto the basin slope by this process and particles that have settled from the surface layer are sorted and reworked through the year by the more persistent mechanism associated with the internal tide.

The study in this chapter illustrates the strong physical control on particle distribution below the surface pycnocline. The results described in this chapter present a good contrast to the study in the coastal basin (Bedford Basin) described in Chapter Two, where biological control is the dominant factor in the distribution

of particles. In both studies strong features in particle distribution below the surface mixed layer, i.e., the formation of bottom nepheloid layers and intermediate nepheloid layers, appear to be unrelated to the density structure of the water column.

Chapter Four



*Measuring physical characteristics of particles:
A new method of simultaneous measurement for size,
settling velocity and density of constituent matter*

INTRODUCTION

The distribution of particles in the ocean results from the combination of water structure including flow, density (salinity, temperature and pressure) structure and turbulence, and the physical characteristics of particles themselves. However, the chemical properties of the water such as oxygen concentration and biological effects such as abundance of heterotrophic organisms, including both microbes and higher trophic level animals, modify and sometimes strongly influence the distribution of particles. The particle distribution is the result after particles are sorted by various oceanic processes. In Chapters Two and Three, the particle distribution was studied in two marine environments for the purpose of investigating the effect of density gradient on marine particle distributions. Results of these studies demonstrate the dominance of biological and physical controls. In this chapter, study of the distribution of particles is approached from another perspective - the physical characteristics of the particles.

Size, density and settling velocity are fundamental physical parameters for evaluating the settling behaviour of particles in the water column and consequently the distribution of particles in the water column. Of these physical parameters, density has proven especially difficult to measure directly (Taghon et al. 1984). Moreover, two kinds of density must be considered. The bulk density, the density of aggregate including interstitial sea water, is of primary importance in settling rate.

The density of constituent matter, the density of materials comprising the aggregate but not including interstitial water, is one of the factors in combination with permeability (Gardner et al., 1991) that is suggested to determine the settling behaviour of an aggregate in a pycnocline or at a density discontinuity.

Until now no direct measurement of bulk density of aggregates has been reported. The most common method for obtaining estimates of the bulk density of aggregates is to calculate it from observed aggregate size and settling velocity and Stokes' equation. Using this method, Riley (1970) gave densities ranging from 1.152 g/cm³ for 2 to 6 μm particles to 1.033 g/cm³ for particles of high organic content and size >60 μm . Krone (1972) reported 1.164 to 1.056 g/cm³ for <1 mm particles. Kawana and Tanimoto (1979) reported that the density of suspended particles with diameter from 10 to 100 μm ranged from 2.0 to 1.1 g/cm³ and decreased with increasing particle diameter. Shiozawa et al. (1985) using *in situ* measurements of size and settling velocity found the density to range from 1.38 to 1.03 g/cm³ for 10 μm to 1 mm particles. In his review of available data, McCave (1975) concluded that the considerable variability in the data leads to uncertainty of up to a factor of 3 in particle settling rates whatever particle shape is assumed.

More recent studies by Alldredge and Gotschalk (1988) measured the settling velocity of macro-organic aggregates with SCUBA in surface waters off southern California. The excess density, or difference between bulk density of the aggregate and sea water density, was determined to range from 2.2×10^{-2} to 1.3×10^{-5} g/cm³. These limits were calculated from the volume and dry weight of the aggregates, the fluid

density and an assumed density of the solid hydrated matter comprising the aggregates, i.e. the density of constituent matter. For this last parameter the density of wet euphausiid faecal pellets, 1.23 g/cm^3 (Komar et al. 1981), was used. This is the only estimate of the density of constituent matter that we have been able to find in the literature, although Syvitski and Lewis (1980) demonstrated the importance of constituent matter density in settling rate of faecal pellets comprised of clays of different types.

The density gradient method described by Taghon et al. (1984) was modified and a simple system was developed to measure the size, density of constituent matter and settling velocity, all independently, and for each aggregate. Constituent matter density measurements reduce the number of unknown physical characteristics of aggregates that affect the particle settling behaviour, and in addition, can be used to estimate bulk density and porosity.

METHODS

The system consists of a column for measuring the settling velocity and density of constituent matter of aggregates, a microscope for size determination and a camera for recording images for shape information. The column, made of Pyrex, is 3.2 cm in diameter, 150 cm long, and is marked off in 1 mm increments. An acrylic water jacket keeps the column temperature at $15 \pm 0.5^\circ\text{C}$. For imaging aggregates for

size and shape determination a Wild stereoscopic dissecting microscope equipped with a 35 mm camera (Pentax ME Super) is mounted on a travelling stage that allows focus in any part of the gradient column (Fig. 4-1).

The upper 110 cm of the column is filled with filtered (0.45 μ m Millipore) sea water, and sterilized with 0.2 % sodium azide. The lower 40 cm of the column contains a sea water-Metrizamide mixture. Metrizamide, 2-(3-acetamido-5-N-methyl-acetamido-2,4,6-tri-iodobenzamido)-2-deoxy-D-glucose, a tri-iodinated benzamido derivative of glucose, has many advantages as a density gradient medium. It is nonionic, chemically inert, and has a low degree of hydration in solution. In addition, when mixed with sea water, the solution has a low viscosity and gives a wide range of densities (Rickwood and Birnie, 1975).

To set up an "instant" density gradient column, the Metrizamide stock solution (1.4579 g/cm³) and filtered, sterilized sea water are connected by a peristaltic pump. Metrizamide solution is pumped into the sea water beaker and mixed by a magnetic stirrer. The resulting mixture is then passed into the bottom of the column at half the rate of the Metrizamide stock solution flow to form a linear density gradient. This density gradient is calibrated using four hollow glass floats with known densities. The linearity of the gradient is described in our experiments by

$$\rho = -0.1936 + 0.01088 * h \quad (r^2=0.99) \quad (1)$$

in which ρ is the density of the medium in g cm⁻³ and h is the height in cm from the

Fig. 4-1 System configuration

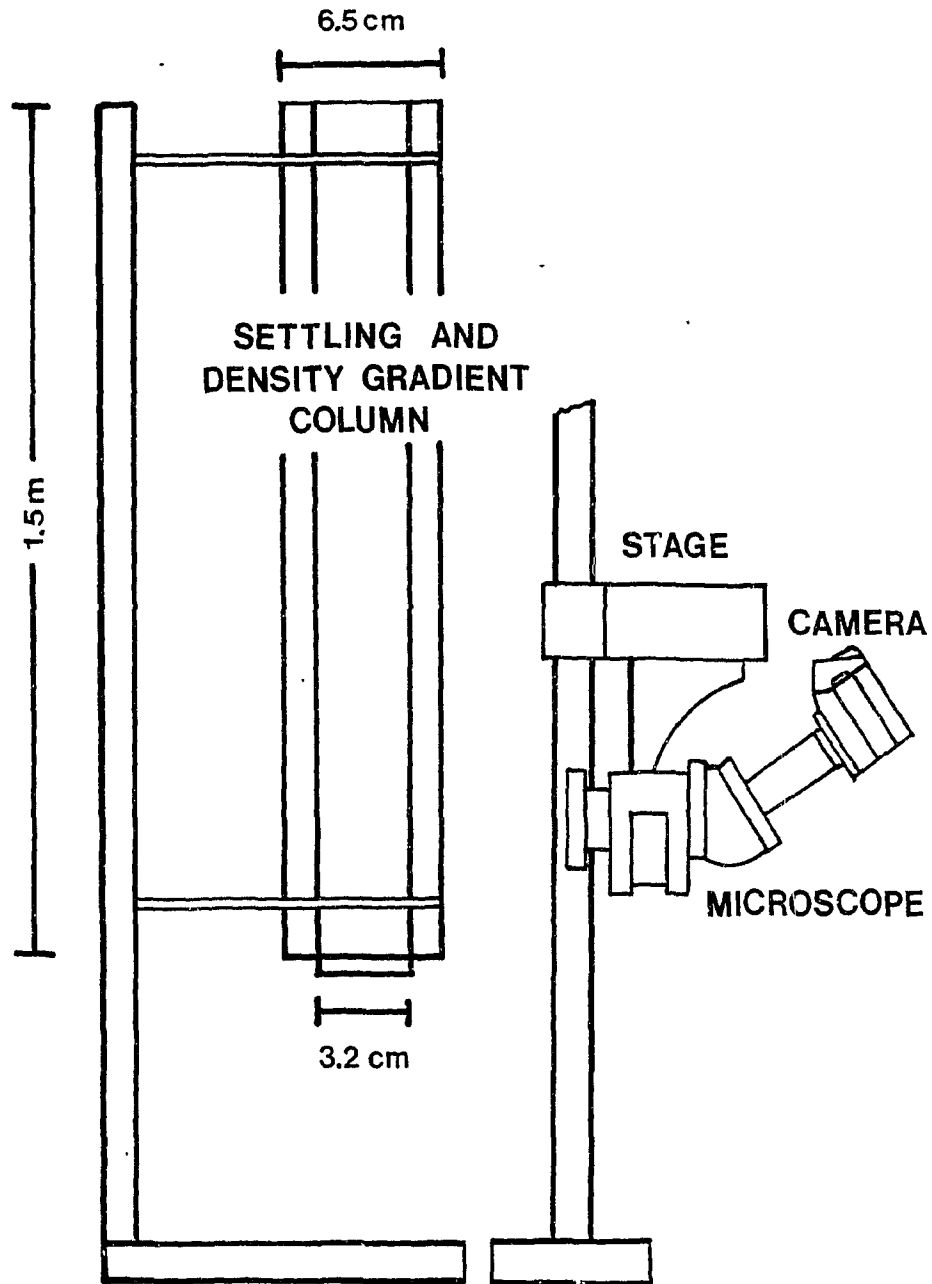


Fig. 4-1

top of the column ($h > 110\text{cm}$). The linearity of the gradient was very stable through the entire 44 day period in which measurements were made (Fig. 4-2).

Two groups of particles were used to test the system in this study. One group was from a small coastal basin, Bedford Basin, Nova Scotia, and was collected on Oct. 31 and Nov. 2, 1989. The suspended particle concentration of the water sampled on Nov. 2, determined using a $0.45\ \mu\text{m}$ Millipore filter, was $2.76\ \text{mg/l}$. Many zooplankton were visible on the filter surface and in the water samples. The other group of particles was taken from a laboratory diatom batch culture (*Chaetoceros*). $0.2\ \%$ Sodium Azide was added to both samples to eliminate biological effects such as microbial decomposition of particles and possible buoyancy regulation by living organisms incorporated into the aggregates. Laboratory aggregation of the samples from Bedford Basin and the diatom culture was created in upwelling as sample water was convected slowly in a glass container. The resulting aggregates were sampled using very slow flow into a wide-bore pipet designed to minimize aggregate breakup.

To measure settling velocity, particles were introduced to the top of the column and velocity was measured in the sea water layer (Fig. 4-2). To avoid error caused by measuring settling velocity before aggregates reached terminal velocity (W_∞), the length of this transient region was estimated. Newton's second law applied to an aggregate of radius, r , yields

$$\rho_s V \frac{dw}{dt} = (\rho_s - \rho_f)gV - \frac{1}{2}V\rho_f \frac{dw}{dt} - 6\pi\mu r w \quad (2)$$

where ρ_s is particle bulk density in g/cm^3 , V is the volume of the particle in cm^3 , w

Fig. 4-2 **Density profile of the column**

0-110 cm : sea water layer with density 1.0217 g/cm³

**110-150 cm : sea water and Metrizamide mixture with
linear density gradient from 1.0217 to 1.429 g/cm³**

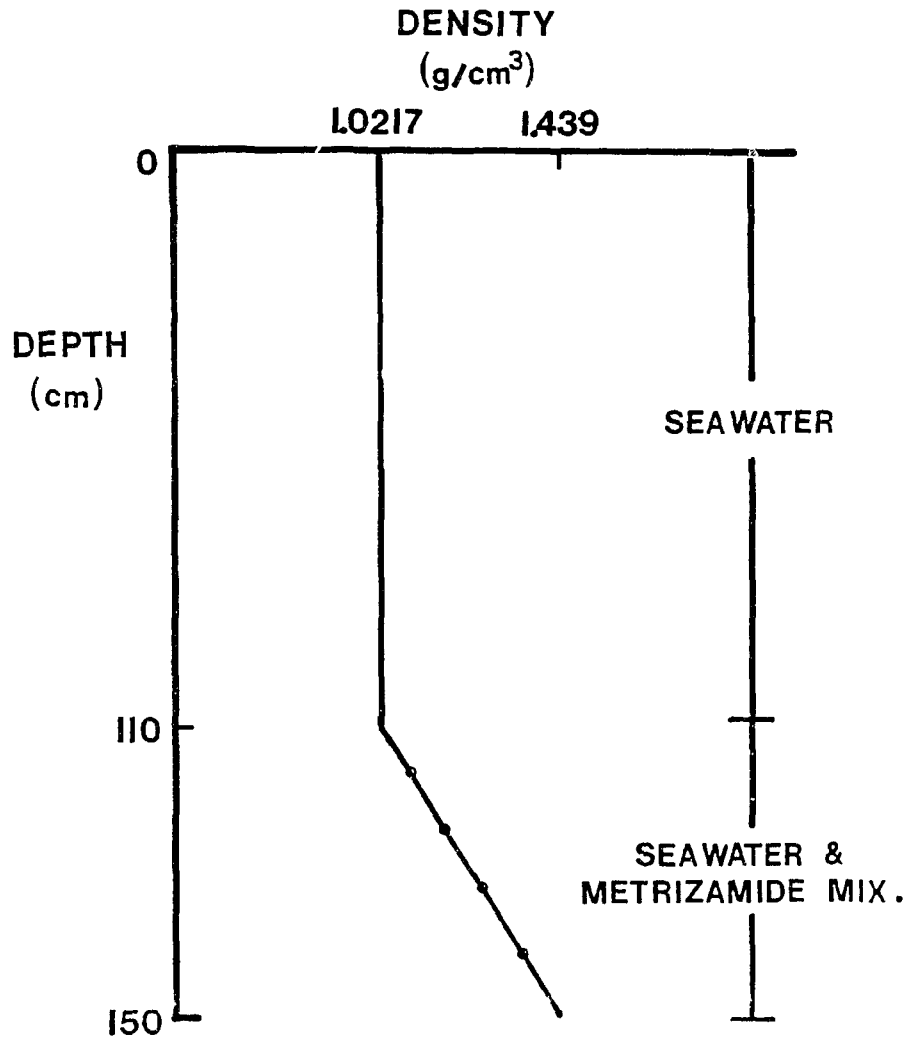


Fig. 4-2

is the settling velocity in cm/s, g is the gravitational constant 980 cm/sec^2 , ρ_f is the density of the fluid in g/cm^3 , and μ is the dynamic viscosity in $\text{g/cm}\cdot\text{s}$. The first term on the right hand side of the equation is the gravitational force, the second term is the virtual inertia due to particle settling (Batchelor, 1967), and the third term is the frictional viscous drag (assuming $\text{Re} < 1$). From this equation, the settling velocity is

$$w = \frac{2(\rho_s - \rho_f)gr^2}{9\mu} [1 - \exp(\beta t)] \quad (3)$$

in which

$$\beta = \frac{-9\mu}{2(\rho_s + \rho_f/2)r^2}$$

The distance particles sink as a function of time is

$$\begin{aligned} X &= \int w dt \\ &= \frac{2(\rho_s - \rho_f)gr^2}{9\mu} \left[t + \frac{2(\rho_s + \rho_f/2)r^2}{9\mu} \exp(\beta t) + \frac{1}{\beta} \right] \end{aligned} \quad (4)$$

In order to reach 99% of terminal velocity ($w_{0.99}$), the particle sinks for time t

$$t = \beta^{-1} \log 0.01 \quad (5)$$

$$X_{0.99} = \frac{4(3.61)(\rho_s - \rho_f)(\rho_s + \rho_f/2)r^4 g}{81\mu^2} \quad (6)$$

$$\doteq 1.7 \cdot 10^6 (\rho_s - \rho_f)(\rho_s + \rho_f/2)r^4$$

When $(\rho_s - \rho_f) = 10^4 \text{ g/cm}^3$ and $r=1 \text{ mm}$, $X_{0.99} = 2.6 \cdot 10^2 \text{ cm}$; when $(\rho_s - \rho_f) = 10^2 \text{ g/cm}^3$ and $r=1 \text{ mm}$, $X_{0.99} = 2.6 \text{ cm}$; when $(\rho_s - \rho_f) = 10^1 \text{ g/cm}^3$ and $r=1 \text{ mm}$, $X_{0.99} = 27.8 \text{ cm}$. Most of particles in this study were less than 1 mm in radius. When $(\rho_s - \rho_f)$ varies from 10^1 to 10^4 g/cm^3 , $X_{0.99}$ is less than 30 cm. Therefore 30 cm should provide sufficient distance for most of the particles in this study to reach terminal velocity.

The use of equation 2 with the Stokes condition for settling is strictly applicable to spheres settling at $Re \ll 1$, but is reasonably accurate for spheres at $Re < 1$ (Batchelor, 1967). Clearly, aggregates in the ocean are not typically spherical nor are they limited by $Re < 1$, although in the case of $Re > 1$ the length of the transition region should be shorter than that predicted from the above treatment.

While more comprehensive equations of aggregate settling that include the influence of shape can be found in the literature, equation 2 is sufficiently accurate for our purpose to estimate the length of the settling transition region. Note too that replicate measurements of settling velocity were made for each aggregate. A stopwatch was used to measure the time of particle sinking through specific depth intervals in the settling velocity region of the column. Settling velocities were sufficiently low that at least three measurements were made during the descent of each aggregate from the Bedford Basin samples, and at least ten measurements were made during the descent of each aggregate from the *Chaetoceros* culture. When the first measurement was significantly lower than the subsequent measurements, the first result was discarded, the assumption being that the particles had not yet reached terminal velocity. In most cases settling velocity results for each particle were in good

agreement (the coefficient of variation, $CV < 6\%$).

The maximum diameter (that perpendicular to the settling direction) and the maximum length (that parallel to the settling direction) were measured to 0.01 mm using an ocular micrometer fitted to the microscope eyepiece. These measurements were made after particles had settled into the density gradient portion of the column and had slowed in sinking rate.

Measurement of the density of constituent matter was performed in the density gradient portion of the column. Since settling velocity is a function of the density difference between the aggregate and ambient fluid, settling velocity decreases as the aggregate sinks into the density gradient portion of the column. Particles stop sinking when the density of constituent matter is equivalent to the density of the ambient fluid. Therefore the aggregate constituent matter density is obtained from the ambient fluid density where the particle stops settling. In any part of the column, the fluid density is calculated from the calibration floats and the linearity of the gradient (Equation 1 and Fig. 4-2).

Aggregates contain interstitial fluid. As an aggregate settles in a medium of different density, exchange of the fluid between interior and exterior of the aggregate occurs. Here, only the final position of the aggregates is needed to evaluate the density of constituent matter. Most of the aggregates required only 3 to 4 hours to reach either an equilibrium position in the density gradient or to settle to the bottom of the column.

Uniform latex particles (styrene divinylbenzene) were used to test the

precision of our density measurements. The latex used has a diameter of $25.7 \mu\text{m}$ and ρ of 1.05 g cm^{-3} . One ml. of latex suspension (10% by volume) containing approximately 10^7 latex particles was introduced at the top of the column. The particles settled to form a band 8 mm thick, corresponding to a density range of $7 \times 10^{-3} \text{ g cm}^{-3}$. From equation 1, this band is between 1.047 and 1.054 g cm^{-3} . Since this result includes real variation in the density of the latex particles, error from the experiment is less than 0.7%.

For aggregates that settled to the bottom of the column, densities of constituent matter were determined from extrapolation of the time vs. density curves (Fig. 4-3a); i.e. after sufficient time, all interstitial water is exchanged with the ambient water and therefore the asymptote for density vs. time curve represents the density of the constituent matter of aggregates. To do this, the curve of density vs. time in Fig. 4-3a is approximated by assuming the density change due to water exchange occurs as $y = at/(b + ct)$, known as a saturation curve, in which y is the density in g/cm^3 , t is time in minutes, and a , b and c are constants. The saturation curve was empirical and there is no mechanisms implied. Time scale for the density change of aggregates due to the water exchange by diffusion and advection processes was estimated in a two-layer system in chapter 5. When $t \rightarrow \infty$, $y \rightarrow a/c$. Therefore a/c is the extrapolated density of constituent matter of the aggregate. In order to obtain a/c , t/y was plotted against t (Fig. 4-b). Since $t/y = b/a + (c/a)t$, the reciprocal of the slope of the linear regression is a/c , and gives the density of constituent matter of an aggregate. At $t < 40$, t/y did not follow a straight line; however, the linear region of the plot ($t > 40$ minutes) gave a very high correlation coefficient ($r = 0.99$, $p < 0.001$). For example,

- Fig. 4-3 (a) Settling of a particle (sample no.21 in Table 4-1) through the density gradient column as a function of time. This curve is assumed to be expressed as a saturation curve : $y = at/(b+ct)$
- (b) Plot of $Y = t/y$ against t and linear regression for $t > 40$ minutes
- $Y = 6.022 + 0.683t$ ($r=0.99, p<0.001$)

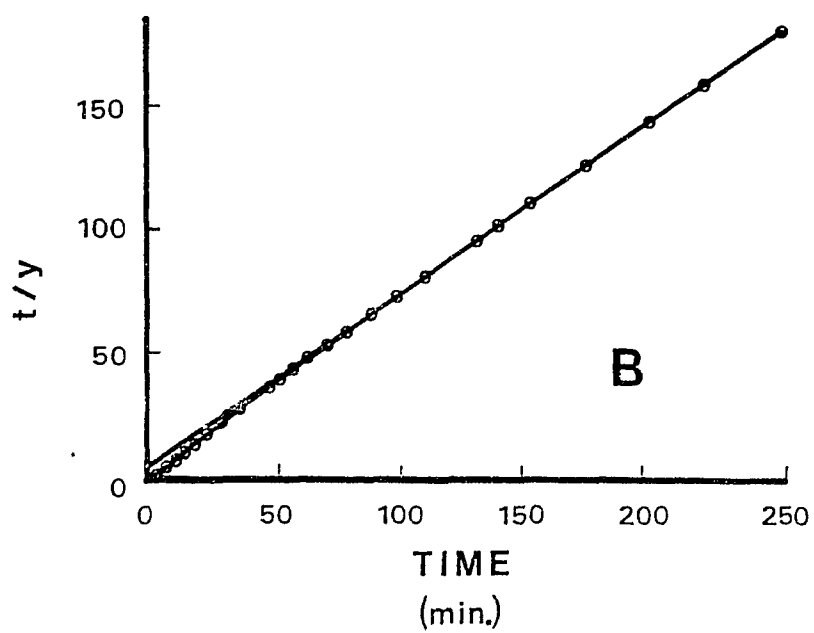
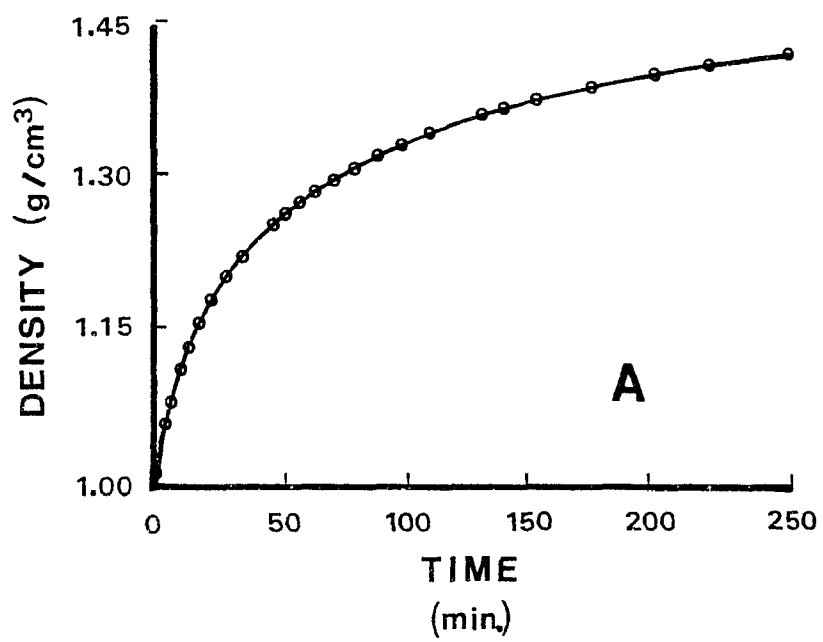


Fig. 4-3

for one aggregate (No.24 in Table 4-1) the linear regression was $t/y = 6.022 + 0.683t$. The reciprocal of the coefficient of t gave the density of constituent matter for this aggregate as 1.464 g/cm^3 .

RESULTS AND DISCUSSION

System

The system was used to determine properties of 24 aggregates produced in the Bedford Basin sea water samples (0.5 m, 5 m and 65m depth) and of 20 aggregates produced in the *Chaetoceros* culture. Some of the aggregates from the Bedford Basin samples contained intact copepod bodies while others were aggregates of small minerals and organic debris. Diameter, settling velocity and density of constituent matter of each aggregate are shown in Table 1 for the Bedford Basin samples and in Table 2 for the *Chaetoceros* samples.

The size, shape and porosity of aggregates undoubtedly depend on the flow regime, chemical composition of the water and surface properties of constituent particles. Since the aggregates in this study were reaggregated in the laboratory, they might not be representative of those in a particular marine environment; however, they do serve to demonstrate the method.

The diameters of the aggregates in this study ranged from 0.29 mm to 1.79 mm. Maximum length, that parallel to the settling direction, ranged from 0.24 to 2.22 mm. These dimensions are well within the range reported for marine aggregates. During

Table 4-1

Diameter, maximum length, settling velocity, density of constituent matter, excess density, bulk density and porosity of aggregates produced in Bedford Basin sea water samples. (The two results in parenthesis for density of constituent matter were obtained by extrapolation using the method described in this paper.) Estimated errors for diameter and length measurements are ± 0.03 mm. For settling velocity it was $\pm 6\%$ of the measurement and for the density of constituent matter it was $\pm 0.7\%$ of the measurement.

Sample No.	depth (M)	Diameter (mm)	Length (mm)	Settling Velocity (m/day)	Constituent Density (g/cm ³)	Excess Density (g/cm ³)	Bulk Density (g/cm ³)	Porosity
1	65	0.71	1.18	126	1.358	0.0053	1.0270	0.984
2				144	>1.439			
3				183	>1.439			
4		0.94	1.29	114	>1.439	0.0027	1.0244	
5		0.53	0.47	136	>1.439(1.497)	0.0103	1.0320	0.978
6	5	0.88	1.29	36		0.0010	1.0227	
7		0.59	1.35	91	>1.439	0.0056	1.0273	
8		0.89	1.18	110	>1.439	0.0030	1.0247	
9		0.41	0.47	67	>1.439	0.0085	1.0302	
10		0.76	0.88	51	1.267	0.0019	1.0236	0.992
11	0.5	0.53	0.59	86	1.306	0.0065	1.0282	0.977
12		0.47	0.53	54		0.0052	1.0269	
13		0.29	0.53		1.095			
14		0.35	0.59		1.100			
15		0.59	0.59		1.274			
16		0.53	0.35		1.274			
17		0.35	0.53		1.313			
18		0.29	0.53		1.314			
19		0.65	1.18	116	1.397	0.0058	1.0275	0.984
20		0.88	0.71	245		0.0067	1.0284	
21		0.71	1.06	26	1.321	0.0011	1.0228	0.996
22		0.53	0.59		1.218			
23		0.59	0.29		1.216			
24		0.45	0.88	262	>1.439(1.464)	0.0275	1.0492	0.938

Table 2-1 *continued*

Porosity (α) is calculated as follows;
Bulk density (ρ_s) is

$$\rho_s = (1 - \alpha)\rho_c + \alpha\rho_f \quad (1)$$

$$\therefore \alpha = \frac{\rho_c - \rho_s}{\rho_c - \rho_f}$$

From Stokes' equation

$$v = \frac{2(\rho_s - \rho_f)gr^2}{9\mu}$$

Excess density ($\rho_s - \rho_f$) is

$$(\rho_s - \rho_f) = \frac{9v\mu}{2gr^2}$$

$$\therefore \rho_s = \frac{9v\mu}{2gr^2} + \rho_f$$

v and r are measured.

ρ_f is measured or calculated from the salinity and the temperature.

μ is calculated.

g is 980 cm/su²

$\therefore \rho_s$ is calculated.

Use this ρ_s and measured ρ_c , α can be calculated from (1)

α : Porosity	v : settling velocity
ρ_s : bulk density	g : gravitational acceleration
ρ_c : density of constituent matter	r : particle diameter
ρ_f : density of the ambient fluid	μ : dynamic viscosity

Table 4-2

Diameter, maximum length, settling velocity, density of constituent matter, excess density, bulk density and porosity of aggregates produced in laboratory diatom (*Chaetoceros*) culture. Estimated error for diameter and length measurements are ± 0.03 mm. For settling velocity it was $\pm 6\%$ of the measurement and for the density of constituent matter it was $\pm 0.7\%$ of the measurement.

sample No.	Day	Diameter (mm)	Length (mm)	Settling Velocity (m/day)	Constituent Density (g/cm ³)	Excess Density (g/cm ³)	Bulk Density (g/cm ³)	Porosity
25	1	0.64	0.95	21		0.0011	1.0228	
26	1	0.95	1.11	14		0.0003	1.0220	
27	1	0.79	2.22	18		0.0006	1.0223	
28	3	0.86	1.24	11	1.341	0.0003	1.0220	0.999
29	3	0.80	1.11	15	1.347	0.0005	1.0222	0.998
30	3	0.99	1.30	18	1.356	0.0004	1.0221	0.999
31	3	1.36	1.48	25	1.341	0.0003	1.0220	0.999
32	3	0.86	1.17	14	1.344	0.0004	1.0221	0.999
33	7	0.99	1.17	13	1.264	0.0003	1.0220	0.999
34	7	0.74	1.24	14	1.275	0.0005	1.0222	0.998
35	10	1.67	2.16	51	1.275	0.0004	1.0221	0.998
36	10	0.93	1.17	14	1.268	0.0003	1.0220	0.999
37	10	0.80	0.93	9	1.267	0.0003	1.0220	0.999
38	14	1.05	1.36	30	1.326	0.0006	1.0223	0.998
39	14	1.24	1.85	20	1.320	0.0003	1.0220	0.999
40	14	1.11	1.17	24	1.324	0.0004	1.0221	0.999
41	44	1.24	1.11	97	1.289	0.0013	1.0230	0.995
42	44	0.74	0.80		1.322			
43	44	1.79	1.54	138	1.257	0.0009	1.0226	0.996
44	44	1.30	1.48	83		0.0011	1.0228	

the settling observations I noted that some aggregates change shape and sometimes break up into smaller pieces. Deformation usually resulted in a more comet-like shape, and was observed mainly in the upper part of the column. Aggregates for which breakup or significant deformation occurred were not included in the results described in Tables 2-1 and 2-2.

Settling velocity ranged from 9.2 m/day to 262 m/day, giving a range within that of reported data (Aldredge and Silver, 1988 a review).

Density of constituent matter of particles ranged from 1.095 g/cm³ to more than 1.439 g/cm³. Eight particles out of 24 produced in the Bedford Basin samples were more dense than 1.439 g/cm³, requiring that their densities be determined from extrapolation of settling data. The only information on density of aggregate constituent matter available in the literature for marine macroaggregates, 1.23 g/cm³ for the wet density of euphausiid faecal pellets (Komar et al., 1981) lies within the range of measured values in this study. Clays incorporated into faecal pellets in the laboratory feeding studies of Syvitski and Lewis (1980) had densities significantly higher than our constituent particle density measurements.

Excess density, the difference between particle bulk density and the density of surrounding water, was calculated assuming Stokes settling (Tables 2-1 and 2-2). Bulk density, used to estimate fluxes from aggregate size (e.g., Gardner and Walsh, 1990), is obtained by adding the density of surrounding water (in our study, 1.0217 g/cm³) to the excess density. The excess density ranged from 3.00×10^{-4} to 1.03×10^{-2} . This is within the range of reported values (Aldredge and Gotschalk, 1988). The

porosity is the ratio of volume that is filled with sea water to the volume of the aggregate. The porosity was calculated from the estimate of the bulk density and the measurement of the constituent matter density. The resulting porosities were greater than 0.938 (Tables 2-1 and 2-2).

The relationships between measured physical parameters for particles sampled both from Bedford Basin and diatom culture are shown in Fig. 4-4. Most of the particles are larger in the axis of settling direction than the one perpendicular to it. These two parameters have a very good correlation ($P < 0.001$) (Fig. 4-4a). No clear relationship was observed between aggregate size and the density of constituent matter nor aggregate size and settling velocity (Fig. 4-4b,c), while the density of constituent matter and settling velocity had a very weak correlation (Fig. 4-4d).

Aggregates from Bedford Basin

In the Bedford Basin sample, aggregate diameter and length had a significant correlation ($P < 0.001$) and particles are elongated in the settling direction. This tendency is clearer in aggregates with larger diameter (Fig. 4-5a). The correlation between diameter and density of constituent matter and between the density of constituent matter and settling velocity are very weak ($P < 0.1$). There was no significant correlation between diameter and settling velocity of aggregates. There are not enough data to discuss the difference of physical parameters with sampling depths. However, it is worth noting that the settling velocities of aggregates sampled from 65 m depth are relatively constant and slightly higher (average = 140.6 m/d,

Fig. 4-4 The relationships between diameter and length, diameter and settling velocity, diameter and density of constituent matter and density of constituent matter and settling velocity of aggregates from both Bedford Basin and diatom culture. Diameter and length of aggregates are correlated at the significance level $P < 0.001$ ($Y = 0.99x + 0.24$), while the correlation between diameter and settling velocity is weak ($P < 0.01$, $Y = 580x - 718$). There is no significant correlation for others. Points in parenthesis are particles that have the density of constituent matter more than 1.439 g/cm^3 , and the constituent matter density was not obtained by extrapolation. These points were excluded from the correlation calculation.

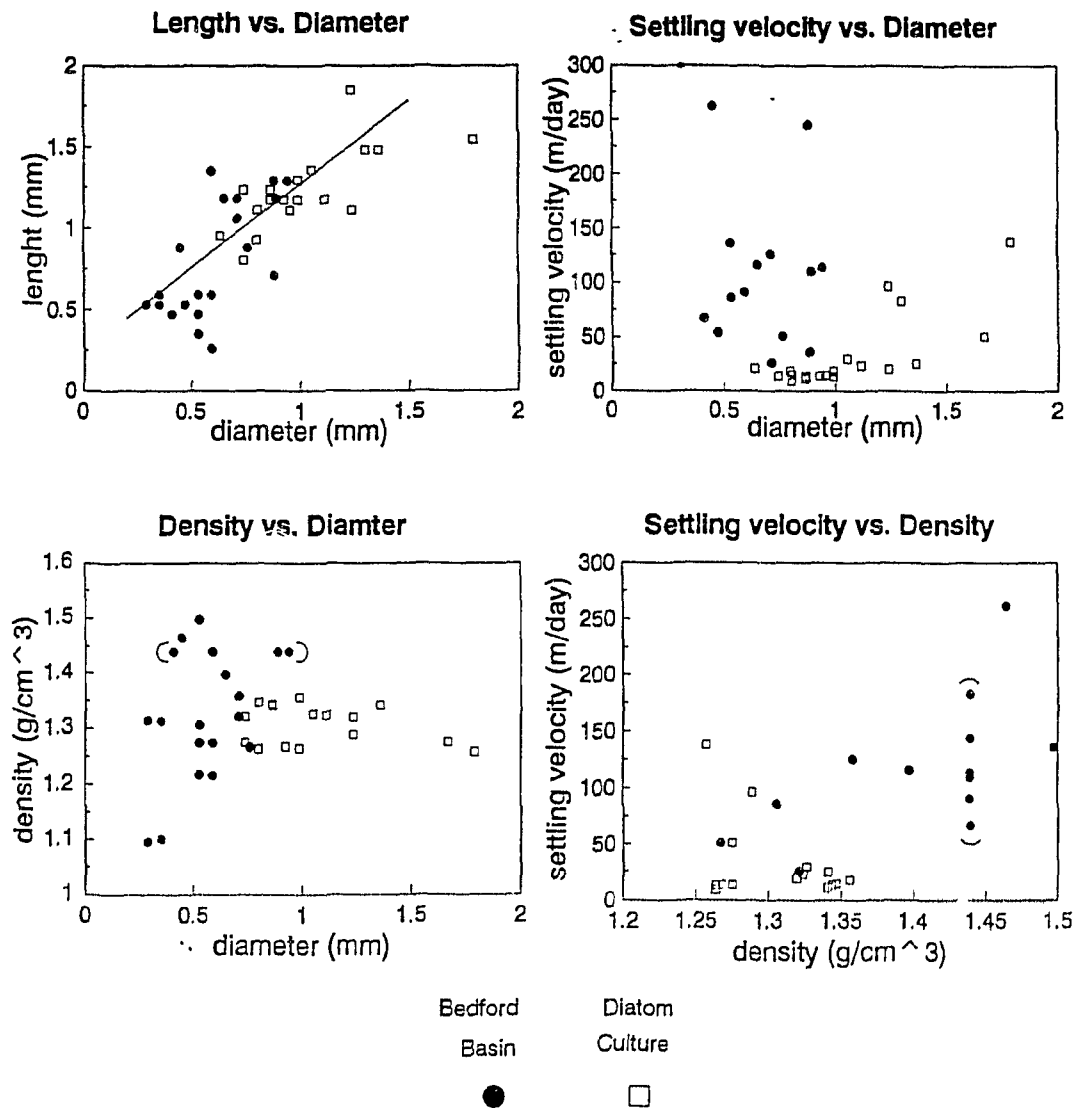


Fig. 4-4

Fig. 4-5 **The relationships between diameter and length, diameter and settling velocity, diameter and density of constituent matter and density of constituent matter and settling velocity of aggregates from Bedford Basin. Diameter and length of aggregates are correlated at the significance level $P < 0.001$ ($Y = 1.15x + 0.24$), while the correlation between diameter and density of constituent matter and between density of constituent matter and settling velocity are weak (for both, $P < 0.1$, $Y = 0.137x + 0.894$ and $Y = 675x - 809$, respectively). Points in parentheses are particles that have the density of constituent matter more than 1.439 g/cm^3 , and constituent matter density was not obtained by extrapolation. These points were excluded from the correlation calculation.**

Bedford Basin

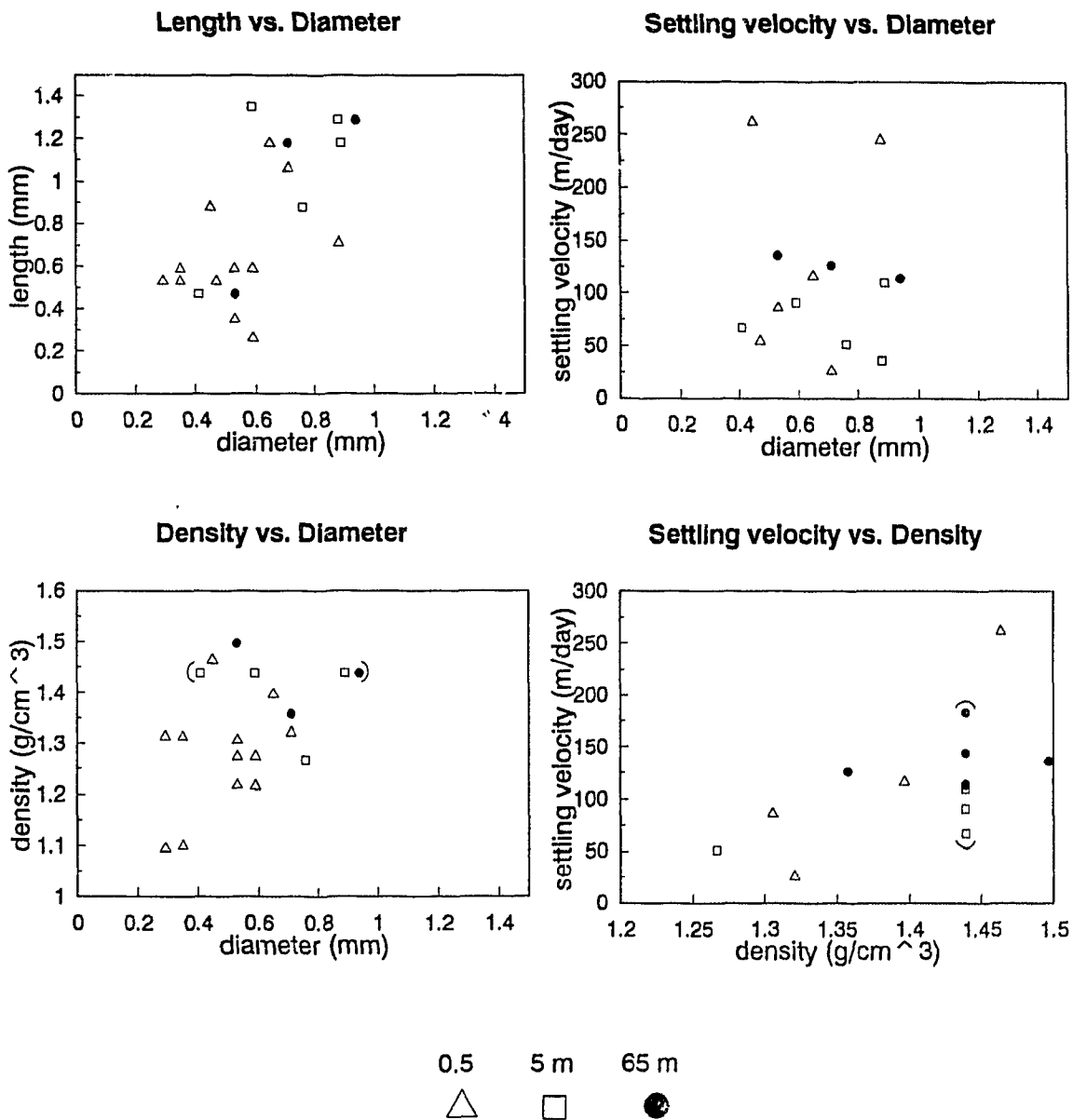


Fig. 4-5

SD=26.2 m/d), compared to that of aggregates from surface waters (0.5 m and 5 m, mean=114 m/d, SD=75.28 m/d), even though diameter and the density of constituent matter are variable. As a result of reworking of marine particles - aggregation, disaggregation, shape modification or being compacted, during settling or resuspension, many aggregates in deeper water might become adjusted to the ambient hydrodynamic conditions and tend to have a constant settling velocity towards the bottom, compared to the aggregates in surface waters that have not experienced much reworking.

Aggregates from the Diatom Culture

Aggregates from Bedford Basin are composed of phytodetritus, the parts of zooplankton and other biogenic materials and inorganic minerals. Aggregates collected from the diatom (*Chaetoceros*) culture, however, include only aggregates of diatom detritus. *Chaetoceros* is a major spring phytoplankton bloom species and known to be a primary marine snow constituent in Bedford Basin, Nova Scotia (Kranck and Milligan, 1988) and in California coastal waters (Aldredge and Gotschalk, 1989). Aggregates of day 1 were taken right after the diatom bloom started flocculating (Chl a. concentration was 132.12 $\mu\text{g/l}$ and 4 days later value dropped to 71 $\mu\text{g/l}$). Samples were taken until 44 days after the first sampling. Time series of diameter, length, diameter/length ratio, settling velocity and density of constituent matter of aggregates are shown in Fig. 4-6. As the culture aged, the settling velocity of aggregates and diameter/length ratio of aggregates increased with time, while there was no significant relationship in diameter vs. time, length vs. time

Fig. 4-6 The changes of size, length, settling velocity, size/length and constituent matter of aggregates from diatom (*Chaetoceros*) culture with time.

Diatom Culture

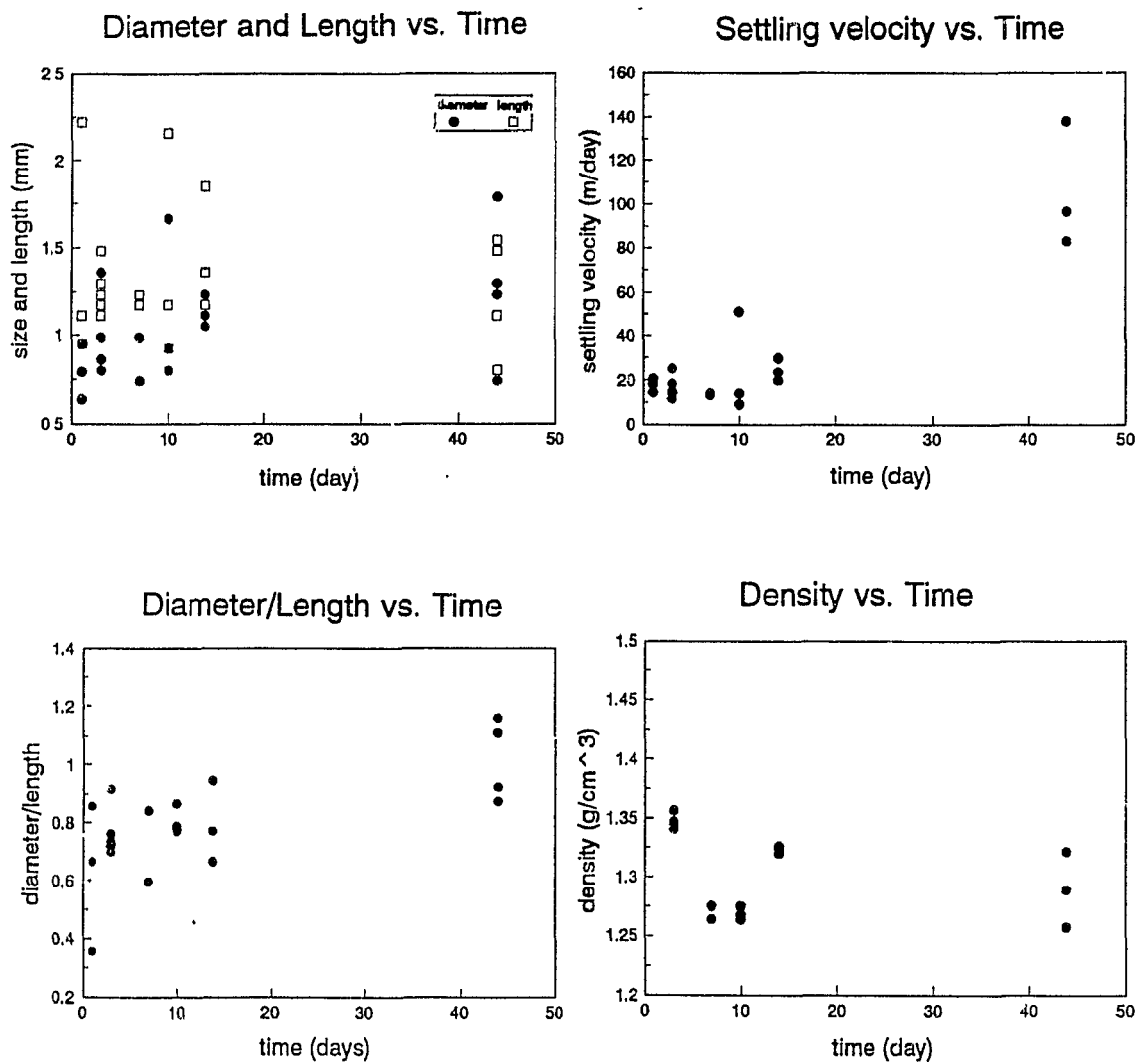


Fig. 4-6

and the density of constituent matter of aggregates vs. time. As a result, decrease in porosity of aggregate (calculation for porosity is described in Table 4-1), with time is indicated (Fig. 4-7). The diameter/length change with time suggests that aged aggregates become more robust and that the shape of the aggregates is not modified as readily as for fresh aggregates, which were often observed to form a comet shape during settling. Moreover aggregates found in the aged culture settle faster, since they are more compact and have lower porosity (larger bulk density) with time.

Fig. 4-7 Change of the porosity of aggregates from diatom (*Chaetoceros*) culture with time.

Porosity vs. Time

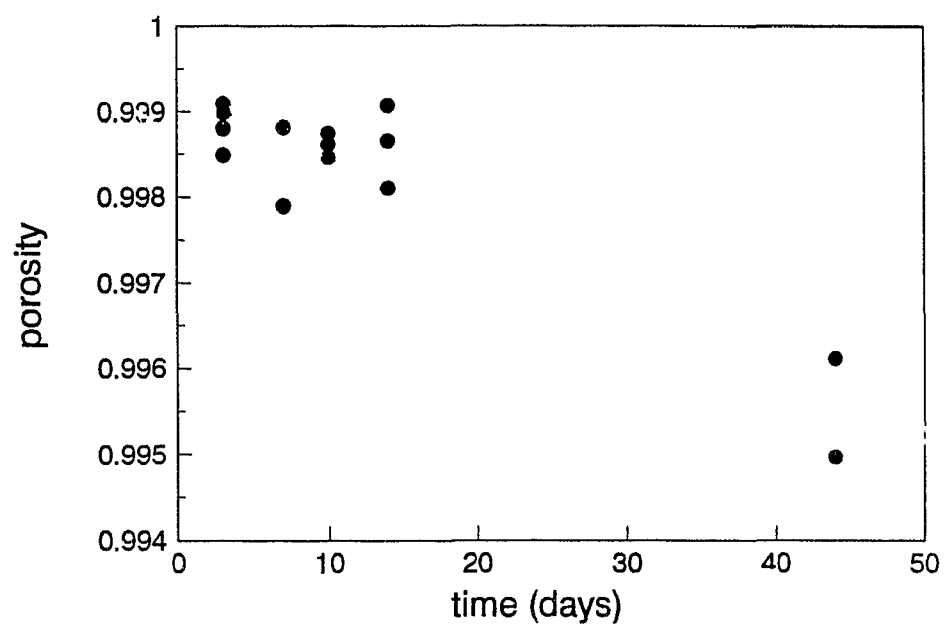


Fig. 4-7

CONCLUSIONS

Measurements of physical properties of particle aggregates, including size, density and shape, are important for understanding the dynamics of suspended particulate material in the ocean. A system was developed that gives simultaneous and independent measurements of size, settling velocity and density of constituent matter of aggregates. Especially important among these parameters is density of aggregate constituent matter, a measurement not previously made on marine aggregates and considered an important parameter for influencing the particle distribution at the pycnocline. Aggregates produced in the laboratory from diatom culture and from particles collected in coastal waters have been used to test the system. Results showed that the density of constituent matter was $>1.095 \text{ g/cm}^3$ for aggregates from Bedford Basin and $>1.257 \text{ g/cm}^3$ for aggregates from the diatom culture. Settling velocity ranged from 26 to 262 m/d for Bedford Basin aggregates and from 9 m/d to 138 m/d for the diatom aggregates. Particle size ranged from 0.29 mm to 0.94 mm for Bedford Basin aggregates and 0.64 mm to 1.79 mm for diatom aggregates. From these measurements, the calculated porosity was very high (>0.938 for Bedford Basin sample and >0.995 for the diatom culture sample). These values are used in the next chapter to model the effect of density discontinuity on the particle distribution.

Chapter Five

Density Structure of the Water Column and the Marine Particle Distribution

INTRODUCTION

Marine particles experience various discontinuities in water characteristics during lateral and vertical transport from sites of generation or introduction. A vertical density discontinuity, the pycnocline, is one of them. Since particle settling velocity is controlled by density differences between the particle and the ambient fluid as well as particle size and shape, there have been suggestions in the literature that density stratification and particle distribution should be correlated. In the early 1970's, Carder (1971) reported a correlation between light-scatter and Brunt-Väisälä frequency for water samples collected using bottles. Using submersibles, Russian (Aybulatov and Novikova, 1984) and Japanese researchers (Ebara and Asaoka, 1985) reported on abundance and shape of marine snow at discontinuity layers. Their results indicated a rapid decrease in concentration, an increase in size and change in shape of aggregates below the density interface.

Introduction of *in situ* optical methods, including transmissometers and light-scatter meters, that enable continuous measurement of the particle distribution offered new insights into the role of the density discontinuity in particle distribution and transport. An early study by Drake (1971) concluded that there was a close relationship between turbid layers and vertical thermal gradients off southern California, although the study did not contain a detailed comparison of light-scatter and temperature profiles. Many recent studies have shown the accumulation of

particulate matter on the seasonal or permanent thermoclines, (e.g. Pak *et al.*, 1980a,b, Thorpe and White, 1988); however, the mechanism that sustains particle accumulation is still unknown. Moreover, very few studies have been conducted on the relationship between the small scale density structure observed in mid- and deep water and the particle distribution.

In this chapter, measurements of light-scatter and density of the water column, which were collected from the western North Atlantic, "Halifax Transect" July, 1989, from Bedford Basin (Chapter 2) and from Emerald Basin (Chapter 3), are investigated and compared to identify the relationship between density stratification and the distribution of particles. A simple model, using the measurements of physical properties of marine particles (described in Chapter 4), is developed to test the effect of a density discontinuity on the retardation of particle settling and attendant particle accumulation in this layer.

The words "discontinuity" and "interface" are used in this study to describe an abrupt change in water characteristics. The "pycnocline" is one type of discontinuity or interface and refers only to the density of the water.

RESULTS AND DISCUSSION OF THE FIELD DATA

Light-scatter measurements and calculated densities of the water column from the "Halifax Transect" (Fig. 5-1) are shown in Fig. 5-2 (because of the depth limitation

Fig. 5-1 "Halifax Transect" stations in the western North Atlantic.

Station 1 The Scotian Shelf Station (100 m depth)

Station 2 The Scotian Slope Station (200 m depth)

Station 3 The Gulf Stream Station (4000 m depth)

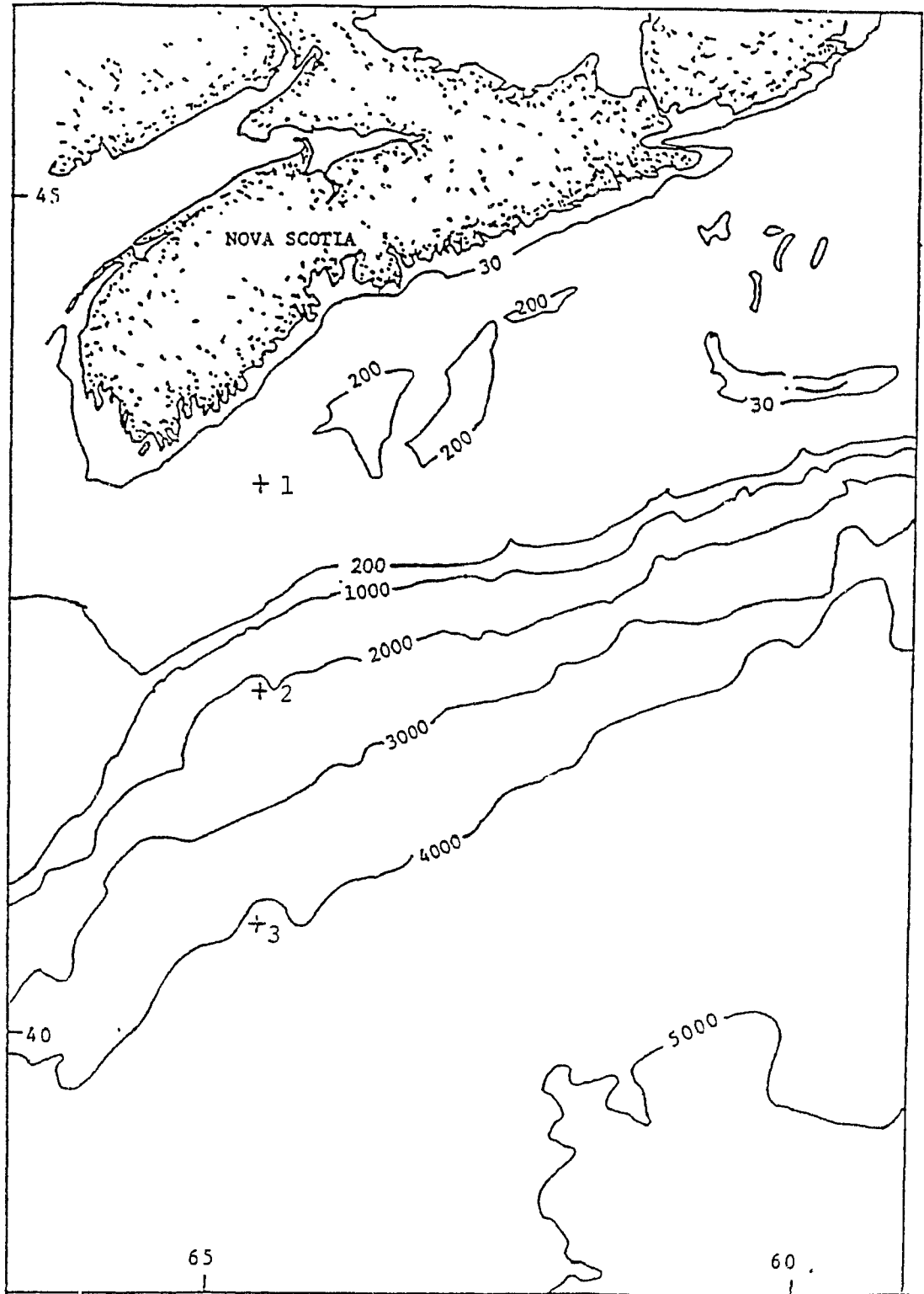


Fig. 5-1

Fig. 5-2 **Vertical distribution of light-scatter and sigma t at three stations from "Halifax Transect".**

Halifax Transect

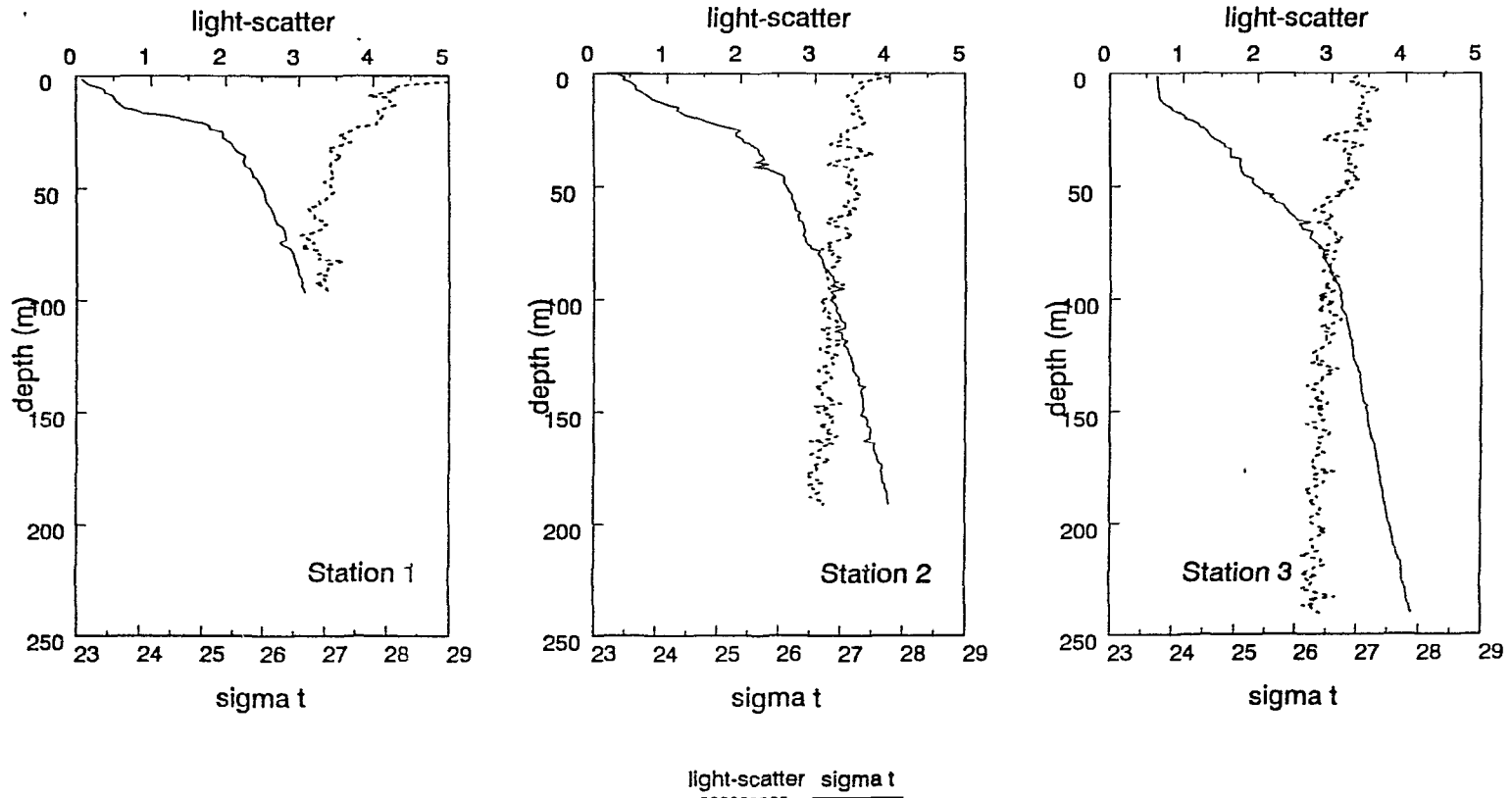


Fig. 5-2

of the light-scatter meter, only the uppermost the 200 m of data are presented). The "Halifax Transect" is located south of Halifax ($64^{\circ}33'$) and is a regular hydrographic study area that includes the Scotian Shelf, the Scotian Slope and Gulf Stream. Detailed studies of the water mass structure are available. The Scotian shelf station (station 1) consists of three layers. The upper 30 m water is called "coastal water", flowing from the Gulf of St. Lawrence through the western side of Cabot Strait and is characterized by low salinity (<32 ‰) and seasonal temperature variations (in this study, $10-15$ °C). The intermediate layer, which has cold temperatures ($< 5^{\circ}\text{C}$) and a salinity of $32-33$ ‰, extends from 30 m to 75 m depth. A warm saline (>5 °C, >33 ‰) water forms the bottom layer of the Shelf (Houghton et al., 1978; Smith *et al.*, 1978). The Scotian Slope station (station 2) also has roughly 3 water masses in the uppermost 200 m. "Coastal water" extends to 40 m depth, warm slope water (Gatien, 1976) below 100 m depth and a mixing layer between 40-100 m. The Gulf Stream station has a very warm saline (26 °C, 36 ‰) surface mixed layer (about 20 m deep) with a wide pycnocline occupying the 20-100 m depth range of the water column. The pycnocline is underlain by warm (13 °C), more saline (>36 ‰) water.

General features of the light-scatter data are an indication of a relatively high particle load above the pycnocline in all three stations (in a shallow mixed layer observed at station 3), and a decrease of the particle load with depth. At station 1, the particle distribution is characterized by a high particle load in the coastal water layer (<30 m), followed by a minimum particle load at the bottom of the intermediate layer (75 m) and a small bottom nepheloid layer below 70 m depth.

The surface particle load at station 2 was not as strong as at stations 1 and 3, however, there was a narrow light-scatter peak at the bottom of the pycnocline (40 m). At station 3, a weak light-scatter peak in the surface mixed layer (0-20 m) and clear bottom water (light-scatter signals are at the detection limit of the instrument, that condition is same as the study in Chapter Two) below 80 m depth were observed.

To understand the relationship between density stratification and the distribution of particles, the gradient of the water density ($d(\text{density})/dz$) was calculated using a five points ($\approx 5\text{m}$) least square fit and compared to the light-scatter profile (Fig. 5-3). The general decreasing trend of light-scatter with depth was removed by calculating the deviation of light-scatter from the linear regression of light-scatter on depth, which was obtained by using the data below the pycnocline. The density gradient is stronger and more variable in surface water than in mid- and deep water. A weak, low variability of the density gradient is especially evident below 100 m at station 3. Because of the high light-scatter at the pycnocline observed in the surface water and decrease of light-scatter with depth, overall correlations between light-scatter and the gradient of the density of the water column should be significant (Fig. 5-4). However there was no significant correlation below the pycnocline; i.e, particle accumulation is observed at surface pycnoclines possessing sufficient gradient ($0.05 \text{ kg/m}^3/\text{m}$ is the lowest gradient among surface pycnoclines of three stations), but there is no apparent accumulation of particles in small scale ($<0.05 \text{ kg/m}^3/\text{m}$) density gradients below the pycnocline. Response of particle distribution to the density

Fig. 5-3 Profiles of light-scatter and the density gradient of the water column ($\text{kg/m}^3/\text{m}$) from the "Halifax Transect". The density gradient was calculated using 5 points ($\approx 5\text{m}$) least square fit.

Halifax Transect, July, 1989

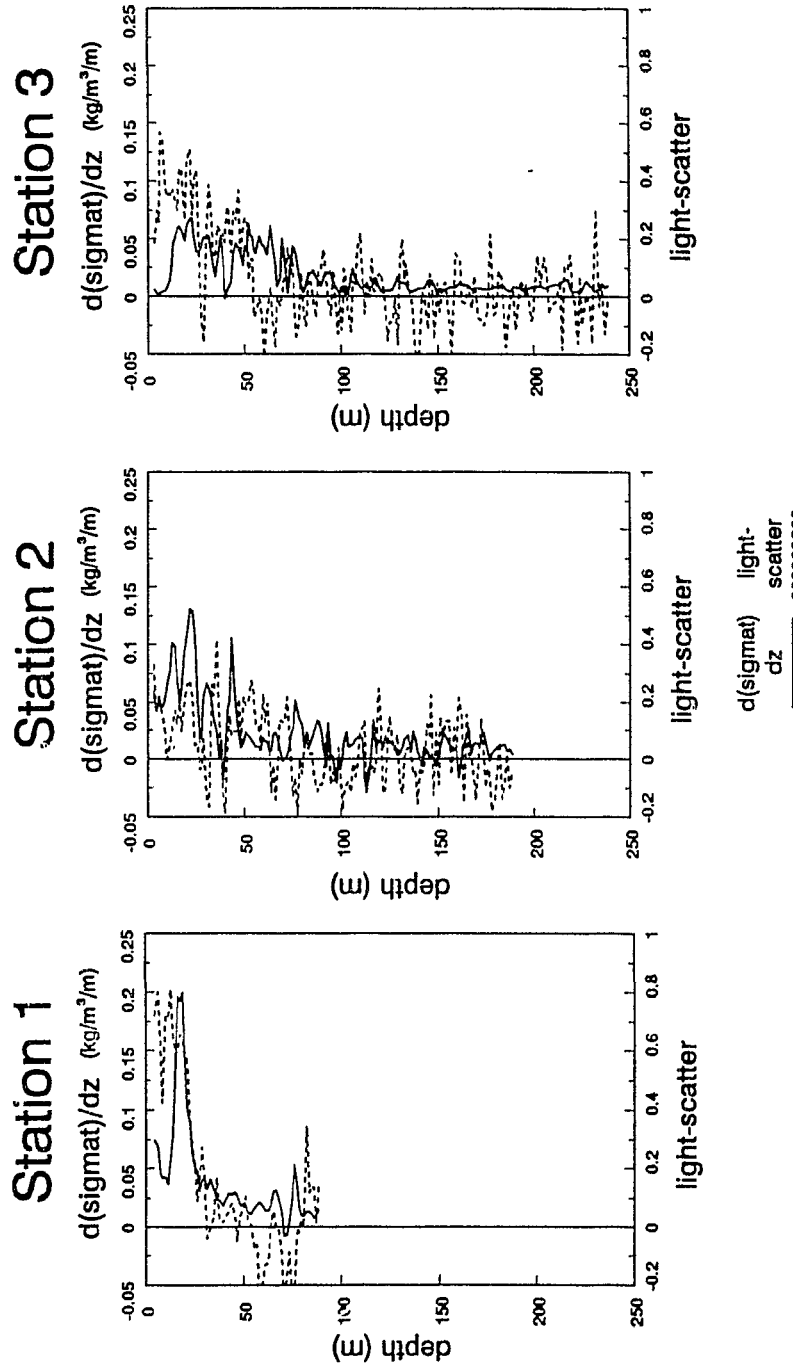


Fig. 5-3

Fig. 5-4 The relationship between light-scatter (after general trend was removed) and the density gradient of the water column

		significance level for the regression (P)
1-1	Station 1. all data	<0.001 ($r^2=.46$, $Y=4.395*X-0.019$)
1-2	Station 1. >30 m	no significance
2-1	Station 2. all data	<0.001 ($r^2=.10$, $Y=1.381*X+0.005$)
2-2	Station 2. >100 m	no significance
3-1	Station 3. all data	<0.001 ($r^2=.15$, $Y=3.635*X-0.002$)
3-2	Station 3. >100 m	no significance

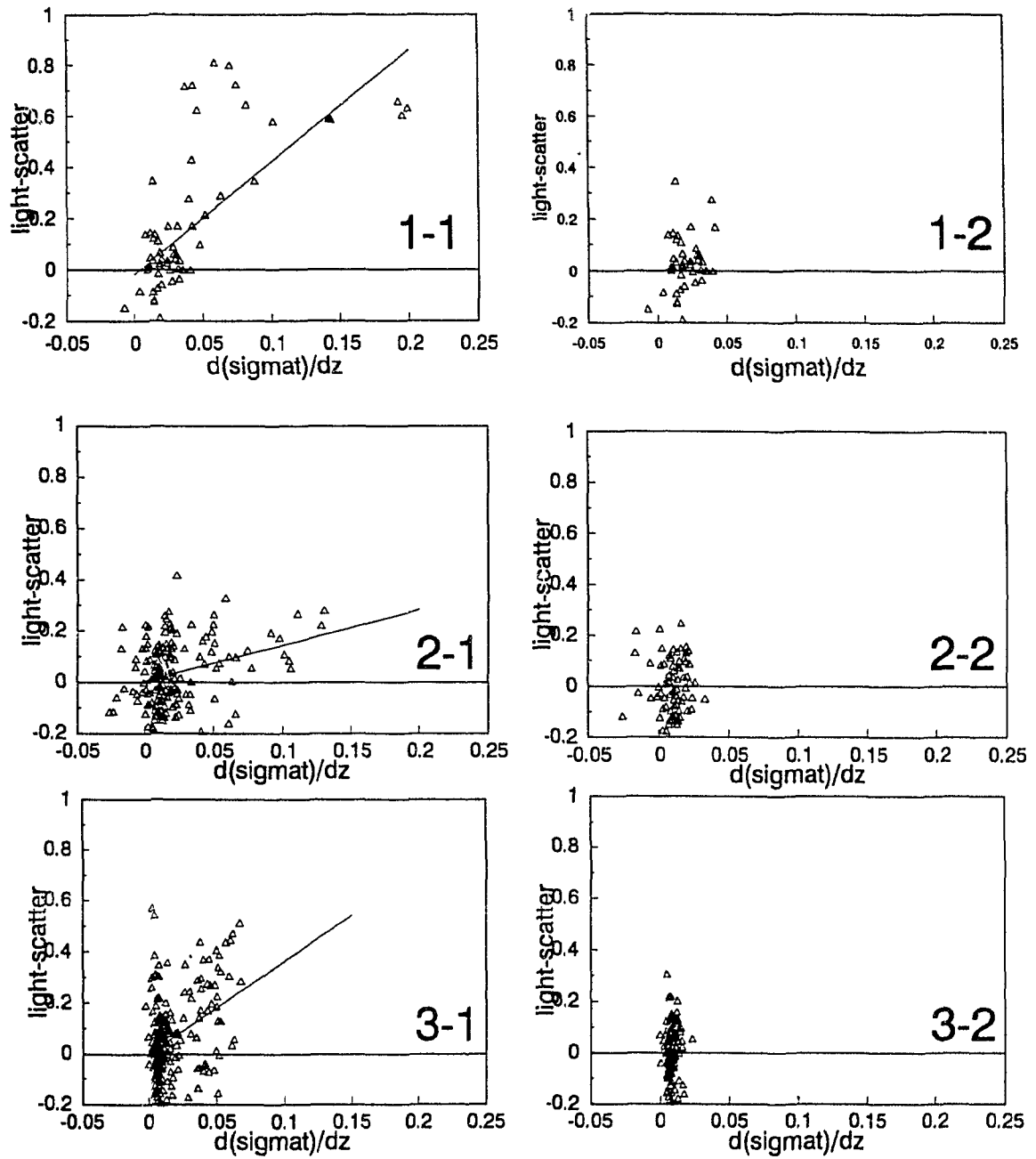


Fig. 5-4

stratification depends not only on the strength of the density gradient of the water column but also on the physical characteristics of the particles. Therefore the criterion for the density gradient to trap particles may change regionally and seasonally. Standard error of estimate of light-scatter using linear regression, which is the variance of light-scatter after the general trend was eliminated, demonstrate that there were larger variances of light-scatter in the pycnocline layers than in the layers below them (Table 5-1). This result may suggest that there are sorting mechanisms for particle distribution in the pycnocline layer.

Some of the light-scatter profiles and water column density gradients from Emerald Basin and Bedford Basin are shown in Fig.5-5 and Fig. 5-6. In Emerald Basin no apparent relationship between density gradient and light-scatter was observed. Rather, in intermediate nepheloid layers the density gradient was low, because the water is well mixed in these layers (Chapter 3). Density stratification is not a major control of the particle distribution there. The surface pycnocline in Bedford Basin becomes stronger towards the summer and light-scatter is always high in this layer. However, the formation of the bottom nepheloid layers are obviously not caused by the density structure of the water. Thus, it is concluded that relatively high particle load was observed in strong density gradients (for example, $>0.05 \text{ kg/m}^3/\text{m}$) in surface water, especially in coastal basin, however, there was no apparent relationship between particle distribution and weak density structure in the mid- and deep water columns.

Table 5-1

Linear regressions of light-scatter on depth in each water mass in Halifax Transect and their standard errors of estimate

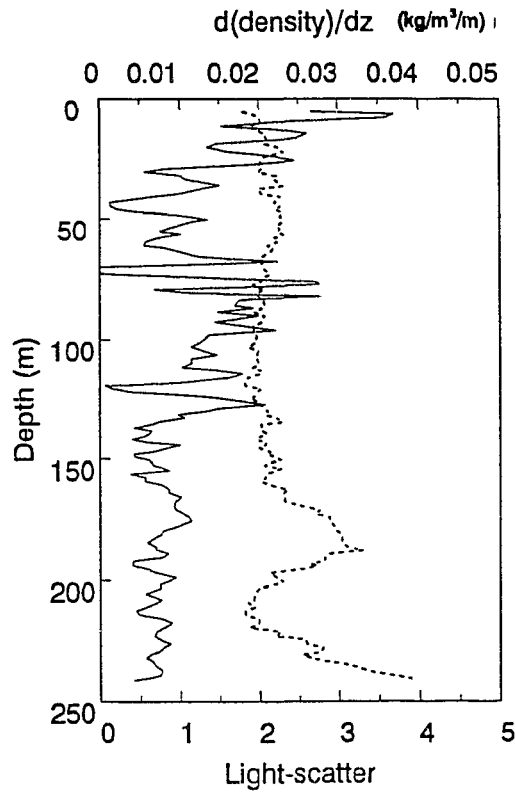
Station	Depth range (m)	Regression	Significance level (P)	Standard error of estimate
1	0-30	$Y = -0.037 * X + 4.648$	<0.001	0.23
	30-75	$Y = -0.008 * X + 3.757$	<0.001	0.09
	>75	$Y = 0.009 * X + 2.530$	<0.001	0.12
2	0-40	$Y = -0.009 * X + 3.703$	<0.001	0.15
	40-100	$Y = -0.006 * X + 3.716$	<0.001	0.11
	>100	$Y = -0.002 * X + 3.412$	<0.001	0.10
3	0-20	N		
	20-80	$Y = -0.007 * X + 3.514$	<0.001	0.14
	>80	$Y = -0.001 * X + 3.078$	<0.001	0.10

N: There was no significant correlation between depth and light-scatter signals.

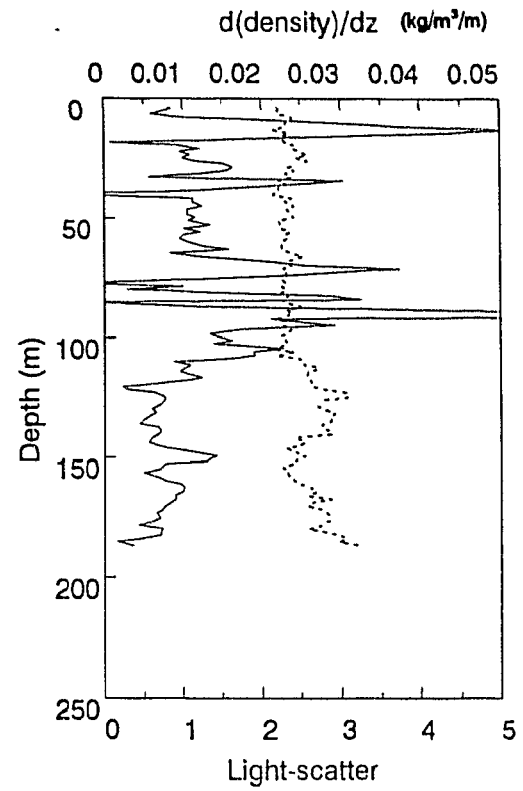
Fig. 5-5 Profiles of light-scatter and the density gradient of the water column ($\text{kg/m}^3/\text{m}$) from Emerald Basin, Station 1 and Station 4. The density gradient was calculated using 5 points ($\approx 5\text{m}$) least square fit. Note the low density gradient at the depth of intermediate nepheloid layers. (N.B. The condition of light-scatter meter is different from the one used in Bedford Basin and in Halifax Transect.)

Emerald Basin

Station 1



Station 4



$d(\text{density})/dz$ light-scatter

Fig. 5-5

Fig. 5-6 Profiles of light-scatter and the density gradient of the water column ($\text{kg/m}^3/\text{m}$) from Bedford Basin, Mar. 10, Apr. 13 and Aug. 16 data. The density gradient was calculated using 5 points ($\approx 5\text{m}$) least square fit. Note the low density gradient at the depth of bottom nepheloid layers.

Bedford Basin

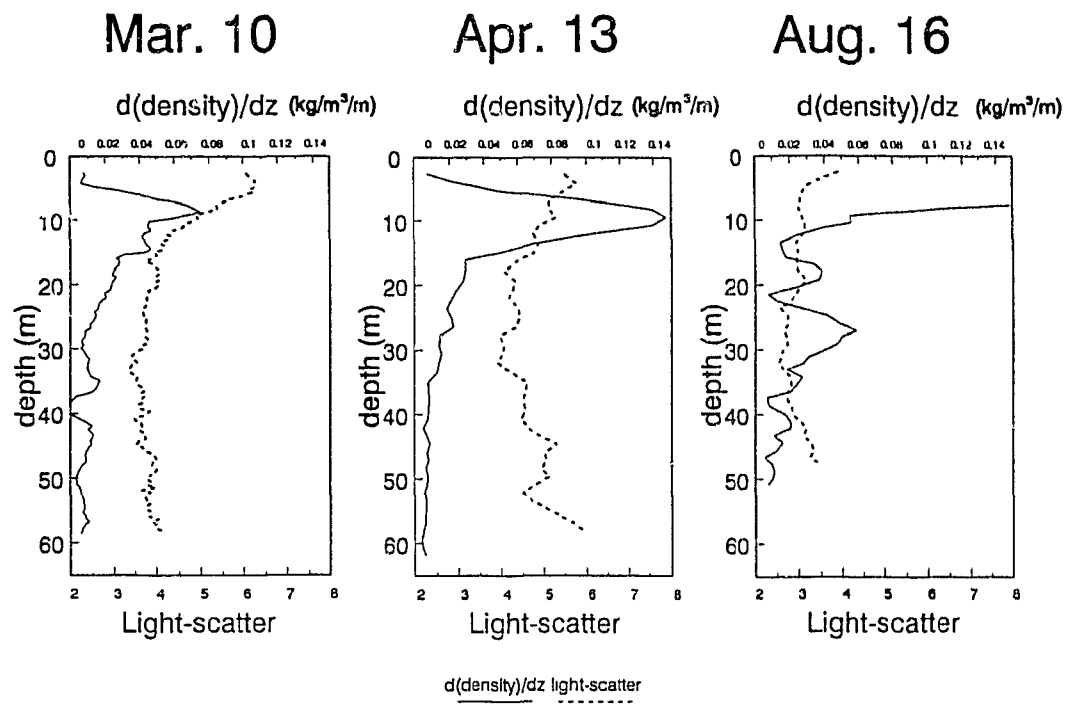


Fig. 5-6

**A Model for the Effect of a Density Discontinuity on
The Distribution of Particles**

A model for evaluating the effect of a density discontinuity in the water column on the distribution of particles was developed. One goal of the model is to assess whether observed accumulation of particulate matter at the surface pycnocline and no accumulation of particulate matter at small scale density discontinuities in the mid- and deep- water, can be explained in terms of the retardation of aggregate settling velocity due to increase of ambient water density.

Assumptions are as follows;

- (i) Steady-state (particle distribution does not change with time)
- (ii) All particles have the same size r and this does not change with depth. Also, particles have the same initial bulk density ρ_p , which is subject to change due to the exchange of water inside and ambient sea water outside of the aggregates.
- (iii) There is no resuspension and the system is laterally homogeneous.
- (iv) Particulate matter concentration and light-scatter measurements are linearly related.

In the two compartment model used, the first compartment represents the water mass above the pycnocline and the second compartment represents the water mass

at the pycnocline (Fig. 5-7). Since steady state is assumed,

$$\begin{aligned} dC_2(t)/dt &= (C_1(t)v_1 - C_2(t)v_2)/\Delta z \\ &= 0 \end{aligned} \quad (1)$$

where $C_1(t)$ and $C_2(t)$ are the concentration, and v_1 and v_2 are the settling velocity of particulate matter in compartments 1 and 2, respectively. From equation (1),

$$C_2/C_1 = v_1/v_2 \quad (2)$$

Consequently, when the particle settling velocity decreases at a density discontinuity, there is an accumulation of particles.

When Stokes' equation is applied to the settling velocity, particle settling is a function of the density difference $\Delta\rho$ between particle (ρ_s) and the ambient fluid (ρ_f) and particle size r . Here r is constant from assumption (ii), so particle settling velocity is only a function of $\Delta\rho$. A change of dynamic viscosity (μ) due to salinity and temperature is not included in this model, however, the effect of μ enhances the retardation of particle settling velocity at the pycnocline.

The bulk density of aggregates (ρ_s) is expressed as a combination of the density of the aggregate constituent matter (ρ_c) and the density of the interstitial fluid (ρ_f) with porosity (α).

$$\rho_s = (1-\alpha)\rho_c + \alpha\rho_f \quad (3)$$

The density profile of the water column (ρ_f), of constituent matter of particle (ρ_c), change of the particle bulk density (ρ_s) due to the interstitial water exchange and of the density difference between the particle and the ambient water ($\Delta\rho$) at the density discontinuity are sketched in Fig. 5-8. As a particle falls through the density discontinuity, ambient water density changes from ρ_{f1} to ρ_{f2} . The interstitial water will

Fig. 5-7 Two compartment model for the particle distribution at the pycnocline. C_1 and C_2 are the concentrations of particles in the water above the pycnocline and at the pycnocline, respectively. v_1 and v_2 are the settling velocities of particles in each layer. ρ_1 and ρ_2 are the densities of the ambient water in compartments 1 and 2.

Two Compartment Model

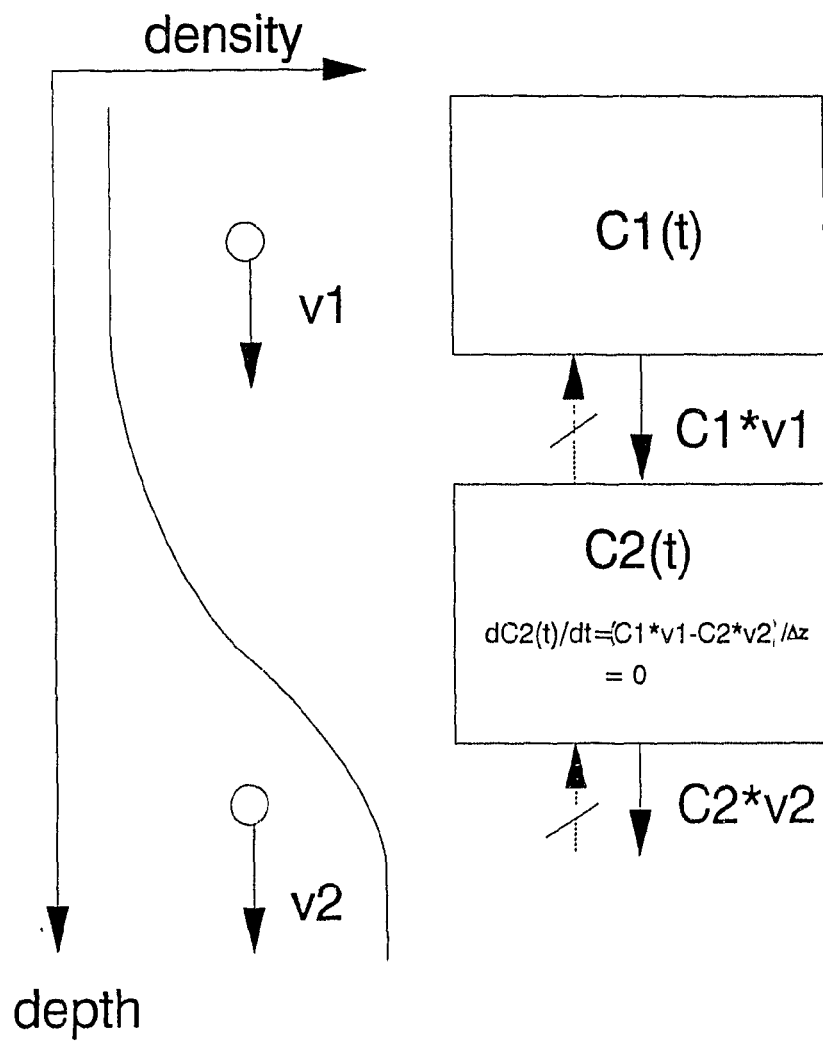


Fig. 5-7

Fig. 5-8 A sketch of the density profile for the constituent matter (ρ_c), ambient water (ρ_t), bulk density of particle (ρ_s) and density difference between the particle bulk density and ambient water ($\Delta\rho$) at the density discontinuity layer.

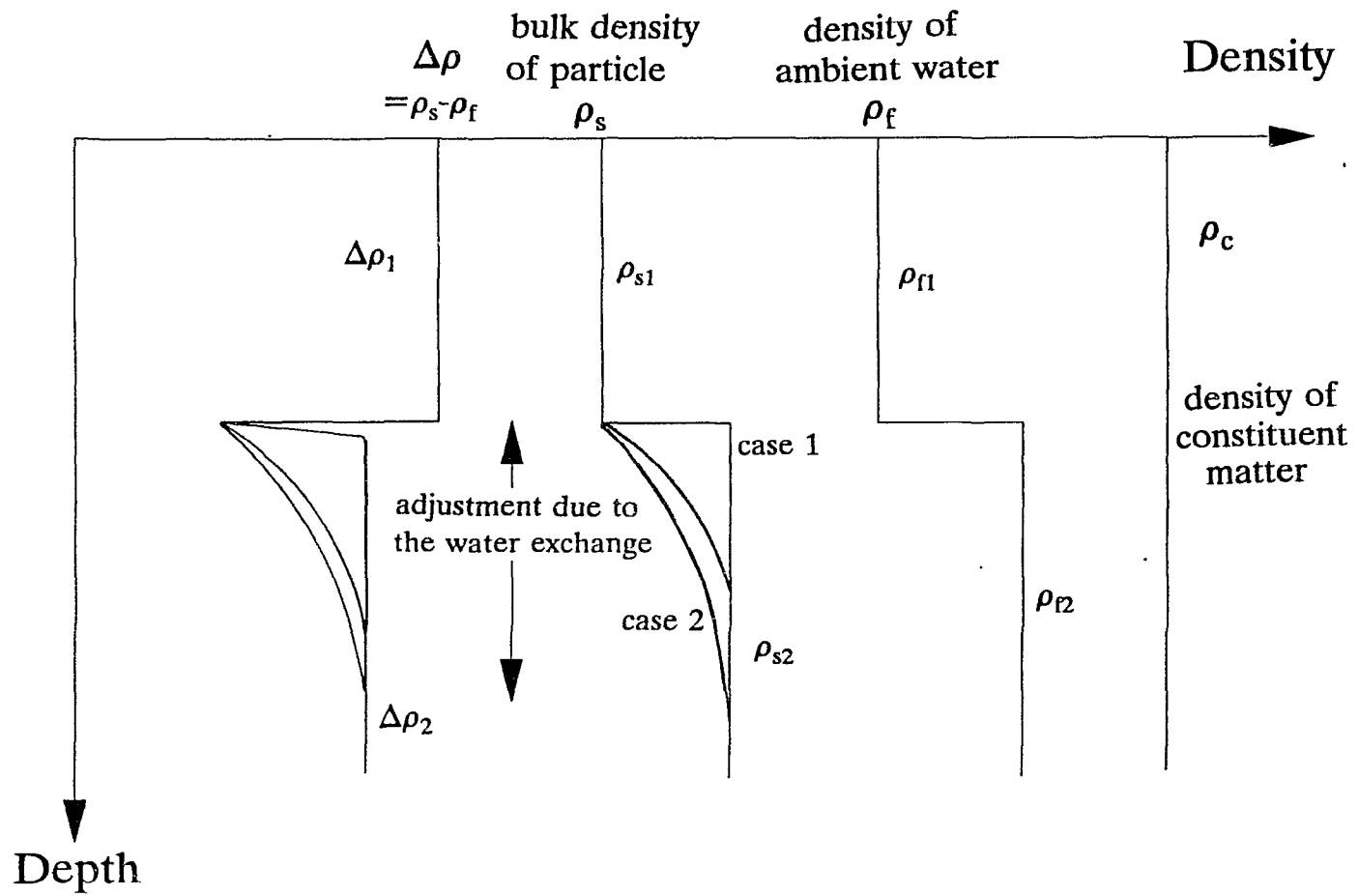


Fig. 5-8

exchange with the ambient water according to the laws of diffusion and advection in the surrounding water and permeability of the particles (Lerman, 1979). The density of the aggregate interstitial water will change from ρ_{n1} to ρ_{n2} as the proportion of the ambient water in aggregate ($\beta(t)$) increase from 0 to 100 %. $\beta(t)$ is expressed asymptotically as $\beta(t) = 1 - \exp(-t/\tau)$. τ is a time scale for the water exchange, but there is no observation of τ for marine particles available at this stage. Estimate of τ is done using a theoretical frame work later in the discussion. From equation (3), the bulk density of the particle is

$$\begin{aligned} \rho_s(t) &= (1-\alpha)\rho_c + \alpha(1-\beta)\rho_{n1} + \alpha\beta\rho_{n2} \\ &= (1-\alpha)\rho_c + \alpha\rho_{n1} + \alpha(1-\exp(-t/\tau))(\rho_{n2}-\rho_{n1}) \end{aligned} \quad (4)$$

The density difference between the particle and ambient water ($\Delta\rho$) shows a minimum value just below the density discontinuity, because the particle contains interstitial water of lower density (ρ_{n1}) than that of the ambient water (ρ_{n2}). As particle bulk density changes with time - therefore with depth, $\Delta\rho$ reaches the new adjusted value $\Delta\rho_2$ as follows,

$$\begin{aligned} \Delta\rho(t) &= (1-\alpha)\rho_c + \alpha(1-\beta)\rho_{n1} + \alpha\beta\rho_{n2} - \rho_{n2} \\ &= \{(1-\alpha)\rho_c + \rho_{n1} - \rho_{n2}\} + \alpha(1-\exp(-t/\tau))(\rho_{n2} - \rho_{n1}) \end{aligned} \quad (5) \quad \text{In the}$$

following example, two extreme cases, (1) instantaneous water exchange ($\tau \rightarrow 0$, $\therefore \beta \rightarrow 1$), and (2) no water exchange ($\tau \rightarrow \infty$, $\therefore \beta \rightarrow 0$), are demonstrated.

(case 1)

When water exchange inside with ambient water outside of aggregates occurs instantaneously, particles have a new settling velocity adjusted to the ambient fluid

density at the pycnocline (ρ_{12}),

$$\begin{aligned}\Delta\rho_2 &= \rho_{12} - \rho_{12} \\ &= (1-\alpha)\rho_c + \alpha\rho_{12} - \rho_{12} \\ &= (1-\alpha)(\rho_c - \rho_{12})\end{aligned}\quad (6)$$

Therefore

$$\begin{aligned}\Delta\rho_2/\Delta\rho_1 &= v_2/v_1 \\ &= \{(1-\alpha)(\rho_c - \rho_{12})\}/\{(1-\alpha)(\rho_c - \rho_{11})\} \\ &= (\rho_c - \rho_{12})/(\rho_c - \rho_{11})\end{aligned}\quad (7)$$

This result shows that when the water within exchanges with water outside of aggregates instantaneously, the ratio of settling velocity between the two layers, above and just below the pycnocline, is independent of the porosity and becomes a function of the density of constituent matter of aggregates and the density of water masses.

From equation (2),

$$\begin{aligned}C_2/C_1 &= v_1/v_2 \\ &= (\rho_c - \rho_{11})/(\rho_c - \rho_{12}) \\ &= 1 + (\rho_{12} - \rho_{11})/(\rho_c - \rho_{12})\end{aligned}\quad (8)$$

At the surface pycnocline, where a density discontinuity is usually strong, ($\rho_{12} - \rho_{11}$) \approx 0.002 g/cm³ and $\rho_{12} = 1.026$ g/cm³ are used from the data from "Halifax Transect" (Fig. 5-2); and from Chapter 1, $\rho_c > 1.1$ g/cm³. Using these values,

$$C_2/C_1 < 1.027$$

and when $\rho_c = 1.497$ (Table 2-1),

$$C_2/C_1 = 1.004$$

A linear relationship between light-scatter and SPM concentration in the Halifax Transect data is shown in Fig. 5-9 and is,

$$Y=4.679X+2.584$$

(X=SPM concentration, Y=light-scatter measurement)

So C_2/C_1 calculated above is equivalent to < 0.5 % of light-scatter change when the SPM concentration is 0.1 mg/l (value at the pycnocline at station 3) and < 0.9 % when the SPM concentration = 0.25 mg/l (value at the pycnocline at station 1). This range is much smaller than the observed light-scatter change at the pycnocline (\approx 10 % at station 1 and 20 % at station 3 in Fig. 5-2) and is of the same range as the noise level (0.9 %). At the smaller scale density discontinuity, $(\rho_{12} - \rho_{11}) < 0.002$, the change of light-scatter signal is much less than the values calculated above.

The results suggest that under the condition of instantaneous water exchange the effect of density discontinuity of the water column on the retardation of particle settling velocity does not explain the observed accumulation of particles at the pycnocline.

(case 2)

If exchange of water inside with ambient water outside of the aggregate is minimal, (4) is

$$\begin{aligned} \Delta\rho_2 &= \rho_{12} - \rho_{11} \\ &= (1-\alpha)\rho_c + \alpha\rho_{11} - \rho_{11} \\ &= \alpha(\rho_{11} - \rho_c) + (\rho_c - \rho_{11}) \end{aligned} \quad (9)$$

Fig. 5-9 Light-scatter measurement and SPM concentration relationship for the "Halifax Transect" data. A linear regression for the data is

$$Y=4.679*X+2.584$$

(Y=light-scatter, X=SPM concentration)
(r=0.68, significance at the level $P<0.05$)

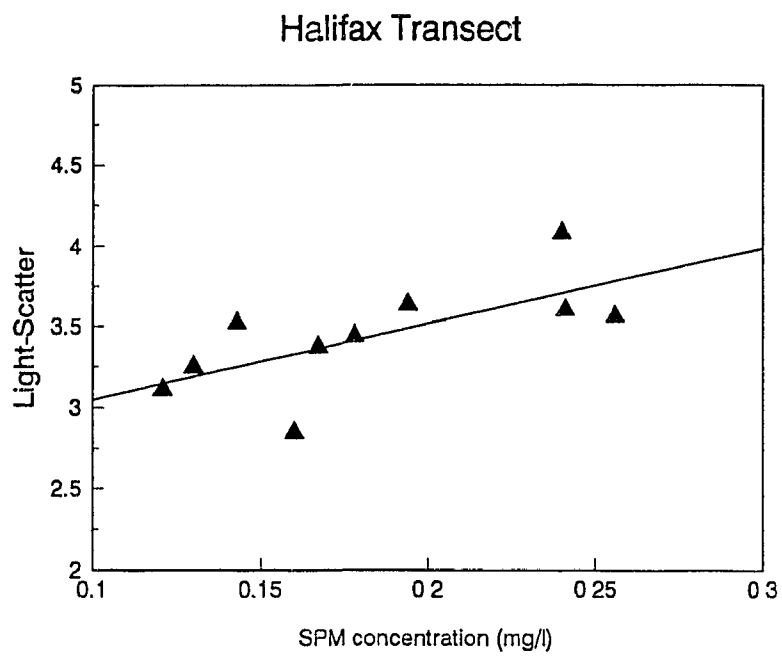


Fig. 5-9

Therefore,

$$\begin{aligned}\Delta\rho_2/\Delta\rho_1 &= v_2/v_1 \\ &= \{\alpha(\rho_n - \rho_c) + (\rho_c - \rho_w)\} / \{(1-\alpha)\rho_c + \alpha\rho_n - \rho_n\}\end{aligned}\quad (10)$$

and,

$$\begin{aligned}C_2/C_1 &= v_1/v_2 \\ &= \{(1-\alpha)(\rho_c - \rho_n)\} / \{\alpha(\rho_n - \rho_c) + (\rho_c - \rho_w)\}\end{aligned}\quad (11)$$

Equations (9) and (11) indicate that when $\alpha \rightarrow 0$, i.e., solid particles that do not include interstitial water, $C_2/C_1 \rightarrow \rho_c / (\rho_c - \rho_w)$ and when $\alpha \rightarrow 1$, i.e., particles that do not include much constituent material, and water inside of particles does not escape, a particle cannot sink below its equivalent density. Under the same conditions of ρ_n , ρ_w and ρ_c as in case 1 with a porosity $\alpha = 0.938$ (Chapter 4, Table 2-1),

$$C_2/C_1 = 1.75$$

This is equivalent to 11 % and 23 % of light-scatter increase, when SPM = 0.1 mg/l and 0.25 mg/l, respectively. This is the same range as the observed light-scatter peaks at the pycnocline. As porosity increases, C_2/C_1 will become larger; however, at the point when particle bulk density is equivalent to the ambient density, particles become neutrally buoyant and stop sinking. When the density difference of ambient water is 0.002 g/cm^3 ($1.024\text{-}1.026 \text{ g/cm}^3$) and constituent matter density is 1.1 g/cm^3 , the particles become neutrally buoyant when the porosity is 0.998 with no water exchange. Porosity of 0.998 was observed for the diatom aggregates (Chapter 4, Table 2-2).

The general form for C_2/C_1 with the saturation of the ambient water in aggregate β (% of interstitial water) is,

$$C_2/C_1 = v_1/v_2 = \{(1-\alpha)(\rho_c - \rho_n)\} / \{(1-\alpha)\rho_c + (1-\beta)\alpha\rho_n + \beta\alpha\rho_n - \rho_n\} \quad (12)$$

Changes of C_2/C_1 depending on β under different conditions are shown in Fig. 5-10.

When the constituent matter density is large ($\rho_c = 1.5 \text{ g/cm}^3$), or density discontinuity is weak ($\rho_n = 1.024 \text{ g/cm}^3$ and $\rho_n = 1.02405 \text{ g/cm}^3$), with a low proportion of interstitial water exchanged, increase of SPM concentration at the pycnocline is small. As the proportion of interstitial water exchange with ambient water becomes higher, there is less accumulation of particulate matter at the pycnocline; however, when stratification is weak there is no significant difference.

DISCUSSION

This simple model demonstrates the relationship between the strength of water density stratification, density of the particle and the accumulation of particles at a density discontinuity. The importance of the rate of water exchange between the aggregate interior and ambient sea water for influencing the distribution of particles at a density discontinuity layer is illustrated. Of primary importance in this exchange is the permeability of marine particles - a parameter that is little known and needs to be studied. The time scale of water exchange, τ , is estimated from the diffusion and advection flux into the aggregates. To evaluate the magnitude of diffusion and

Fig. 5-10 Particle accumulation (C_1/C_2) change with the proportion of the interstitial water exchange with various conditions.

(a) $\rho_c = 1.1 \text{ g/cm}^3$, $\rho_{n1} = 1.024$, $\rho_{n2} = 1.026$, $\alpha = 0.938$

(b) $\rho_c = 1.5 \text{ g/cm}^3$, $\rho_{n1} = 1.024$, $\rho_{n2} = 1.026$, $\alpha = 0.938$

(a change of constituent matter density)

(c) $\rho_c = 1.1 \text{ g/cm}^3$, $\rho_{n1} = 1.024$, $\rho_{n2} = 1.02405$, $\alpha = 0.938$

(a change of the density gradient)

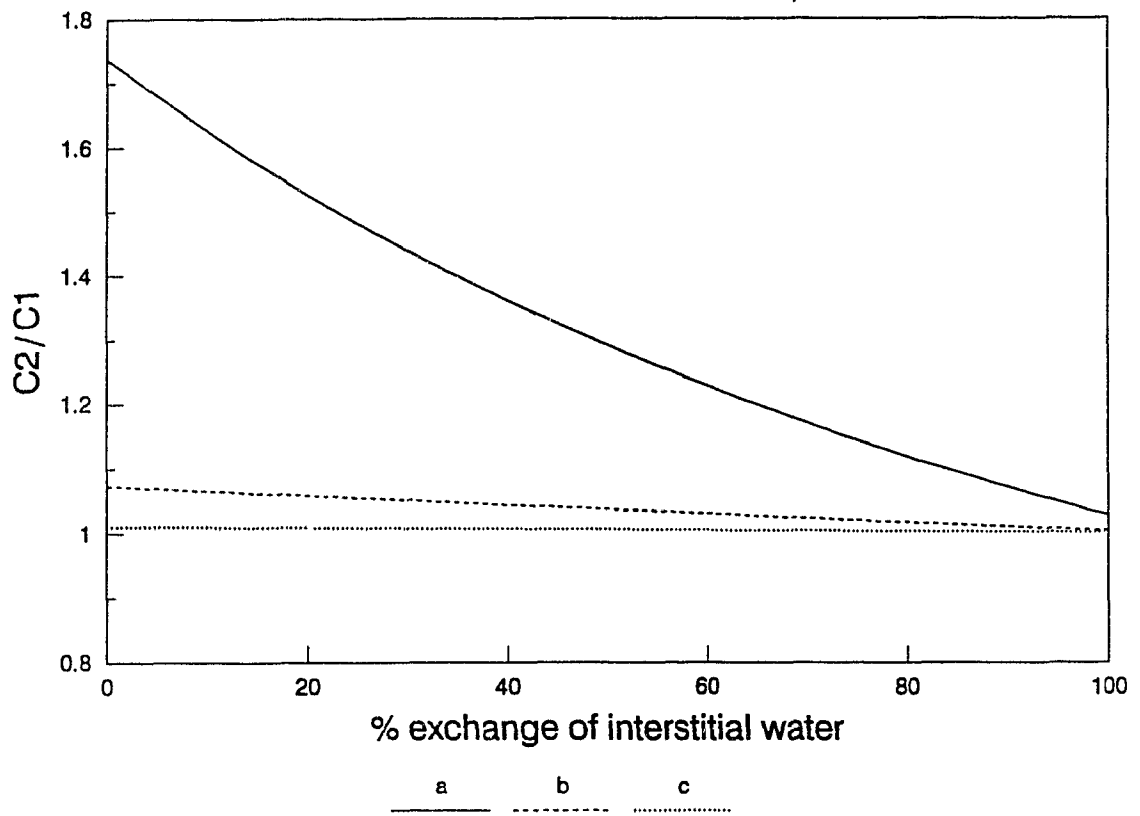


Fig. 5-10

advection flux, the Peclet number is calculated. Peclet number is a dimensionless number, defined as $Pe=LU/D$. Here, D is the diffusion coefficient, L is the average distance of migration and U is interstitial water flow velocity. When $Pe \ll 1$, diffusion is the major process and when $Pe \gg 1$, advection is the major process. Logan and Hunt (1987) predicted velocities of intra-aggregates flow from $1 \mu\text{m s}^{-1}$ for organic aggregates with constituent density $\rho_c=1.06 \text{ g cm}^{-3}$, and $100 \mu\text{m s}^{-1}$ for the heavier mineral aggregates with density of constituent matter $\rho_c=2.65 \text{ g cm}^{-3}$. The diffusion coefficient for a porous medium is approximately related to the porosity (α) and is given as $D=D_0\alpha^2$ (Lerman, 1979). Diffusivity of heat (D_T) is $1 \times 10^{-3} \text{ cm}^2/\text{s}$, and of salt (D_s) is $1 \times 10^{-5} \text{ cm}^2/\text{s}$. Since porosity is >0.938 , D_T for the aggregates is $>0.88 \times 10^{-3} \text{ cm}^2/\text{s}$ and D_s is $>0.88 \times 10^{-5} \text{ cm}^2/\text{s}$. Using these values and $L=1 \text{ mm}$ as typical aggregate size and $U=1 \mu\text{m s}^{-1}$, the range of Peclet numbers for marine organic aggregates is $10^{-2} < Pe < 1$. For mineral aggregates, the Peclet number is $1 < Pe < 10^2$. Therefore for marine organic aggregates, diffusion flux is more important than advection flux in terms of interstitial water exchange and for mineral aggregates, advection flux is more important. Next, the time scale of water exchange due to diffusion is estimated. Water exchange between the aggregate interior and ambient sea water is expressed as a saturation of ambient water in aggregate interior by the diffusion process. Diffusion in spheres is expressed in the following equation (Jacobs, 1967),

$$\frac{\partial C}{\partial t} = \frac{D}{r^2} \left(\frac{\partial}{\partial r} r^2 \frac{\partial C}{\partial r} \right) \quad (13)$$

C is the concentration of the substrate at distance r from the centre of the sphere at

time t and D is the diffusion coefficient. Equation (13) is solved to obtain the saturation of ambient water in the interstitial water ($\beta_d(t)$) by the equation,

$$\beta_d(t) = 1 - \frac{6}{\pi^2} \{ \exp(-\pi^2 Dt/r^2) + \frac{1}{4} \exp(-4\pi^2 Dt/r^2) + \dots \} \quad (14)$$

in which r is the size of aggregates, D is the diffusion coefficient. Using 1 mm as aggregate size and the diffusion coefficients of salt and heat for a porous medium, $\beta_d(t)$ is calculated (Fig. 5-11). From equation (14) and Fig. 5-11, the time scale of water exchange (τ) ranges from 2-3 seconds to 10 minutes. The sinking velocities of particles (v) is about 10 m/day to 100 m/day for organic aggregates, thus the depth for adjustment of particle bulk density due to water exchange is $v\tau = 0.2$ mm to 0.7 m. For the fast settling heavy mineral aggregates (settling velocity of 100-200 m/day), advective flux is a primary process of water exchange and interstitial water flow velocity is estimated as $100 \mu\text{m s}^{-1}$ by Logan and Hunt (1987). Therefore the time scale for the 1 mm size particle is about 10 seconds and depth for the adjustment is 1 cm to 2 cm. These results show that interstitial water exchange occurs within 1 m from the density discontinuity for slow sinking (10-100 m/day) organic aggregates and within 2 cm for fast sinking (100-200 m/day) mineral aggregates. However these results represent a very rough scaling. The time scale of diffusion processes in a permeable object is variable due to the complication of porous structure and hydrodynamic effects associated with the surfaces of settling aggregates. For convective exchange of water, the tortuosity of marine particles must be known. Moreover, the organic films produced by microbes on the surface of marine particles (Wangersky, 1977) may hinder diffusion and advection flux of ambient sea water into aggregates.

Fig. 5-11 Saturation of ambient water in aggregates by diffusion process as a function of time. Solid line is for the saturation using the diffusion coefficient of salt for porous medium ($D_s=0.88 \times 10^{-5} \text{ cm}^2 \text{ s}^{-1}$) and dashed line is for the saturation using the diffusion coefficient of heat for porous medium ($D_T=0.88 \times 10^{-3} \text{ cm}^2 \text{ s}^{-1}$).

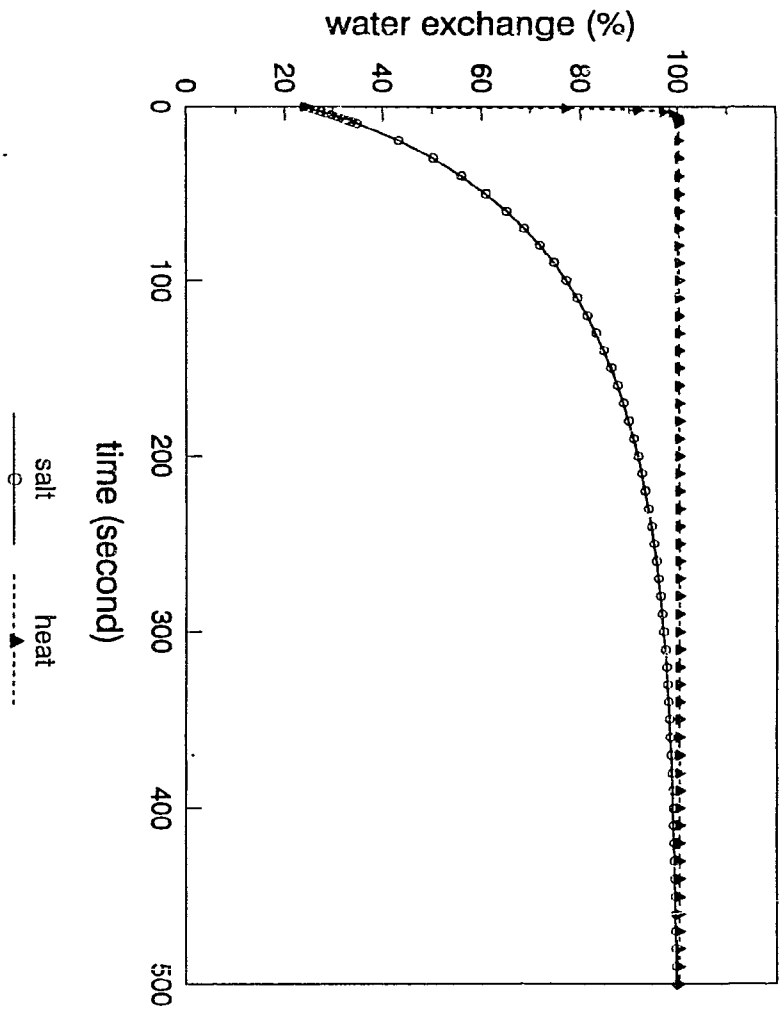


Fig. 5-11

To explain the accumulation of particulate matter at the surface pycnocline, for example $(\rho_2 - \rho_1) > 0.002 \text{ g/cm}^3$, in terms of the retardation of settling velocity in this layer, it is necessary to assume that the water exchange rate between the interior of the aggregate and ambient sea water is slow compared to the settling velocity. Since there is no measurement for permeability of aggregates, other possible mechanisms need to be considered as well. One such possibility is the existence of neutrally buoyant particles. Neither light-scatter measurements nor SPM measurements can distinguish between neutrally buoyant or sinking particles, hence the distribution of suspended (neutrally buoyant) particles is unknown in the ocean. However, if neutrally buoyant particles are distributed homogeneously over the range of sea water density, more particles will be observed for a unit depth at the pycnocline. Moreover, it is known that phytoplankton regulate their buoyancy due to light intensity, nutrient concentration and physiological stage (Smayda, 1970; Steel and Yentsch, 1960; Ballek and Swift, 1986). This abundance of a living phytoplankton population is a part of the cause of observed light-scatter signals in the surface water. However, it is important to note that nonliving POC represents something like 10 times the living fraction in the ocean.

Another possible mechanism for accumulation of particulate matter at the pycnocline is the turbulent effect that keeps particles in suspension. Lande and Wood (1987) modeled the suspension times of particles in the upper ocean as a two layer system, and demonstrated that particles with a slow sinking rate make many rapid excursions between the interior of the mixed layer and the top few meters of

the thermocline. The result is a reduced sinking rate at the thermocline. However, the turbulent effect on particle distribution is still little known in either theoretical studies or in measurements in the laboratory or in the field.

The model described here does not include a viscosity change in the pycnocline. Where the pycnocline is derived from thermal stratification, the viscosity change in this layer can be important for particles of small size. At this stage, it is not possible to evaluate such effects quantitatively.

The model in this study shows that meso- and micro- scale density discontinuities ($\Delta\rho_t < 0.00005 \text{ g/cm}^3$) are not sufficient to trap settling particles and cause the accumulation of particulate matter detected in the light-scatter measurements of this study. Narrow peaks exceeding instrument noise level probably represent the occurrence of a single large aggregate (Thorpe and White, 1988). The decrease of light-scatter observed below the pycnocline indicates an increase in settling velocity or dissolution of particles.

CONCLUSIONS

Data describing vertical particle distributions, obtained by light-scatter measurements, together with the density structure of the water column, were collected from the western North Atlantic, "Halifax Transect". Comparisons were made for measurements on the Scotian Shelf, Slope and Gulf Stream stations, a coastal basin, Bedford Basin, and an offshore basin, Emerald Basin. Accumulation of particulate matter was observed at the surface strong density interface ($\Delta\rho > 0.002 \text{ g/cm}^3$), but there was no apparent relationship between the weak density stratification observed in mid- and deep- water and the light-scatter measurements.

A simple model was used to assess the effect of density stratification on the particle distribution. The model demonstrates the importance of the density of constituent matter of particles and aggregate permeability for settling through a density discontinuity. The higher the aggregate permeability and density of constituent matter of particles, the lower tendency for particles to accumulate at a density discontinuity. Where the density stratification is weak ($\Delta\rho_f < 0.05 \text{ kg/m}_3/\text{m}$ which is the range of most of observed density discontinuities in mid- and deep water column), particle accumulation is not sufficient to be detected by the light-scatter measurement used in this study.

Chapter Six
Summary and Conclusions

Summary and Conclusions

(I) A high particle accumulation on top of the pycnocline was observed from coastal to offshore regions; however, there was no apparent relationship between meso- to microscale density structure and particle distribution in mid- and deep water. Instead, the particle patchiness below the mixed layer was influenced by biological and physical processes.

Light-scatter measurements together with the simultaneous measurements of salinity and temperature were conducted in the western North Atlantic, "Halifax Transect" - including the Scotian Shelf, the Scotian Slope and the Gulf Stream stations, in a coastal basin in Nova Scotia and Emerald Basin on the Scotian Shelf. Results showed high particle accumulation on top of the surface pycnocline in all sites; accumulation was especially evident in the coastal basin during the spring bloom period. In mid- and deep- water, strong patchiness of particle abundance was observed in Bedford Basin and in Emerald Basin, however there was no apparent relationship with density profile of the water column. Instead, particle distributions below the mixed layer were strongly influenced by biological effects in the coastal site, e.g., in formation of a bottom nepheloid layer. In contrast, intermediate nepheloid layers observed in Emerald Basin were caused by physical control of particle transport. In the "Halifax Transect", there was no strong light-scatter peak below the

surface pycnocline, and small narrow nephel signals there do not appear to be associated with the density structure of the water column.

Bottom nepheloid layer formation was observed through a time series study of the vertical distribution of suspended particles conducted during and after a phytoplankton bloom in a small coastal basin, Bedford Basin, Nova Scotia, Canada. Through the period of the study three general stages were observed; however, the profiles of the particle distribution also reflected episodic events such as fresh water river input and storm mixing. During the peak of the spring bloom in March, the water column was characterized by a high particle load in the surface mixed layer (0-8 m) with a smaller but uniform particle load in the middle and bottom water. The second stage (mid-April to July) featured bottom nepheloid layer formation (45-65 m) and a high particle load in the surface water with minimum light-scatter at mid-depth. This formation of the bottom nepheloid layer started 2-3 weeks after the settling of the surface spring phytoplankton bloom and persisted for a much longer period (3 months) than has been reported for the open ocean (20 days). In the third stage, in late July to August, the bottom nepheloid layer thinned and the mid-water became progressively clear. The light-scatter measurements revealed a patchiness in the vertical particle distribution. Water samples were selectively collected from the depths corresponding to light-scatter peaks for measurements of particulate organic carbon (POC) concentration, weight/volume concentration of suspended particulate matter (SPM), and microscope observation to identify particle characteristics. These

observations demonstrated that the distribution of particles is heterogeneous with depth as well as with time, not only in concentration but also in particle composition. As a bottom nepheloid layer developed, particles in this layer changed from predominantly intact diatom chain assemblages with high POC concentration to small and degraded aggregates with low POC concentration.

Optical methods allow continuous measurement of the distribution of particles. One important application of optical methods is detection of intermediate nepheloid layers - nepheloid layers that are below the mixed layer and separated from the bottom nepheloid layer. These intermediate nepheloid layers are considered very important for transporting particulate matter from the ocean margin to the ocean interior.

Strong intermittent intermediate nepheloid layers were observed on the Scotian Shelf in late April, 1987. These nepheloid layers were at 180-190 m in Emerald Basin and at 120-140 m in the adjacent basin-both well below the mixed layer and about 90 m above the sea bed. A slightly higher Chlorophyll a concentration was measured in the intermediate nepheloid layer, compared to the concentration of the water above and in the bottom nepheloid layer. Mechanisms that may cause these observed intermediate nepheloid layers are assessed from both biological and physical considerations. Depths of intermediate nepheloid layers coincide with the critical depth for possible generation, amplification and breaking of internal waves with semi-diurnal (M_2) internal tide frequency. The criterion for generation or concentration

of energy of internal waves is met when the characteristic slope is close to the topographic slope. Intermittent particle resuspension at the "critical" depth on the Basin slope, along with temporal variability of the currents, appears to be the cause of the observed intermittency of the intermediate nepheloid layers. Observations of intermediate nepheloid layers at three stations in Emerald Basin (40 km apart, from the west side of the slope to the east side of the slope) and the adjacent basin (north of Emerald Basin) indicate that this process is not a rare event, but rather a basin wide phenomenon. Low-frequency slope water intrusion driven by storm surges during winter is predicted to result in mass transport of sediment from the outer shelf to the inner shelf basin. However, freshly deposited particles during the non-storm season, especially biogenic particles after a spring phytoplankton bloom, are sorted, reworked and transported by more regularly occurring processes such as internal waves.

(II) A system was developed that enables measurements of physical characteristics of marine particles, including size, settling velocity and density of constituent matter simultaneously and independently for each aggregate. Density of aggregate constituent matter was presented for the first time for marine aggregates.

Knowledge of physical characteristics of particles, including size, density and shape, are important for understanding distribution and transport processes of suspended particulate material in the ocean. Methods for determining size, shape

and settling velocity of marine particles have progressed rapidly over the past ten years and include: *in situ* optical methods, e.g., photography coupled with sediment traps, holographic methods and methods using SCUBA diving. The density of marine particles, however, is not well known and has proven especially difficult to measure directly.

The system for measuring aggregate characteristics consists of a linear density gradient column, made from a solution of metrizamide in sea water, that permits the direct measurement of the constituent matter density. The density gradient column has been integrated into a system that also allows independent measurements of settling velocity, and aggregate size and shape. The measurements reported here are the first direct density measurements of any type for marine aggregates, and although the constituent matter density does not relate directly to settling velocity, these measurements will help reduce errors in estimates of other physical parameters, e.g., porosity. Aggregates produced in the laboratory from a diatom culture and from particles collected in coastal waters have been used to test the system. The results show that the density of constituent matter from these sources is $>1.095 \text{ g/cm}^3$ and porosity >0.938 .

(III) A model was developed to evaluate the role of physical characteristics of marine aggregates in settling through density discontinuity layers. The important parameters include density of constituent matter, porosity and exchange rate of interstitial water with ambient sea water. The model was developed using the measurements from the

field and the laboratory.

High constituent matter density and high porosity of aggregates produced in the laboratory, both suggest that the small density gradients ($<0.05 \text{ kg/m}^3/\text{m}$) that were found below the surface pycnoclines in the field, were not sufficiently strong to trap a sufficient amount of particulate matter to be detected by the light-scatter meter. Accumulation of marine particles on the surface pycnocline is partly explained by the retardation of settling velocity due to the density effect. The model demonstrates the importance of physical parameters of aggregates for settling behaviour and distribution of marine particles at density discontinuity layers. Important parameters include density of constituent matter, porosity and exchange rate of interstitial water of aggregates. The first parameter has not previously been known for marine particles.

APPENDIX I

***Estimate of the Noise Level for
Light-Scatter Measurements***

The noise level of the light-scatter measurement was calculated to evaluate the significance of the light-scatter peaks observed in the field. The light-scatter signal includes both light-scatter by the particle patchiness ("true" light-scatter) and the noise. The noise is composed of instrumental (electronics) noise and statistical noise by particles. The autocorrelation coefficient (r) with lag Δz is defined as

$$\begin{aligned} r &= \frac{E[LS(z)LS(z+\Delta z)]}{(E[LS(z)^2]E[LS(z+\Delta z)^2])^{1/2}} \\ &= \frac{E[LS(z)LS(z+\Delta z)]}{\text{Var}(LS(z))} \end{aligned} \quad (1)$$

Here E is the mathematical expectation, $LS(z)$ is the light-scatter measurement at depth z and the mean of light-scatter is moved to 0. $\text{Var}(LS(z))$ is a variance of light-scatter measurement. Since light-scatter measurement includes both "real" light-scatter signal ($LS'(z)$) and noise ($N(z)$), $LS(z)$ is expressed as

$$LS(z) = LS'(z) + N(z) \quad (2)$$

Using relation (2), (1) is expressed as follows,

$$\begin{aligned} r &= \frac{E[(LS'(z) + N(z))(LS'(z + \Delta z) + N(z + \Delta z))]}{\text{Var}(LS(z))} \\ &= \frac{E[LS'(z)^2]}{\text{Var}(LS(z))} \\ &= \frac{\text{Var}(LS'(z))}{\text{Var}(LS(z))} \end{aligned}$$

r is calculated for lag Δz (Fig. I-1). When lag is 0, r is extrapolated to 0.787. $\text{Var}(\text{LS}(z))$ is calculated from the light-scatter measurement on Mar. 10 in Bedford Basin and is 0.043. Therefore the variance of "true" light-scatter signals is 0.034. Since variance of light-scatter contains the variance of "true" light-scatter and noise, the variance of the noise is calculated from the difference between the variance of the light-scatter ($\text{Var}(\text{LS}(z))$) and the variance of the "true" light-scatter ($\text{Var}(\text{LS}'(z))$). Variance of the noise is 0.009 and 95% of confidence interval is $\text{LS}(z) \pm 0.024$. This value, 0.009, is in good agreement with the observed noise level at the "Halifax Transect" Station 3, the below 100m water mass (standard error of Y estimate is 0.10, so variance is 0.01), where light-scatter signals are at the level of the detection limit of the instrument.

Fig. I-1 Autocorrelation coefficient of light-scatter with lag Δz
 $Y = -0.5596X + 0.7865$ ($r = 0.98$, significant at the level of
 $P < 0.001$)

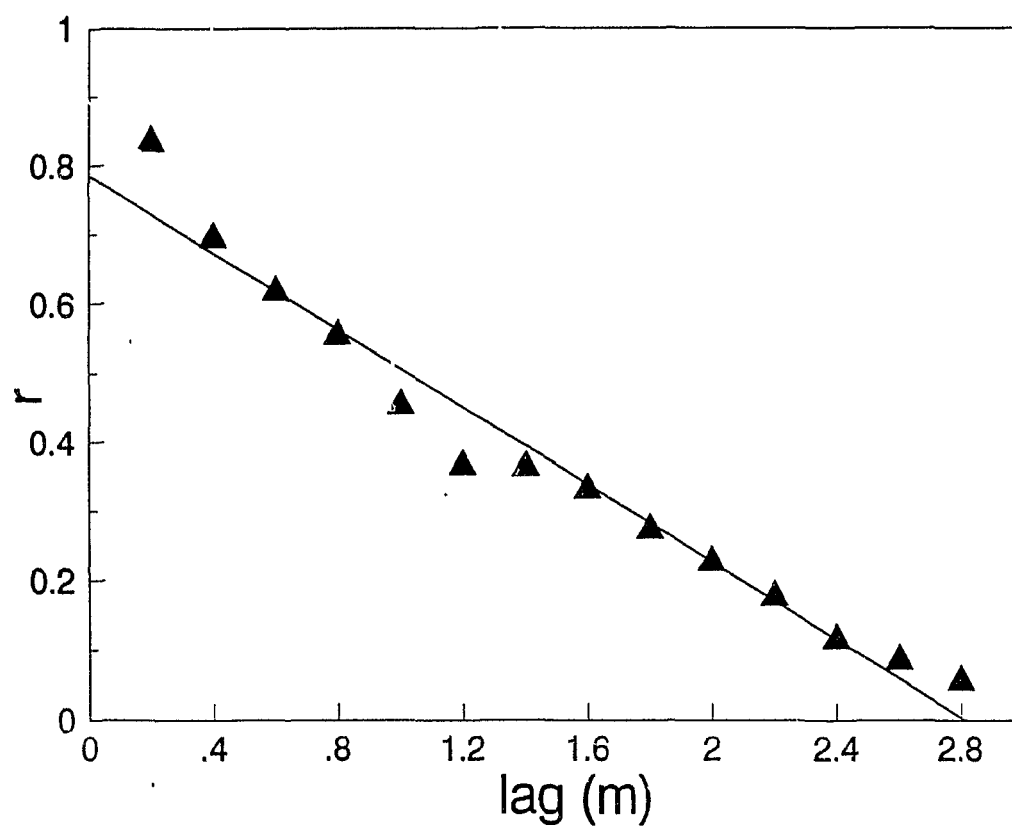


Fig. I-1

References

- Allredge, A.L. (1972) Abandoned larvacean houses: A unique food source in the pelagic environment. *Science*, **117**, 885-887.
- Allredge, A.L. (1976) Discarded appendicularian houses as source of food, surface habitat, and particulate organic matter in planktonic environments. *Science*, **21** 14-23.
- Allredge, A.L. (1979) The chemical composition of macroscopic aggregates in two neritic seas. *Limnology and Oceanography*, **24**, 855-887.
- Allredge, A.L. and Y. Cohen (1987) Can microscale chemical patches persist in the sea? Microelectrode study of marine snow, faecal pellets. *Science*, **235**, 689-691.
- Allredge, A.L., J.J. Cole and D.A. Caron (1986) Production of heterotrophic bacteria inhabiting macroscopic organic aggregates (marine snow) from surface waters. *Limnology and Oceanography*, **31**, 68-78.
- Allredge, A.L. and C. Gotschalk. (1988). In situ settling behaviour of marine snow. *Limnology and Oceanography*, **33**(3), 339-351.
- Allredge A.L. and C.C. Gotschalk (1989) Direct observation of the mass flocculation of diatom blooms: characteristics, settling velocities and formation of diatom aggregates. *Deep-Sea Research*, **60**, 159-171.
- Allredge, A.L. and M. W. Silver (1988) Characteristics, dynamics and significance of marine snow. *Progress in Oceanography*, **20**, 41-82.
- Albert, M. A., W. G. Deuser, S. Honjo and C. Stienen (1991) Seasonal and depth-related change in the source of sinking particles in the North Atlantic. *Nature*, **354**, 136-1139.
- Amos, C.L. and J.T. Judge (1991) Sediment transport on the eastern Canadian continental shelf. *Continental Shelf Research*, **11**, 1037-1068.
- Asper, V.L. (1987a) A review of sediment trap technique. *Marine Technology Society Journal* **21**, 18-25.
- Asper, V.L. (1987b) Measuring the flux and sinking speed of marine snow aggregates. *Deep-Sea Research*, **34**, 1-17

- Aybulatov, N.A. and Z.T. Novikova (1984) Quantitative distribution of suspended matter in shelf waters of the Black Sea. *Oceanology*, **24**, 721-726
- Azetsu-Scott K. and B.D. Johnson (1992) Measuring physical characteristics of particles: A new method of simultaneous measurement for size, settling velocity and density of constituent matter of particles. *Deep-Sea Research* (in press)
- Bacon, M. P. and R. F. Anderson (1982) Distribution of thorium isotopes between dissolved and particulate forms in the deep sea. *Journal of Geophysical Research*, **87**, 2045-2056
- Bacon, M. P., C. Huh, A. P. Fleer and W. G. Deuser (1985) Seasonality in the flux of natural radionuclides and plutonium in the deep Sargasso Sea. *Deep-Sea Research*, **32**, 273-286
- Baines, P.G. (1974) The generation of internal tides over steep continental slopes. *Phil. Trans. Roy. Soc. London*, **227**, 1263, 27-58.
- Baker, E. T, H. B. Milburn and D. A. Tennant (1988) Field assessment of sediment trap efficiency under varying flow conditions. *Journal of Marine Research* **46**, 573-592
- Ballek, R.W. and E. Swift (1986) Nutrient- and light-mediated buoyancy control of the oceanic non-motile dinoflagellate *Pyrocystis noctiluca* Murray ex Haeckel (1890). *Journal of Experimental Marine Biology and Ecology*, **101**, 175-192.
- Banse, K. (1990) New views on the degradation and disposition of organic particles as collected by sediment traps in the open sea. *Deep-Sea Research*, **37**, 1177-1195.
- Batchelor, G.K. 1967. *An Introduction to Fluid Dynamics*. Cambridge University Press, 615pp.
- Berger, W.H. (1989) Global maps of ocean productivity. In: *Productivity of the Ocean: Present and Past*, W.H. Berger, V.S. Smetacek and G. Wefer, editors, Wiley, New York, pp. 429-455.
- Berner, R.A. (1982) Burial of organic carbon and pyrite sulphur in the modern ocean: its geochemical and environmental significance. *American Journal of Science*, **282**, 451-473.
- Billett D.S.M., R.S. Lampitt, A.L. Rice and R.F.C. Mantoura (1983) Seasonal sedimentation of phytoplankton to the deep sea benthos. *Nature*, **302**, 520-522

- Biscaye, P.E. and S.L. Eittreim (1977) Suspended particulate loads and transport in the nepheloid layer of the abyssal Atlantic Ocean. *Marine Geology*, **23**, 155-172.
- Bishop J.K.B., and J.M. Edmond (1976) A new large volume *in situ* filtration system for sampling oceanic particulate matter. *Journal of Marine Research*, **34**, 181-198
- Bishop, J. K., and J. Marra (1984) Variations in primary production and particulate carbon flux through the base of the euphotic zone at the site of the sediment trap intercomparison experiment (Panama Basin). *Journal of Marine Research*, **42**, 189-206
- Brewer, P. G., D. W. Spencer, P. E. Biscaye, A. Hanley, P. L. Sachs, C. L. Smith, S. Kadar and J. Fredericks (1976) The distribution of particulate matter in the Atlantic Ocean. *Earth and Planetary Science Letters*, **32**, 393-402
- Bruland, K. W. (1983) Trace elements in sea-water. In: *Chemical Oceanography*, J.P. Riley and R. Chester, editors, Academic Press, London, **8**, 157-220.
- Bruland, K.W. and M.W. Silver (1981) Sinking rate of faecal pellets from gelatinous zooplankton (salps, pteropods, doliolids). *Marine Biology*, **63**, 295-300.
- Buat-Ménard, P, J. Davies, E. Remoudaki, J.C. Miquel, G. Bergametti, C.E. Lambert, U. Ezar, C. Quetel, J.La Rosa and S.W. Fowler (1989) Non-steady-state biological removal of atmospheric particles from Mediterranean surface waters. *Nature*, **340**, 131-134
- Buckley, D.E. (1991) Deposition and diagenetic alteration of sediment in Emerald Basin, the Scotian Shelf. *Continental Shelf Research*, **11**, 1099-1122.
- Buesseler, K. O. (1991) Do upper-ocean sediment traps provide an accurate record of particle flux ? *Nature*, **353**, 420-423
- Butman, C. A. (1986) Sediment trap biases in turbulent flows: Results from a laboratory flume study. *Journal of Marine Research*, **44**, 645-693
- Butman, C. A., W.D. Grant and K.D. Stolzenback (1986) Predictions of sediment trap biases in turbulent flows: A theoretical analysis based on observations from the literature. *Journal of Marine Research*, **44**, 601-644
- Cacchione, D.A. and D.E. Drake (1986) Nepheloid layers and internal waves over continental shelves and slopes. *Geo-Marine Letters*, **6**, 147-152.

- Calvert, S.E. and M.J. McCartney (1979) The effect of incomplete recovery of large particles from water samplers on the chemical composition of oceanic particulates. *Limnology and Oceanography*, **24**, 532-536.
- Carder, K.L., G.F. Beardsley and H. Pak (1971) Particle size distribution in the eastern equatorial Pacific. *Journal of Geophysical Research*, **76**, 5070-5077.
- Carder, K.L., P.R. Betzer and D.W. Eggimann (1974) Physical, chemical and optical measures of suspended particulate concentrations: their intercomparison and application to the West African shelf. In: *Suspended Solids in Water*. R.J. Gibbs (ed.), Plenum, New York, 173-193.
- Caron, D.A., P.G. Davis, L.P. Madin and J.McN. Sieburth (1982) Heterotrophic bacteria and bacterivorous protozoa in oceanic macroaggregates. *Science*, **218**, 795-797.
- Caron, D.A., P.G. Davis, L.P. Madin and J.McN. Sieburth (1986) Enrichment of microbial populations in macroaggregates (marine snow) from surface waters of the North Atlantic. *Journal of Marine Research*, **44**, 543-565.
- Cole, J. J., S. Honjo and J. Erez (1987) Benthic decomposition of organic matter at a deep-water site in the Panama Basin. *Nature*, **327**, 703-704
- Comita, P. B., R. B. Gagosian and P. M. Williams (1984) Suspended particulate organic material from hydrothermal vent waters at 21°N. *Nature*, **307**, 450-453
- Deuser W.G. (1979) Marine biota, nearshore sediments, and the global carbon balance. *Org. Geochem.* **1**, 243-247.
- Deuser, W.D. (1985) Seasonal and interannual variations in deep-water particle fluxes in the Sargasso Sea and their relation to surface hydrography. *Deep-Sea Research*, **33**, 225-246
- Deuser, W.G., F.E. Muller-Karger and C. Hemleben (1988) Temporal variations of particle fluxes in the deep subtropical and tropical North Atlantic: Eulerian versus Lagrangian effects. *Journal of Geophysical Research*, **93**, C6, 6857-6862
- Deuser W.G., E.H. Ross and R.F. Anderson (1981) Seasonality in the supply of sediment to the deep Sargasso Sea and implications for the rapid transfer of matter to the deep ocean. *Deep-Sea Research*, **28A**, 495-505
- Dickson R.R. and I.N. McCave (1986) Nepheloid layers on the continental slope west of Porcupine Bank. *Deep-Sea Research*, **33**, 791-818

- Drake, D.E. (1971) Suspended sediment and thermal stratification in Santa Barbara Channel, California. *Deep-Sea Research*, **18**, 763-769.
- Drake, D.E. (1974) Distribution and transport of suspended particulate matter in submarine canyons off southern California. In: *Suspended Solids in Water*. R.J. Gibbs, ed. Plenum Press, N.Y. 133-153.
- Drinkwater, K. and G. Taylor (1982) Monthly means of the temperature, salinity and density along the Halifax Section. *Can. Tech. Rep. Fish. Aquat. Sci.*, **1093**, 67pp.
- Ebara, S. and O. Asaoka (1985) Direct or optical observations for vertical distribution of suspended material in sea water by the use of the research submersible "SHINKAI 2000". *Technical Reports of Japan Marine Science and Technology Center*, **13**, 7-16.
- Eckman J.E., A.R.M. Nowell and P.A. Jumars (1981) Sediment destabilization by animal tubes. *Journal of Marine Research*. **39**, 361-374
- Emery, K.O. and S. Honjo (1979) Surface suspended matter off western Africa: relations of organic matter, skeletal debris and detrital minerals. *Sedimentology*, **26**, 775-794.
- Eppley, R. W. and B. J. Peterson (1979) Particulate organic matter flux and planktonic new production in the deep ocean. *Nature*, **282**, 677-680
- Fournier, R.O., J. Marra, R. Bohrer and M. Van Det (1977) Plankton dynamics and nutrient enrichment of the Scotian Shelf. *Journal of Fishery Research Board of Canada*, **34**, 1004-1018.
- Fournier, R.O., M. Van Det, J.S. Wilson and N.B. Hargreaves (1979) Influence of the shelf-break front off Nova Scotia on phytoplankton standing stock in winter. *Journal of Fishery Research Board of Canada*, **36**, 1228-1237.
- Fowler, S. W. and G. A. Knauer (1986) Role of large particles in the transport of elements and organic compounds through the oceanic water column. *Progress in Oceanography*, **16**, 147-194
- Gardner W.D. (1977) Incomplete extraction of rapid settling particles from water samples. *Limnology and Oceanography*, **22**, 764-768
- Gardner, W.D. (1980a) Sediment trap dynamics and calibration: a laboratory evaluation. *Journal of Marine Research*, **38**, 17-39.

- Gardner, W.D. (1980b) Field assessment of sediment traps. *Journal of Marine Research*, **38**, 41-52.
- Gardner, W.D. (1985) The effect of tilt on sediment trap efficiency. *Deep-Sea Research*, **32**, 349-361.
- Gardner, W.D. (1989a) Baltimore Canyon as a modern conduit of sediment to the deep sea. *Deep-Sea Research*, **36**, 323-258.
- Gardner, W.D. (1989b) Periodic resuspension in Baltimore Canyon by focusing of internal waves. *Journal of Geophysical Research*, **94**, 18185-18194.
- Gardner W.D., P.E. Biscaye, J.R.V. Zaneveld and M.J. Richardson (1985) Calibration and comparison of the LDGO nephelometer and the OSU transmissometer on the Nova Scotia Rise. *Marine Geology*, **66**, 323-344
- Gardner, W.D., K.R. Hinga and J. Marra (1983) Observations on the degradation of biogenic material in the deep ocean with implications on accuracy of sediment trap fluxes. *Journal of Marine Research*, **41**, 195-214.
- Gardner, W.D., M. J. Richardson, I. D. Walsh and B. L. Berglund (1991) In-situ optical sensing of particles for determination of oceanic processes. *Oceanography*, November, 11-17
- Gardner W.D. and L.G. Sullivan (1981) Benthic storms: temporal variability in a deep-ocean nepheloid layer. *Science*, **213**, 329-331
- Gardner, W.D. and I.D. Walsh (1990) Distribution of macroaggregates and fine-grained particles across a continental margin and their potential role in fluxes. *Deep-Sea Research*, **37**, 401-411
- Gatien, M.G. (1976) A study in the slope water region south of Halifax. *Journal of Fishery Research Board of Canada*, **33**, 2213-2217.
- Gibbs, R.J. (1974) The suspended material of the Amazon shelf and tropical Atlantic Ocean. In: *Suspended Solids in Water*. edit. R.J. Gibbs, Plenum Press, N.Y. 203-210.
- Gibbs, R.J. and L.N. Konwar (1983) Sampling of mineral flocs using Niskin bottles. *Environmental Science and Technology*, **16**, 374-375.
- Gooday A.J. and P.J.D. Lambshead (1989) Influence of seasonally deposited phytodetritus on benthic foraminiferal populations in the bathyal northeast Atlantic: the species response. *Marine Ecology Progress Series*, **58**, 53-67

- Gooday, A.J. and C.M. Turley (1990) Responses by benthic organisms to inputs of organic material to the ocean floor: a review. In: *The Deep-sea Bed: its Physics, Chemistry and Biology*. H. Charnock, J.M. Edmond, I.N. McCave, A.L. Riu and T.R.s. Wilson (eds), *Phil. Trans. Roy. soc. Lond.*
- Gordon Jr., Donald C. (1979) A microscopic study of organic particles in the North Atlantic Ocean. *Deep-sea Research*, **17**, 175-185
- Gowing, M.M. and M.W. Silver (1985) "Minipellets": A new and abundant size class of marine faecal pellets. *Journal of Marine Research*, **43**, 395-418.
- Grant J., C.W. Emerson, B.T. Hargrave and J.L. Shortle (1991) Benthic oxygen consumption on continental shelves off Eastern Canada. *Continental Shelf Research*, **11**, 1083-1097.
- Gregory D.N. and P.C. Smith (1988) Current statistics of the Scotian Shelf and Slope. *Canadian Technical Report of Hydrography and Ocean Sciences*, No. 106.
- Grimalt, J.O., B.R.T. Simoneit, J.I. Gómez-Belinchón, K. Fisher and J. Dymond (1990) Ascending and descending fluxes of lipid compounds in North Atlantic and North Pacific abyssal waters. *Nature*, **345**, 147-150.
- Gross, T.F., A.J. Williams III and A.R.M. Nowell (1988) A deep-sea sediment transport storm. *Nature*, **331**, 518-521.
- Hargrave B.T. (1978) Seasonal changes in oxygen uptake by settled particulate matter and sediment in a marine bay. *Journal of Fishery Research Board of Canada*, **35**, 1621-1628
- Hargrave B.T. and S. Taguchi (1978) Origin of deposited material sedimented in a marine bay. *Journal of Fishery Research Board of Canada*, **65**, 1604-1613
- Hecker B. (1990) Photographic evidence for the rapid flux of particles to the sea floor and their transport down the continental slope. *Deep-Sea Research*, **37**, 1773-1782.
- Herman, A.W., D.D. Someoto, C. Shunian, M.R. Mitchell, B. Petrie and N. Cochrane (1991) Sources of zooplankton on the Nova Scotia shelf and their aggregations within deep-shelf basin. *Continental Shelf Research*, **11**, 211-238.
- Hollister C.D. and I.N. McCave (1984) Sedimentation under deep-sea storms. *Nature*, **309**, 220-225.

- Honjo, S. (1978) Sedimentation of materials in the Sargasso Sea at a 5,367 m deep station. *Journal of Marine Research*, **36**, 459-492.
- Honjo, S. (1980) Material fluxes and modes of sedimentation in the mesopelagic and bathypelagic zones. *Journal of Marine Research*, **38**, 53-97.
- Honjo, S. (1982) Seasonality and interaction of biogenic and lithogenic particulate flux at the Panama Basin. *Science*, **218**, 883-884
- Honjo, S., K.W. Doherty, Y.C. Agrawal and V.L. Asper (1984) Direct optical assessment of large amorphous aggregates (marine snow) in the deep ocean. *Deep-Sea Research*, **31**, 67-76
- Honjo, S., S.J. Manganini and J.J. Cole (1982) Sedimentation of biogenic matter in the deep ocean. *Deep-Sea Research*, **29**, 609-625.
- Houghton, R.W., P.C. Smith and R.O. Fournier (1978) A simple model for cross-shelf mixing on the Scotian Shelf. *Journal of Fishery Research Board of Canada*, **35**, 414-421.
- Irwin B. (1991) Coulometric measurement of primary production, with comparison against dissolved oxygen and ^{14}C methods in a seasonal study. *Marine Ecology Progress Series*, **71**, 97-102
- Ittekkot, V. (1988) Global trends in the nature of organic matter in river suspension. *Nature*, **332**, 436-438.
- Ittekkot, V. and E.T. Degens and S. Honjo (1984) Seasonality in the fluxes of sugars, amino acids, and amino sugars to the deep ocean: Panama Basin. *Deep-Sea Research*, **9**, 1071-1083.
- Ittekkot, V., R.R. Nair, S. Honjo, V. Ramaswamy, M. Bartsch, S. Manganini and B.N. Desai (1991) Enhanced particle fluxes in Bay of Bengal induced by injection of fresh water. *Nature*, **351**, 385-387.
- Jacobs, M.H. (1967) *Diffusion Processes*. Springer-Verlag, New York, pp160
- Johnson B.D. and R.C. Cooke (1980) Organic particle and aggregate formation resulting from the dissolution of bubbles in seawater. *Limnology and Oceanography*, **25**, 653-661.
- Johnson, B.D., K. Kranck and D.K. Muschenheim (1990) Physico-chemical factors in particle aggregation. In: *The Biology of Particles in Aquatic Systems*. R.S. Wotton (ed), CRC Press, 57-82.

- Johnson B.D. and P.J. Wangersky (1985) A recording backward scattering meter and camera system for examination of the distribution and morphology of macroaggregates. *Deep-Sea Research*, **32**, 1143-1150.
- Jumars P. A. and A. R. M. Nowell (1984) Effects of benthos on sediment transport: difficulties with functional grouping. *Continental Shelf Research*, **3**, 115-130
- Kajihara, M. (1971) Settling velocity and porosity of large suspended particles. *Journal of the Oceanographic Society of Japan*, **22**, 158-161.
- Karl, D. M., G. A. Knauer and J. H. Martin (1988) Downward flux of particulate organic matter in the ocean: a particle decomposition paradox. *Nature*, **332**, 438-441.
- Kawana, K. and T. Taniyoto (1979) Suspended particles near the bottom in Osaka Bay. *Journal of Oceanographical Society of Japan*, **35**, 75-81.
- King, L.H. (1970) Surficial geology of the Halifax-Sable Island Map area. *Marine Science Paper 1*, Department of Energy, Mines and Resources, Ottawa, 16pp.
- King, L.H. and G.B. Fader (1986) Wisconsinan glaciation of the continental shelf, southeastern Atlantic Canada. *Geological Survey of Canada Bulletin*, No. 363, 72pp.
- Knauer, G.A., D. Hebel and F. Cipriano (1982) Marine snow: major site of primary production in coastal waters. *Nature*, **300**, 630-631.
- Knauer, G.A., D.M. Karl, J.J. Martin and C.N. Hunter (1984) *In situ* effects of selected preservatives on total carbon, nitrogen and metals collected in sediment traps. *Journal of Marine Research*, **42**, 445-462.
- Knauer, G.A., J.H. Martin and K.W. Bruland (1979) Fluxes of particulate carbon, nitrogen and phosphorous in the upper water column of the northeast Pacific. *Deep-Sea Research*, **26**, 97-108.
- Kolpak, P.D., A.P. Morse, and L.F. Small (1981) An analysis of sinking rates of natural copepod and euphausiid faecal pellets. *Limnology and Oceanography*, **26**, 172-180.
- Kranck K. and T.G. Milligan (1988) Macroflocs from diatoms: *in situ* photography of particles in Bedford Basin, Nova Scotia. *Marine Ecology Progress Series*, **44**, 183-189.

- Krone, R.B. (1972) A field study of flocculation as a factor in estuarial shoaling processes. *United States Corps of Engineers, Committee on Tidal Hydraulics, Technical Bulletin*, 19, 62pp.
- Lampitt, R.S. (1985) Evidence for the seasonal deposition of detritus to the deep-sea floor and its subsequent resuspension. *Deep-Sea Research*, 32, 885-897
- Lande, R. and A.M. Wood (1987) Suspension times of particles in the upper ocean. *Deep-Sea Research*, 34, 61-72.
- Lerman, A (1979) *Geochemical Processes of Water and Sediment Environments*. John Wiley and Sons, Inc, New York, pp481.
- Lewis, A.g. and J.P.M. Syvitski (1983) The interaction of plankton and suspended sediment in fjords. *Sedimentary Geology*, 36, 81-92.
- Livingston, H.D. and R.F. Anderson (1983) Large particle transport of plutonium and other fallout radionuclides to the deep ocean. *Nature*, 303, 229-231.
- Lively, R.R. (1988) Current meter, meteorological, sea-level, and hydrographic observations for the CASP experiment off the coast of Nova Scotia November 1985 to April 1986. *Canadian Technical Report of Hydrography and Ocean Sciences*, No. 100.
- Martin, H. and G.A. Knauer (1985) Lateral transport of Mn in the north-east Pacific Gyre oxygen minimum. *Nature*, 314, 524-526.
- McCave, I.N. (1975) Vertical flux of particles in the ocean. *Deep-Sea Research*, 22, 491-502.
- McCave I.N. (1983) Particle size spectra, behaviour and origin of nepheloid layers over the Nova Scotian Continental rise. *Journal of Geophysical Research*, 88, 7644-7666.
- McCave, I.N. (1985) Local and global aspects of the bottom nepheloid layers in the world ocean. *Netherlands Journal of Sea Research*, 20(2/3), 167-181.
- Michaels, A. F. and M. W. Silver (1988) Primary production, sinking fluxes and the microbial food web. *Deep-Sea Research*, 35, 473-490.
- Michaels, A.F., M.W. Silver, M.M. Gowing and G.A. Knauer (1990) Cryptic zooplankton "swimmers" in upper ocean sediment traps. *Deep-Sea Research*, 37, 1285-1296.

- Moore, W. S. and J. Dymond (1988) Correlation of ^{210}Pb removal with organic carbon fluxes in the Pacific Ocean. *Nature*, **331**, 339-341.
- Murray, J.W. (1987) Coastally derived signals to the ocean interior: Stable inorganic species. In: *Ocean Margins In GOFs*. U.S. GOFs Planning Report **6**, 245pp.
- Newberger, P.A. and D.R. Caldwell (1981) Mixing and the bottom nepheloid layer. *Marine Geology*, **41**, 321-336.
- Nishizawa, S., M. Fukuda, N. Inoue (1954) Photographic study of suspended matter and plankton in the sea. *Bulletin of the Faculty of Fisheries of Hokkaido university*, **5**, 36-40.
- Nittrouer, C.A., T.B. Curtin and D.J. DeMaster (1986) Concentration and flux of suspended sediment on the Amazon continental shelf. *Continental and Shelf Research*, **6**, 151-174
- Noriki, S., N. Ishimori, K. Harada and S. Tsunogai (1985) Removal of trace metals from seawater during a phytoplankton bloom as studied with sediment traps in Funaka Bay, Japan. *Marine Chemistry*, **17**, 75-89.
- Noriki, S. and S. Tsunogai (1986) Particulate fluxes and major components of settling particles from sediment trap experiments in the Pacific Ocean. *Deep-Sea Research*, **33**, 903-912
- Novitsky J.A. (1990) Evidence for sedimenting particles as the origin of the microbial community in a coastal marine sediment. *Marine Ecology Progress Series*, **60**, 161-167
- Nowell A.R.M., P.A. Jumars and J.E. Eckman (1981) Effects of biological activity on the entrainment of marine sediments. *Marine Geology*, **42**, 133-153
- Pak, H. (1983) Fluctuations of beam-attenuation coefficient in the lowest 2m on the continental rise off Nova Scotia. *Marine Geology*, **51**, 77-97.
- Pak H., J.R. Zaneveld and J. Kitchen (1980a) Intermediate nepheloid layers observed off Oregon and Washington. *Journal of Geophysical Research*, **85**, 6697-6708.
- Pak H., L.A. Codispoti and J.R.V. Zaneveld (1980b) On the intermediate particle maxima associated with oxygen-poor water off western south America. *Deep-Sea Research*, **27A**, 783-797.
- Parsons T.R., M. Takahashi and B. Hargrave (1984) *Biological oceanographic processes*. (third edition) Pergamon press, pp330.

- Petrie, B. (1974) Surface and internal tides on the Scotian Shelf and Slope. Ph.D. thesis. Dalhousie University, Halifax, Canada, 152pp.
- Petrie, B. (1975) M_2 surface and internal tides on the Scotian shelf and slope. *Journal of Marine Research*, **33**, 303-323.
- Petrie, B. (1983) Current response at the shelf break to transient wind forcing. *Journal of Geophysical Research*, **88**, c14, 9567-9578.
- Petrie, B. and P.C. Smith (1977) Low-frequency motions on the Scotian shelf and slope. *Atmosphere*, **15**(3), 117-140.
- Petrie, B., B.J. Topliss and D.G. Wright (1987) Coastal upwelling and eddy development off Nova Scotia. *Journal of Geophysical Research*, **29**, C12, 12979-12991.
- Piper, D.J.W. (1991) Seabed geology of the Canadian eastern continental shelf. *Continental Shelf Research*, **11**, 1013-1035.
- Pocklington, R., J.D. Leonard and N.F. Crewe (1991) Sources of organic matter to surficial sediments from the Scotian Shelf and Slope, Canada. *Continental Shelf Research*, **11**, 1069-1082.
- Prezelin, B.B. and A.L. Alldredge (1983) Primary production of marine snow during and after an upwelling event. *Limnology and Oceanography*, **28**, 1156-1167.
- Rhoads, D.C., J.Y. Yingst and W. Ullman (1978) Seafloor stability in central Long Island Sound. Part I. Temporal changes in erodibility of fine-grained sediments. In: *Estuarine Interactions*. M.L. Wiley (ed.), Academic Press, New York, 221-244.
- Rice A.L., D.S.M. Billett, J. Fry, A.W.G. John, R.S. Lampitt, R.F.C. Mantoura and R.J. Morris (1986) Seasonal deposition of phytodetritus to the deep-sea floor. *Proceedings of the Royal Society of Edinburgh*, **88**, 265-279
- Richardson M.J. (1987) Particle size, light scattering and composition of suspended particulate matter in the North Atlantic. *Deep-Sea Research*, **34**, 1301-1329.
- Rickwood, D. and G.D. Birnie (1975) Metrizamide, a new density gradient medium. *Fed. Eur. Biochem. Soc. Lett.* **50**, 102-110.
- Riebesell U. (1989) Comparison of sinking and sedimentation rate measurements in a diatom winter/spring bloom. *Marine Ecology Progress Series*, **54**, 109-119.

- Riebesell U. (1991a) Particle aggregation during a diatom bloom. I. Physical aspects. *Marine Ecology Progress Series*, **69**, 273-280.
- Riebesell U. (1991b) Particle aggregation during a diatom bloom. II. Biological aspects. *Marine Ecology Progress Series*, **69**, 281-291.
- Riley, G. A. (1963) Organic aggregates in seawater and the dynamics of their formation and utilization. *Limnology and Oceanography*, **8**, 372-381.
- Riley, G. A. (1964) Organic aggregates in tropical and subtropical surface waters of the north atlantic ocean. *Limnology and Oceanography*, **9**, 546-550.
- Riley, G. A., P. J. Wangersky and D. Van Hemert (1964) Organic aggregates in tropical and subtropical surface waters of the North Atlantic Ocean. *Limnology and Oceanography*, **9**, 546-550.
- Riley, G. A. (1970) Particulate matter in sea water. *Advances in Marine Biology*, **8**, 1-118.
- Robison, B.H. and T.G. Bailey (1981) Sinking rates and dissolution of midwater fish faecal matter. *Marine Biology*, **65**, 135-142.
- Rowe, G.T., S. Smith, P. Falkowski, T. Whitley, R. Theroux, W. Phoel and H. Ducklow (1986) Do continental shelves export organic matter ? *Nature*, **324**, 559-561.
- Ruddick B. (1986) Relevant physical oceanography of Halifax Inlet. In; *The Halifax inlet water quality study: phase 2*, Appendix B. prepared by A.S.A. Consulting Ltd. for the Metro area planning commission. (unpublished manuscript) pp60.
- Sameoto, D.D. and A.W. Herman (1990) Life cycle and distribution of *Calanus finmarchicus* in deep basins on the Nova Scotia shelf and seasonal changes in *Calanus* spp. *Marine Ecology Progress Series*, **66**, 225-237.
- Sasaki, H., H. Hattori and S. Nishizawa (1988) Downward flux of particulate organic matter and vertical distribution of calanid copepods in the Oyashio Water in summer. *Deep-Sea Research*, **35**, 505-515.
- Sasaki, H. and S. Nishizawa (1981) Vertical flux profile of particulate material in the sea off Sanriku. *Marine Ecological Progress Series*, **6**, 191-201.
- Shanks, A.L. and J.D. Trent (1979) Marine snow: microscale nutrient patches. *Limnology and Oceanography*, **24**, 850-854.

- Shanks, A.L. and J.D. Trent (1980) Marine snow: Sinking rates and potential role in vertical flux. *Deep-Sea Research*, **26**, 137-144.
- Shiozawa, T., K. Kawana, A. Hoshika and T. Tanimoto (1985) Suspended matter and bottom sediment in the Seto Inland Sea. *Bulletin on Coastal Oceanography*, **22**, No.2, 149-156.
- Siegel D.A., T.D. Dickey, L. Washburn, M.K. Hamilton and B.K. Mitchell (1989) Optical determination of particulate abundance and production variations in the oligotrophic ocean. *Deep-Sea Research*, **36**, 211-222..
- Siegel, D.A., T.C. Granata, A.F. Michaels and T.D. Dickey (1990) Mesoscale eddy diffusion, particle sinking and the interpretation of sediment trap data. *Journal of Geophysical Research*, **95**, 5305-5311.
- Silver, M.W. and A.L. Aldredge (1981) Bathypelagic marine snow: deep-sea algal and detrital community. *Journal of Marine Research*, **39**, 501-530.
- Silver, M.W., A.L. Shanks and J.D. Trent (1978) Marine snow: microplankton habitat and source of small scale patchiness in pelagic populations. *Science*, **201**, 371-373.
- Simpson, W.R. (1982) Particulate matter in the oceans-sampling methods, concentration, size distribution and particle dynamics. *Oceanography and Marine Biology, an Annual Review*, **20**, 119-172.
- Smayda, T.J. (1970) The suspension and sinking of phytoplankton in the sea. *Oceanogr. Mar. Bilo. Ann. Rev.*, **8**, 353-414.
- Smith, K.L. and R.F. Baldwin (1984) Seasonal fluctuations in deep-sea sediment community oxygen consumption: central and eastern North Pacific. *Nature*, **307**, 624-626.
- Smith, K.L. (1987) Food energy supply and demand: a discrepancy between particulate organic carbon flux and sediment community oxygen consumption in the deep ocean. *Limnology and Oceanography*, **32**, 201-220.
- Smith, J.D. and T.S. Hopkins (1972) Sediment transport on the continental shelf off of Washington and Oregon in light of recent current measurements. In: *Shelf Sediment Transport: Process and Pattern*. D.J.P. Swift, D.B. Duane and O.H. Pilkey, editors, Dowden, Hutchinson and Ross, Inc. Pennsylvania, 143-180.
- Smith, P.C., B. Petrie and C.R. Mann (1978) Circulation, variability, and dynamics of the Scotian Shelf and Slope. *Journal of Fishery Research Board of Canada*,

35, 1067-1083.

Smith, P.C. and F.B. Schwing (1991) Mean circulation and variability on the eastern Canadian continental shelf. *Continental Shelf Research*, **11**, 977-1012.

Spinrad, R.W., J.R.V. Zaneveld and J.C. Kitchen (1983) A study of the optical characteristics of the suspended particles in the benthic boundary layer of the Scotian Rise. *Journal of Geophysical Research*, **88**, 7641-7645.

Steele, J.H. and C.S. Yentsch (1960) The vertical distribution of chlorophyll. *Journal of Marine Biological Association of U.K.*, **39**, 217-226.

Sternberg, R.W., E.T. Baker, D.A. McManus, S. Smith and D.R. Morrison (1974) An integration nephelometer for measuring particle concentrations in the deep sea. *Deep-Sea Research*, **21**, 887-892.

Sternberg, R.W. and D.A. McManus (1972) Sediment transport on the continental shelf off of Washington and Oregon in light of recent current measurements. In: *Shelf Sediment Transport: Process and Pattern*. D.J.P. Swift, D.B. Duane and O.H. Pilkey, editors, Dowden, Hutchinson and Ross, Inc. Pennsylvania, 181-194.

Suess, E. (1980) Particulate organic carbon flux in the oceans-surface productivity and oxygen utilization. *Nature*, **288**, 260-263.

Suzuki, N. and K. Kato (1953) Studies on suspended materials. Marine snow in the sea. I. Sources of marine snow. *Bulletin of the Faculty of Fisheries of Hokkaido University*, **4**, 132-135.

Syvitski, J.P.M. and A.G. Lewis (1980) Sediment ingestion by *Tigriopus Californicus* and other zooplankton: mineral transformation and sedimentological considerations. *Journal of Sedimentology and Petrology*, **50**, 869-889.

Syvitski, J.P.M. and J.W. Murray (1981) Particle interaction in fjord suspended sediment. *Marine Geology*, **39**, 215-242.

Taghon, G.L., A.R.M. Nowell and P.A. Jumars (1984) Transport and Breakdown of faecal pellets: Biological and sedimentological consequences. *Limnology and Oceanography*, **29**, 64-72.

Takahashi, K. (1986) Seasonal fluxes of pelagic diatoms in the subarctic Pacific, 1982-1983. *Deep-Sea Research*, **33**, 1225-1251.

- Takahashi, K and S. Honjo (1981) Vertical flux of sedimentary radiolaria: a taxon-quantitative sediment trap study from the western tropical Atlantic. *Micropaleontology*, **27**, 203-211.
- Takahashi, K and S. Honjo (1983) Radiolarian skeletons: size, weight, sinking speed, and residence time in tropical pelagic oceans. *Deep-Sea Research*, **30**, 543-568.
- Thorpe S.A. and M. White (1988) A deep intermediate nepheloid layer. *Deep-Sea Research*, **35**, 1665-1671.
- Trent, J.D., A.L. Shanks and M.W. Silver (1979) *In situ* and laboratory measurements on macroscopic aggregates in Monterey Bay, California. *Limnology and Oceanography*, **23**, 626-635.
- Vanderploeg, H.A. (1990) Feeding mechanisms and particle selection in suspension-feeding zooplankton. In: *The Biology of Particles in Aquatic Systems*. R.S. Wotton (ed), CRC Press, 183-212.
- Wakeham, S. G., J. W. Farrington and R. B. Gagosian (1984a) Variability in lipid flux and composition of particulate matter in the Peru upwelling region. *Organic Geochemistry*, **6**, 203-215.
- Wakeham, S. G., J. W. Farrington, R. B. Gagosian and E.A. Canuel (1984b) Sterenes in suspended particulate matter in the eastern tropical North Pacific. *Nature*, **308**, 840-843.
- Wakeham, S. G., C. Lee, J. W. Farrington and R. B. Gagosian (1984c) Biogeochemistry of particulate organic matter in the oceans: results from sediment trap experiments. *Deep-Sea Research*, **31**, 509-528.
- Walsh I., K. Fischer, D. Murray and J. Dymond (1988) Evidence for resuspension of rebound particles from near-bottom sediment traps. *Deep-Sea Research*, **33**, 59-70.
- Walsh, J.J. (1991) Importance of continental margins in the marine biogeochemical cycling of carbon and nitrogen. *Nature*, **350**, 53-55.
- Wangersky P. J. (1974) Particulate organic carbon: Sampling variability. *Limnology and Oceanography*, **19**, 980-984.
- Wangersky P. J. (1976) Particulate organic carbon in the Atlantic and Pacific oceans. *Deep-Sea Research*, **23**, 457-465.

- Wangersky, P. J. (1977) The role of particulate matter in the productivity of surface waters. *Helgoländer wiss. Meeresunters*, **30**,546-564.
- Wangersky, P. J. (1978) The distribution of particulate organic carbon in the oceans: ecological implications. *International Revue der gesamten Hydrobiologie*, **63**, 567-574.
- Wangersky, P. J. (1984) Organic material in sea water. In: *The Handbook of Environmental Chemistry. Volume 1/Part C*. ed. by O. Hutzinger. 25-62.
- Wangersky, P.J (1990) Sampling for particulate and dissolved material. In: *The Biology of Particles in Aquatic Systems*. ed. by Roger S. Wotton, CRC Press, Boston, pp303
- Warner, J.L. (1970) Water movement on the Scotian Shelf. Ph.D. Thesis. Dalhousie Univ., Halifax, N.S. 227pp.
- Winneberger J.H., J.H. Austin and C.A. Klett (1963) Membrane filter weight determinations, *Journal WPCF*, **35**, 807-813
- Wotton, R.S. (1990) Particulate and dissolved organic materials as food. In: *The Biology of Particles in Aquatic systems*. R.W. Wotton (ed.), CRC Press, 213-262.
- Yingst, J.Y. and D.C. Rhoads (1978) Seafloor stability in central Long Island Sound: Part II. Biological interactions and their potential importance for seafloor erodibility. In: *Estuarine Interactions*. M.L. Wiley (ed.), Academic Press, New York, 245-260.

COPYRIGHT ACKNOWLEDGEMENTS

The copyright of Chapter 4 belongs to the following organization:

Copyright (1992)
Pergamon Press Ltd,
Headington Hill Hall, Oxford, OX3 0BW, United Kingdom

Azetsu-Scott, K. and B.D. Johnson (1992)
Measuring Physical Characteristics of Particles: A New method of
simultaneous measurement for size, settling velocity and density of
constituent matter. *Deep-Sea Research* (in press)

I have retained the right to include the manuscript as a chapter in my thesis. In addition, my co-author has given permission for the inclusion of Azetsu-Scott and Johnson (1992) in the thesis.

Bruce D. Johnson



Date: 12 June 1992